Neurosurgery Research Group, Biomedicum Helsinki
Department of Neurosurgery, Helsinki University Central Hospital
University of Helsinki
Helsinki, Finland

Microsurgical Aneurysm Model in Rats and Mice: Development of Endovascular Treatment and Optimization of Magnetic Resonance Imaging

Johan Marjamaa

ACADEMIC DISSERTATION

To be publicly discussed,
with the permission of the Medical Faculty
of the University of Helsinki,
in Lecture Hall 1 of Töölö Hospital
on May 29th 2009 at 12 noon.

Helsinki 2009

Supervised by:

Associate Professor **Mika Niemelä**, M.D.,Ph.D.
Department of Neurosurgery
Helsinki University Central Hospital
Helsinki, Finland

Associate Professor **Marko Kangasniemi**, M.D., Ph.D.
Medical Imaging Center
Helsinki University Central Hospital
Helsinki, Finland

Reviewed by:

Associate Professor **Jaakko Rinne**, M.D., Ph.D.
Department of Neurosurgery
Kuopio University Hospital
Kuopio, Finland

Associate Professor **Leo Keski-Nisula**, M.D., Ph.D.
Medical Imaging Center
Tampere University Hospital
Tampere, Finland

Opponent:

Professor **Fady T. Charbel**, M.D., FACS
Department of Neurosurgery
University of Illinois at Chicago
Chicago, USA

Johan Marjamaa, M.D.
Neurosurgery Research Group, Biomedicum Helsinki
Department of Neurosurgery, Helsinki University Central Hospital
johan.marjamaa@hus.fi

ISBN: 978-952-92-5558-0 (paperback)
ISBN: 978-952-10-5572-0 (PDF)

Helsinki University Print

Table of contents

Abstract

The rupture of a cerebral artery aneurysm causes a devastating subarachnoid hemorrhage (SAH), with a mortality of almost 50% during the first month. Each year, 8-11/100 000 people suffer from aneurysmal SAH in Western countries, but the number is twice as high in Finland and Japan. The disease is most common among those of working age, the mean age at rupture being 50-55 years. Unruptured cerebral aneurysms are found in 2-6% of the population, but knowledge about the true risk of rupture is limited. The vast majority of aneurysms should be considered rupture-prone, and treatment for these patients is warranted.

Both unruptured and ruptured aneurysms can be treated by either microsurgical clipping or endovascular embolization. In a standard microsurgical procedure, the neck of the aneurysm is closed by a metal clip, sealing off the aneurysm from the circulation. Endovascular embolization is performed by packing the aneurysm from the inside of the vessel lumen with detachable platinum coils. Coiling is associated with slightly lower morbidity and mortality than microsurgery, but the long-term results of microsurgically treated aneurysms are better.

Endovascular treatment methods are constantly being developed further in order to achieve better long-term results. New coils and novel embolic agents need to be tested in a variety of animal models before they can be used in humans. In this study, we developed an experimental rat aneurysm model and showed its suitability for testing endovascular devices. We optimized noninvasive MRI sequences at 4.7 Tesla for follow-up of coiled experimental aneurysms and for volumetric measurement of aneurysm neck remnants. This model was used to compare platinum coils with polyglycolic-polylactic acid (PGLA) -coated coils, and showed the benefits of the latter in this model. The experimental aneurysm model and the imaging methods also gave insight into the mechanisms involved in aneurysm formation, and the model can be used in the development of novel imaging techniques. This model is affordable, easily reproducible, reliable, and suitable for MRI follow-up. It is also suitable for endovascular treatment, and it evades spontaneous occlusion.

List of original publications

The thesis is based on the following original publications, referred to in the text by their Roman numerals:

I **Mice with a deletion of the first intron of the Col1a1 gene develop dissection and rupture in the absence of aneurysms: high-resolution magnetic resonance imaging, at 4.7 T, of the aorta and cerebral arteries**
Marjamaa J, Tulamo R, Abo-Ramadan U, Hakovirta H, Frösen J, Rahkonen O, Niemelä M, Bornstein P, Penttinen R, Kangasniemi M
Magn Reson Med 2006;55:592-7

II **Contribution of mural and bone marrow-derived neointimal cells to thrombus organization and wall remodeling in a microsurgical murine saccular aneurysm model**
Frösen J, Marjamaa J, Myllärniemi M, Abo-Ramadan U, Tulamo R, Niemelä M, Hernesniemi J, Jääskeläinen J
Neurosurgery 2006;58:936-44

III **High-resolution TOF MR-angiography at 4.7 Tesla for volumetric and morphologic evaluation of coiled aneurysm neck remnants in a rat model**
Marjamaa J, Antell H, Abo-Ramadan U, Hernesniemi J, Niemelä M, Kangasniemi M
(Submitted).

IV **Occlusion of neck remnant in experimental rat aneurysms after treatment with platinum- or polyglycolic-polylactic acid-coated coils**
Marjamaa J, Tulamo R, Frösen J, Abo-Ramadan U, Hernesniemi J, Niemelä M, Kangasniemi M
Surg Neurol 2009 71:458-65 (Epub 2008 Jul 9)

The thesis also contains some unpublished data.

Abbreviations

ACA	Anterior cerebral artery
Acom	Anterior communicating artery
AVM	Arteriovenous malformation
CAP	Cellulose acetate polymer
CE-MRA	Contrast-enhanced magnetic resonance angiography
CNR	Contrast-to-noise ratio
CT	Computed tomography
CTA	Computed tomography angiography
DAVF	Dural arteriovenous fistula
DIND	Delayed ischemic neurological deficit
DSA	Digital subtraction angiography
ECA	External carotid artery
EVAL	Ethylene vinyl alcohol
FBI	Fresh blood imaging
FOV	Field of view
GCS	Glasgow coma scale
GDC	Guglielmi detachable coil
GEFC	Gradient echo imaging sequence, comprising 1st order flow compensation
GOS	Glasgow outcome scale
ICA	Internal carotid artery
IR-RARE	Rapid acquisition with relaxation enhancement and inversion recovery
ISAT	International Subarachnoid Aneurysm Trial
ISUIA	International Study of Unruptured Intracranial Aneurysms
MCA	Middle cerebral artery
MDC	Mechanically detachable coil
MGE	Multiple gradient echo
MIP	Maximum intensity projection
MRA	Magnetic resonance angiography
MRI	Magnetic resonance imaging
MSME	Multi-spin multi-echo
MT	Magnetization transfer
NEX	Number of exitations
PA	Pulse angle (also known as flip angle (FA))
PBS	Phosphate-buffered saline
PCA	Posterior cerebral artery
Pcom	Posterior communicating artery

PGA	Polyglycolic acid
PGLA	Polyglycolic-polylactic acid
RARE	Rapid acquisition with relaxation enhancement
RF	Radio frequency
ROI	Region of interest
SAH	Subarachnoid hemorrhage
SCAA	Saccular cerebral artery aneurysm
SNR	Signal-to-noise ratio
[Sv]	Sievert
[T]	Tesla
TE	Echo time
TIA	Transient ischemic attack
TOF-MRA	Time-of-flight magnetic resonance angiography
TR	Repetition time
USPIO	Ultrasmall superparamagnetic particles of iron oxide
VENC	Velocity-encoding coefficient

1. Introduction

The rupture of a cerebral artery aneurysm causes a devastating subarachnoid hemorrhage (SAH). The 1-month mortality is almost 50% (Sarti et al. 1991), and 24% of patients are left with permanent neurological deficits (Hernesniemi et al. 1993, Hop et al. 1997). The incidence of aneurysmal SAH is 8-11/100 000 in Western countries (Phillips et al. 1980, Ingall et al. 1989, van Gijn et al. 2007, de Rooij et al. 2007, Bederson et al. 2009), but this number is twice as high in Finland and Japan (Sarti et al. 1991, Ohkuma et al. 2002). This disease is most common among those of working age, the mean age at rupture being 50-55 years (Mahindu et al. 2008, van Munster et al 2008). Unruptured cerebral aneurysms are found in 2-6% of the population (Ronkainen et al. 1998, Rinkel et al. 1998), but why only some of them rupture remains unknown. Risk factors associated with aneurysm growth and rupture have been identified: smoking, hypertension, excessive alcohol use, female gender, family history, aneurysm size, and aneurysm site (Hillbom et al. 1981, Bonita 1986, Juvela et al. 2000, Juvela et al. 2001, Wiebers et al. 2003, de Rooij et al. 2007, Ishibashi 2009, Woo et al. 2009). However, no reliable methods exist for estimating the natural progression of an aneurysm (Koffijberg et al. 2008), and thus far it is not possible to predict which aneurysms will rupture. Therefore, all aneurysms must be considered potentially lethal, and patients should be evaluated for their suitability for treatment. The risk of rupture must always be weighted against the age- and comorbidity-adjusted risks associated with treatment.

Both unruptured and ruptured aneurysms can be treated by either microsurgical clipping or endovascular embolization. Endovascular embolization is performed by packing the aneurysm with detachable platinum coils, nowadays often together with balloon remodeling or with stents. Coiling is preferred in many neurosurgical centers since it has been shown to be associated with a slightly lower morbidity, especially in the posterior circulation, than surgery (Koivisto et al. 2000, Molyneux et al. 2002, Taha et al. 2006). However, the initial angiographic results of coiled aneurysm disturbingly often show incomplete occlusion, with persisting neck remnants or filling of the fundus of the aneurysm (Vanninen et al. 1999, Molyneux et al. 2002, Raymond et al. 2003, Taha et al. 2006). In addition, even perfectly coiled aneurysms may undergo coil compaction and recanalization, leading to an increased risk of rupture (Raymond et al. 2003), necessitating angiographic follow-up and eventual re-treatment (Vanninen et al. 1999, Raymond et al. 2003). Although studies with selected patients show good long-term results after coiling, other studies show significantly poorer results depending on aneurysm morphology, size, and location. The clinician is forced to balance the risks and benefits of surgical clipping, which offers a very small risk of recurrence when performed properly (Tsutsumi et al. 2001), with the long-term uncertainties and mandatory long-term follow-up associated with the less invasive coiling. The immediate (24 h) risks of coiling also cannot be

dismissed, as 3.8% patients may suffer from an thromboembolic event or transient ischemic attacks (Derdeyn et.al. 2002). Moreover, according to a meta-analysis by Brilstra et al. (1999), the intraprocedural rupture incidence is 4.5%. Periprocedural complications are seen in 8.4% of endovascularly treated patients and in 19.4% of surgically treated patients (Taha et al 2006). Therefore, development of even safer and especially more efficient endovascular treatment methods is needed.

Today, coiling is dependent on the mechanical occlusion of the aneurysm, and the results are better when higher packing density is achieved. In order to fill the aneurysm as densely as possible, balloon-assisted remodeling techniques and stenting methods have been developed. However, this makes the procedure even more demanding and time-consuming, theoretically increasing the complication rate. Efforts should be directed towards creating simpler endovascular techniques and the ongoing development should emphasize on the biological effect of the coil, made possible by the increasing knowledge on aneurysm pathobiology (Peters et al. 1999, 2001, Frösen et al. 2004, Tulamo et al. 2006, Laaksamo et al. 2008). Coils could be coated with biologically active agents, like growth factors, to induce myointimal hyperplasia and strengthen the aneurysm wall. Hopefully, in the future, biologically active coils will work as a form of local drug delivery into the aneurysm, and their effect will not depend on the packing density, but rather on other properties that will stabilize the aneurysm and progressively occlude it. In this way, aneurysms that depending on their location or local anatomy (e.g. branches arising near the aneurysm), are difficult to treat endovascularly and even more so microsurgically, would be applicable for therapy with a more simple coil. These futuristic tools would enable us to treat aneurysms at difficult sites and with complex angioarchitecture better.

When new endovascular devices are developed, they need to be tested in experimental animal models before being used in humans. A good experimental animal model must be easy to reproduce and reliable, and it also has to evade spontaneous occlusion. Repeated in vivo radiological follow-up examinations of the experimental aneurysm are required, and the chosen imaging technique should have a resolution that enables detection of even small changes at the interface between the aneurysm neck and the coil surface. At the end of the study, animals should be sacrificed and the samples analyzed by histological methods.

Experimental aneurysm models suitable for endovascular treatment have been developed in swine, rabbits, and dogs. In the swine model, a jugular vein graft is used to construct an aneurysm in the carotid artery (Guglielmi et al. 1994). In the rabbit model, elastase-induced aneurysms are formed in ligated stumps of the carotid arteries (Cawley et al. 1996). The follow-up has been performed by digital subtraction angiography (DSA). In order to test the efficacy of the devices, it is important that the untreated aneurysm remains patent or grows.

In this study, we developed a surgically created aneurysm model in rats and mice. The rat model is suitable for endovascular treatment since the experimental aneurysms resemble the smallest ruptured aneurysms in humans. The model is easy to standardize and highly reproducible. Because of the low mortality rate and the inexpensive price of the animals, our model is also more affordable than the other experimental aneurysm models. The mouse model allows the use of widely available transgenic strains in order to dissect mechanisms involved in the pathobiology of aneurysm formation. However, the main reason for choosing to use rats and mice was that noninvasive follow-up with a 4.7 Tesla magnetic resonance (MR) scanner was possible only with animals small enough to fit into the bore of the scanner. For magnetic resonance imaging (MRI), we optimized an imaging protocol including a high-resolution (117 x 117 x 117 µm) time-of-flight magnetic resonance angiography (TOF-MRA) sequence for volumetric measurement of aneurysm neck remnants. Using the rat model and the optimized MR imaging protocol we performed a study comparing the effects of platinum coils with polyglycolic-polylactic acid (PGLA) - coated coils. With MRI, we were able to detect even small changes in the aneurysm neck during follow-up. We also investigated the suitability of a genetically modified mouse strain (Col-IntΔ) for the study of aneurysm formation by optimizing an MR imaging protocol for the mouse aorta and cerebral arteries and scanning these vessels for aneurysms. Murines are the most commonly used animals at our research facility (Biomedicum, Helsinki).

2. Review of the literature

2.1 Cerebral artery aneurysms

2.1.1 Prevalence and etiology

The estimated prevalence of unruptured cerebral artery aneurysms in the general population varies between 0.8% and 8.1% (Byrne et. Guglielmi 1998, Rinkel et al. 1998, Ronkainen et al. 1998). According to a meta-analysis of autopsy and angiographic studies, the incidence of cerebral aneurysms in an adult population without risk factors for SAH is 2%, most aneurysms being less than 10 mm in diameter (Rinkel et al. 1998). In a Finnish forensic autopsy study, the prevalence was 2.2% for aneurysms ≥3 mm (Ronkainen et al. 1998). Based on their morphology, aneurysms can be classified into the more common (98%) saccular or the rare fusiform (Yaşargil 1984) and dissecting types. Saccular aneurysms are most often berry-like protrusions that have a well-defined neck (often narrow), sometimes with a multilobular appearance or a wide neck. The largest diameter of a ruptured saccular cerebral artery aneurysm (SCAA) is on average 11 mm, whereas incidental aneurysms are on average only 6 mm (Juvela et al. 2001). Aneurysms larger than 25 mm in diameter (giant aneurysms) comprise 3-5% of all aneurysms (McCormick et al. 1970, Choi et al. 2003). Up to one-third of patients have multiple aneurysms (Rinne et al. 1994). Most of the saccular aneurysms (85-95%) are located in the anterior circulation (carotid system) and only 5-15% in the posterior circulation (vertebro-basilar system). Aneurysms usually arise in the bifurcations of proximally located cerebral arteries, of these the most frequent sites are the Acom (30%), Pcom (25%) and MCA (20%) (Weir et. MacDonald 1996). In Finland MCA aneurysms are predominant (Pakarinen 1967, Fogelholm 1981, Rinne et al. 1996). The hemodynamic stress in these locations most probably favors aneurysm formation, but this is not the only explanation. The true etiology appears to be much more complex and is incompletely known. On histological inspection, the cerebral arteries lack an external elastic lamina (between the media and adventitia layer) and have gaps in the media layer at bifurcations where muscle is replaced by connective tissue (Wilkinson 1972, Finlay et al. 1998). Moreover, inflammation (Frösen et al. 2004, Tulamo et al. 2006), lipid deposition and the formation of such atherosclerotic changes as myointimal hyperplasia may be important contributing factors. A minority of aneurysms have a traumatic (Benoit et al. 1973) or infectious etiology (Frazee et al. 1980, Clare et al. 1992, Kumar et al. 1998).

Patients with certain relatively rare inherited diseases such as polycystic kidney disease (PKD) (Butler et al. 1996, Belz et al. 2001), fibromuscular dysplasia (FMD) and diseases that affect the connective tissue e.g. Ehlers Danlos type IV and Marfan´s syndrome (ter Berg et al. 1986), have higher risk of developing aneurysms.

2.1.2 Cerebral artery aneurysm rupture

The natural history of cerebral artery aneurysms is not fully known. Thus far, it is not possible to predict which aneurysms will rupture and when. The multinational ISUIA (International Study of Unruptured Intracranial Aneurysms), the largest study on this subject, concluded that the risk of rupture is dependent on aneurysm location, size, and previous history of SAH (Wiebers et al. 2003). According to ISUIA, the risk of rupture of aneurysms less than 7 mm in diameter is only about 0.1% per year if no previous history of SAH exists the risk being higher in posterior than anterior circulation. On the other hand, for example for Pcom aneurysms larger than 25 mm the 5-year cumulative risk of rupture is 50%. The ISUIA results for small aneurysms differ from other studies. Juvela et al. (2000) reported an overall annual risk of rupture of 1.3% in Finland. This risk accumulates over time, being 10.5% at 10 years and 30.3% at 30 years (Juvela et.al. 2000) and also aneurysms ≤ 6 mm in diameter have a 1.1% risk of rupture. However, most patients in their study had a history of previous SAH, which makes it difficult to directly compare these results with ISUIA. In addition to aneurysm size and location, also gender, age, cigarette smoking, hypertension, and alcohol consumption are important risk factors predisposing to rupture (Hillbom et al. 1981, Bonita 1986, Juvela et al. 2000, Juvela et al. 2001, Wiebers et al. 2003, de Rooij et al. 2007, Ishibashi et al. 2009, Woo et al. 2009). Diabetes and hypercholesterolemia, in turn, have not been shown to increase the risk.

Aneurysm rupture most commonly results in a SAH. An intracerebral hematoma with or without SAH is seen in 20-40% of patients, whereas intraventricular hemorrhage occurs in 13-28% (Yeh et al. 1985) and subdural hemorrhage in 2% (Gelabert-Gonzalez et al. 2004).

2.1.2.1 Subarachnoid hemorrhage

Rupture of cerebral artery aneurysms accounts for approximately 80% (Kassell et al 1990a, van Gijn et al 2001) of all nontraumatic cases of SAH, the rest being from e.g. cerebral arteriovenous malformations (AVMs) or unknown causes (Ronkainen et. Hernesniemi 1992). The annual incidence of aneurysmal SAH is 8-11/100 000 in Western countries (Phillips et al. 1980, Ingall et al. 1989, de Rooij et al. 2007, van Gijn et al. 2007, Bederson et al. 2009). In Finland, the risk is more than twice as high, being 25/100 000 among Finnish women and 33/100 000 among Finnish men (Sarti et al 1991). The risk is also higher in the Japanese population, being 21/100 000 (Ohkuma et al. 2002). Most patients are 50-55 years of age (Mahindu et al. 2008, van Munster et al 2008), but the proportion of older and more fragile patients is increasing. The outcome of SAH is still devastating, with a 1-month mortality rate of 46% in women and 48% in men (Sarti et al. 1991). Moreover,

approximately 24% of the survivors are left with moderate to severe disability (Hernesniemi et al. 1993). The case-fatality rate has, however, decreased during the last decades due to improved management (Hop et al. 1997), including ultra early treatment, antifibrinolytic therapy, neurointensive care and monitoring, and vasospasm prevention and treatment.

Acute SAH is a complex and critical condition requiring a dedicated multidisciplinary neurocare team. The clinical presentation of SAH is an acute, severe headache, which can be accompanied by a variety of symptoms such as nausea, vomiting, drowsiness, loss of consciousness, and meningismus. In the case of an intracerebral hematoma, hemiparesis and symptoms of herniation may occur. A significant number of patients (30-60%) suffer from a warning leak and symptoms that pass within a day, some days before the major bleeding. SAH is reliably diagnosed with a computed tomography (CT) scan or lumbar puncture (van Gijn et al. 1980, van der Wee et al 1995). The source of bleeding must be identified, and this is usually done by computed tomography angiography (CTA) or digital subtraction angiography (DSA) and sometimes magnetic resonance angiography (MRA) since the aneurysm itself usually can not be seen on plain CT images.

Patients surviving the initial hemorrhage may deteriorate or die because of rebleeding, vasospasm, or hydrocephalus. The risk of rebleeding after SAH is 15-20% within 2 weeks. This can be avoided by treating the aneurysm in the early phase, within 3 days (Öhman et al. 1989). Angiographic vasospasm is seen in almost 70% of the patients with SAH. Delayed ischemic neurological deficit (DIND) – sometimes still called clinical vasospasm – develops in one-fourth of the patients (Kassell et al 1985). The basic pathophysiology of DIND remains uncertain. It is an elaborate condition, involving more brain arterioles and small vessels than merely reflecting contraction in the main arteries. It can cause clinical deterioration because of decreased cerebral blood flow and may result in permanent cerebral infarction. Nimodipine, a calcium channel antagonist has proven efficacious in preventing vasospasm (Auer et al. 1986, Öhman et al. 1988, Pickard et al. 1990, Rinkel et al. 2002). The effective treatment of vasospasm with induced hypertension, hypervolemia, and hemodilution usually necessitates neurointensive care and invasive monitoring and sometimes angioplasty (Song et al. 1997). To carry out these treatments more safely, the aneurysm must first be repaired. Since the peak of vasospasm is during days 6-8, surgery performed on days 4-10 may exacerbate the vasospasm. Hydrocephalus can be present already at admission to hospital, especially in cases with intraventricular hemorrhage, or develop over the course of months, slowing recovery. The reported incidence of chronic hydrocephalus requiring treatment with a shunt varies between 6% and 67 % (Tapaninaho et al. 1993, Vale et al. 1997, Dorai et al. 2003).

2.2 Treatment of ruptured and unruptured aneurysms

Saccular aneurysms can be treated by either microsurgical clipping or endovascular coiling (Figure 2). In cases involving giant aneurysms, bypass surgery in conjunction with trapping of the aneurysm (proximal ligation) may be needed. Most aneurysms are, in theory, suitable for both microsurgical and endovascular treatments. However, surgical treatment is recommended in patients with a large intracerebral hematoma, a severe hydrocephalus, or a giant aneurysm. Both methods are technically demanding and are associated with even fatal complications.

2.2.1 Microsurgical clipping

In 1937, Dandy was the first to clip an aneurysm. The main evolution of microneurosurgical clipping took place in the 1950s and 1960s, with improvements in aneurysm clips (Norlen et. Olivecrona 1953, Heifetz 1963, Nyström 1966, Mayfield et al. 1971) and development of operating microscopes (Donaghy et al. 1979, Kriss et al. 1998). The foremost publication by Krayenbühl and Yaşargil (1972) reported the results of 231 microsurgically treated aneurysm patients between 1967 and 1971. The mortality rate was only 4%, in a later study dropping further to 2% (Yaşargil et al. 1975). However, no early surgery was performed and treatment was delayed up to 3 weeks after the initial SAH in most cases.

In microsurgical clipping a steel or titanium clip is applied to the neck of the aneurysm, isolating it from the parent artery. The long-term durability and efficacy of clipping are very well known and good. The annual recurrence rate of a completely clipped aneurysm has been reported to be as low as 0.3% (Tsutsumi et al. 2001), and the cumulative risk of rebleeding 2.2% in 10 years and 9.0% in 20 years after clipping of a ruptured aneurysm (Tsutsumi et al. 1998). The cumulative risk of bleeding from an originally unruptured aneurysm is 1.4% in 10 years (Tsutsumi et al. 1999) after complete clipping. Angiographic long-term follow-up is usually not performed for patients with clipped aneurysms after the initial imaging, unless the patient with SAH is exceptionally young. A recent report shows that the complete occlusion rate after clipping is 88% (Kivisaari et al. 2004), unexpected neck remnants remaining a challenge even in experienced hands (Lin et al. 1989). It is important to remember that these patients may also develop de novo aneurysms, especially if such risk factors as smoking and hypertension are ignored or if the patient is very young at the time of the initial bleeding (Rinne et al. 1993). Clipping of previously coiled aneurysms is sometimes indicated, but it requires even more meticulous handling because the coil-mass interferes with visibility and approach, and the aneurysm is usually attached to the surrounding parenchyma.

2.2.2 Endovascular treatment

Endovascular treatment is performed by a trained interventionist (neuroradiologist or neurosurgeon) as a member of a dedicated neurovascular team. The endovascular approach can be used to treat aneurysms, arteriovenous fistulas (AVFs), and arteriovenous malformations (AVMs) and can also be used in conjunction with surgery (Marks et al. 1995). Endovascular occlusion of feeding arteries prior to surgery is also beneficial in highly vascular tumors. In endovascular treatment, the aneurysms is usually filled from inside the vessel lumen with detachable coils, sometimes with the help of neck re-modeling with balloons or stents.

2.2.2.1 History of endovascular treatment

The first steps in the treatment of intracranial vascular lesions (AVFs, AVMs, and aneurysms) by an endovascular approach were taken by a Russian neurosurgeon, Fedor Serbinenko, who started examining the potential of using flow-directed inflatable balloon catheters in 1962 (Serbinenko et al. 1971, 1974). Serbinenko used the balloon system to investigate collateral flow through the circle of Willis and the effect of temporary and permanent occlusion of vessels. In 1969, he treated a carotid cavernous fistula with a nondetachable balloon. He later developed a mechanism for balloon detachment and hypothesized that it could be used for aneurysm occlusion. The technique was further developed by other researchers (Romodanov et al. 1979, Debrun et al. 1981, Hieshima et al. 1986), and in order to prevent the balloon from deflating, causing aneurysm recanalization or embolism to the parent artery balloons were filled with a solidifying agent (Serbinenko et al. 1974, Taki et al. 1980, Goto et al. 1988). However, direct balloon occlusion of aneurysms was associated with rather high mortality and morbidity. In a series of 84 patients, Higashida et al. (1990) reported a treatment-related mortality of 17.9%, mostly due to aneurysm rupture, also in cases with no prior SAH. Moreover, 10.7% of patients developed stroke due to thromboembolism, parent vessel narrowing, or leakage of solidifying agent from the balloon. During the follow-up period of 3 to 68 months, 77.4% of the aneurysms continued to be permanently occluded, but 11.8% were in need of re-treatment.

Metallic coils were later introduced as an alternative embolic material. Copper wire had earlier been placed into aneurysms during an open craniotomy (Mullan et al 1965, Hosobuchi et al 1979). Endovascularly delivered metallic coils were first used to occlude the entire parent vessel (Spaziante et al. 1986) and later to selectively occlude the aneurysm (Takahashi et al. 1988, Dowd et al. 1990). The first coil types were “free” in the sense that once they were deployed into the aneurysms with a pusher wire it was not possible to retrieve them. Optimal positioning of the

coils into the vascular lesion (aneurysm or AVM) is naturally important, and therefore, mechanisms for coil retrieval were developed (Hawkins et al. 1986).

The most significant advance in endovascular technology for the treatment of cerebral aneurysms was the development of the Guglielmi detachable coils (GDCs) (Guglielmi et al. 1991a,b). The GDC system consists of a soft platinum coil, available in different sizes, which is connected to a stainless steel pusher wire by a soft, uninsulated intermediate piece made of steel. The coil can be repositioned in the aneurysm several times and then motionlessly detached from the wire by electrolysis of the intermediate piece. The electrical current that causes the electrolysis was also believed to cause substantial thrombosis of the aneurysm (electrothrombosis). The concept of electrothrombosis had been presented decades earlier by Mullan et al. (1965, 1969) and Araki et al. (1966), who used the technique in combination with stereotactic surgery or open craniotomy, but Guglielmi was the first to combine electrothrombosis with endovascular mechanical occlusion of an aneurysm. Platinum was also suitable because of its biocompatibility (Loeb et al. 1982), radiopacity, and thrombogenicity compared with steel coils. Moreover, the soft platinum coil adapts to the shape of the aneurysm and is less traumatic than a balloon or a stiffer steel coil (Guglielmi et al 1991a). The initial results in 15 patients were good (Guglielmi et al. 1991b), and in a matter of years the technique was adopted by others and reports of larger series were published (Vinuela et al. 1997, Cognard et al. 1998).

2.2.2.2 Safety and efficacy of endovascular coiling

A meta-analysis by Brilstra et al. (1999) showed a 12% mortality and morbidity associated with coiling, including a 3.7% risk of permanent deficit and a 1.1% risk of death. Ischemic events and aneurysm perforations were the most common causes of adverse outcome (Brilstra et al. 1999). It should be emphasized, though, that these figures are from the very early era of endovascular treatment. These figures may be acceptable, but a larger concern is the high rate of incomplete occlusion, seen in 46% of cases (Brilstra et al. 1999), the high rate of angiographic recurrence (recanalization), and the lack of long-term follow-up (i.e. several decades) (Vanninen et al. 1999, Molyneux et al. 2002, Raymond et al. 2003, Taha et al. 2006). Follow-up has proven to be necessary, with subsequent treatment frequently needed (Vanninen et al. 1999, Raymond et al. 2003) to avoid rebleeding. Also, completely coiled aneurysms may undergo coil compaction and recanalization, leading to an increased risk of rupture (Raymond et al. 2003). It is still somewhat open how, when, by whom, and how long these patients should be followed.

The occlusion rate after endovascular treatment is usually evaluated with the three-grade Raymond scale: 1) complete occlusion, 2) contrast agent filling in the neck of the aneurysm, and 3) contrast agent filling in the sac of the aneurysm (Roy et al. 2001) (Figure 1).

The rate of angiographic recurrence has been assessed in many short- and medium-term studies. Raymond et al. (2003) conducted a thorough retrospective study of 501 aneurysms treated with GDC coils. Overall angiographic recurrences were found in 33.6% of patients after a mean follow-up of 12.31 ± 11.33 months. Major recurrences, permitting re-treatment, were seen in 20.7% of patients after 16.49 ± 15.93 months. Half (49.4%) of the major recurrences were re-treated, and of these, a second recurrence was found in 48.6% of cases (at 15.56 ± 18.43 months). Major recurrence significantly more often occurred in aneurysms larger than 10 mm (34.4%) and aneurysms with necks wider than 4 mm (34.8%). Ruptured aneurysms showed major recurrence more often than unruptured ones (25.1% vs. 16.3%). Complete initial occlusion was achieved in 35.9% of aneurysms, and in this group, major recurrence was found in only 9.0%. The aneurysm rupture rate, being 0.8%, was far less than the angiographic recurrence rate, so even incomplete coiling may protect against rebleeding.

Kuether et al. (1998) reported a series of 77 patients treated with platinum coils and with an average angiographic follow-up time of 1.4 years. Initial complete occlusion was achieved in 40% of cases, and 14% of patients needed further embolization. Two patients (2/70 = 2.9%) suffered from rebleeding 5 months after coiling; neither one of them exhibited complete initial occlusion.

In their study of 145 aneurysms treated with GDCs, Sluzewski et al. (2004) found that large aneurysm volume is associated with low packing density and increased risk of aneurysm recurrence. Cognard et al. (1998) followed 169 coiled aneurysms with an initial complete occlusion rate of 56% and observed recurrence in 14% of the lesions between 3 and 40 months.

The long-term durability of coiling appear less certain than with clipping. When assessing validity of older series, one should bear in mind that endovascular techniques and devices have been – and still are – under constant development. A long-term, prospective, randomized trial comparing clipping and coiling has not yet been performed. Thus far, prospective studies have demonstrated follow-up times of 1 year (Koivisto et al. 2000) and 7 years (Molyneux et al. 2005).

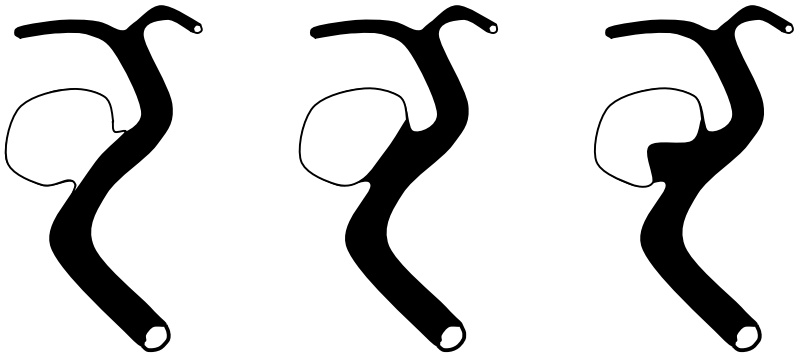

Figure 1:
Raymond scale, used for evaluation of aneurysm filling.

2.2.2.3 *Further development of endovascular treatment*

Embolizing aneurysms with detachable platinum coils is performed under general anesthesia by first inserting a guiding catheter via femoral approach into the cervical arteries (internal carotid artery or vertebral artery), after which a microcatheter can be advanced into the aneurysm. Through the microcatheter, the aneurysm can be packed with a sufficient number of coils of different lengths and diameters. During the procedure intravenous heparin is routinely administered in order to avoid thromboembolic complications. Antiplatelet drugs can also be used. Endovascular embolization should cause clotting of the blood inside the coil scaffold, this blood cloth should become organized and fibrosed. Moreover, for the treatment results to be long-lasting, the neck of the aneurysm should become endothelialized.

Coiling was initially unsuited for aneurysms with an unfavorable dome-to-neck ratio (width of dome / width of neck < 2.0) or a wide neck (>4mm) (Debrun et al. 1998, Wanke et al. 2003). In 1997, Moret et al. (1997) introduced the so called “remodeling technique”, in which an inflated balloon is temporary placed at the neck of the aneurysm during coil placement to ensure that the coils do not protrude into the parent artery. The same thing can be accomplished by placing a self-expanding stent at the neck of the aneurysm (Wanke et al. 2003) (Figure 2). Compared with the balloon-expandable (coronary) stents used in a few early case reports (Higashida et al. 1997, Mericle et al. 1998, Sekhon et al. 1998, Lanzino et al. 1999), deployment of the self-expanding stent is less traumatic, and since the stent is more flexible, it is safer to deliver and the risk of vessel dissection is smaller. The self-expanding stent is preloaded into the microcatheter. A stabilizer wire is put into the microcatheter to keep the stent in place. Deployment of the stent occurs when the microcatheter is pulled back while simultaneously keeping the stent in place with the stabilizer. The latest stents are electrically detachable and can be repositioned before detachment. The microcatheter with the coil is pushed into the aneurysm already prior to stenting,

entrapping it between the stent and the vessel wall. In this way, the microcatheter is kept in place during coiling, but afterwards it is possible to remove it. In addition to heparin, patients undergoing stenting are given antiplatelet therapy consisting of clopidogrel (30 days) and aspirin (rest of life) (Wanke et al. 2003). Interestingly, it has been shown that the stent alters the blood flow in the inflow zone of the aneurysm, seen as stasis of contrast media inside the vessel (Wanke et al. 2003). Therefore, in certain cases stenting alone can cure the aneurysm (Vanninen et al. 2003). There is an ongoing development of intraluminal flow-diverting stents, which would principally be used alone without coiling (Kallmes et al. 2007).

In addition to making wide-necked aneurysms more favorable for endovascular treatment, stenting also enables higher packing densities to be achieved, which might provide better long-term results. However, no data yet exist on the long-term result of stenting. Other inventions have also been devised in an attempt to prevent recanalization, e.g. different modifications of the three-dimensional shape of the coil (Malek et al. 1999, Cloft et al. 2000). 3D coils more easily produce a basket into which subsequent filling-coils are easier to deploy, thereby improving the packing density.

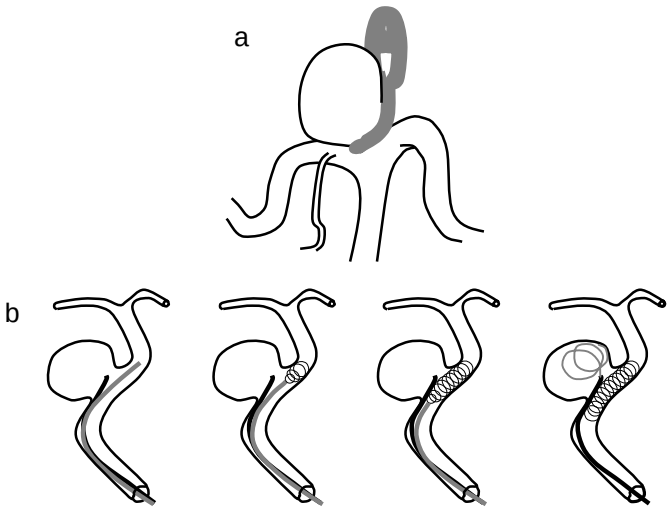

Figure 2:
Illustration of aneurysm clipping (a), and of stent assisted coiling (b).

2.2.2.4 *Surface-modified coils in clinical use*

Attempts have also been made to modify the surface of the platinum coils since they are sometimes only surrounded by an unorganized thrombus, which does not provide much anatomic support. Second-generation coated coils were developed to enhance maturation of the thrombus, formation of fibrosis, and endothelialization of the neck.

The first second-generation coil introduced into clinical use was the Matrix coil (Boston Scientific, Fremont, CA, USA). Matrix is a GDC coil that is coated with polyglycolic-polylactic acid (PGLA), a bioabsorbable polymeric material. Materials like this have been used for a variety of purposes, including sutures, implants, drug delivery vehicles, and scaffolds for tissue engineering (Langer et al. 1993).

PGLA-coated coils were tested in two experimental aneurysm models, in swine and rabbits (discussed further), before being introduced for use in humans. In human studies, the safety of PGLA-coated coils has been shown to be equal to platinum coils (Katz et al. 2005, Linfante et al. 2005, Taschner et al. 2005, Pierot et al. 2006), but the results on efficacy have been very confusing (Katz et al 2005, Murayama et al 2006, Niimi et al 2006). Murayama et al. (2006) achieved promising results; 80.5% of aneurysms treated with PGLA-coated coils remained stable or showed progressive occlusion after a mean follow-up of 8 months. Moreover, recanalization did not appear in aneurysms that were initially completely occluded. However, Katz et al. (2005) and Pierrot et al. (2006) found the recanalization rate to fall within the range of platinum coils, with rates of 14.3% (12 months) and 25.6% (14 months), respectively. The worst results when using PGLA-coated coils were reported by Niimi et al. (2006); their recanalization rate at 12 months was as high as 57.4%. One explanation for the unsatisfactory result is that they had the lowest primary occlusion rate, only 17.6%, compared with 56.3% in the Katz study. Volumetric occlusion (packing density) seems to be an important factor also with these second-generation coils. The first large, prospective, randomized study comparing PGLA-coated coils with platinum coils is about to begin.

Modifications of the Matrix coil have also been made, in the Cerecyte coil (Micrus Endovascular, San Jose, CA, USA), polyglycolic acid (PGA) is loaded within the coil loops rather than on the surface (Bendszus et al. 2006, Geyik et al. 2008). Further studies are needed to verify the benefits of this coil compared with others.

Hydrogel (acrylic) polymer coating was developed to achieve higher packing densities. Hydrogel is biologically inert, but it expands to provide additional filling of the aneurysm. It can expand up to 11 times its size and does not degrade. These coils (HydroCoil, Microvention Inc., Aliso Viejo, CA, USA) have already been in clinical use (Cloft et al. 2006, 2007a), but the longest follow-up thus far has only been 6 months, and the coils were not simultaneously compared with other coils. Despite the higher packing densities achieved with these expandable coils, the overall recanalization rate was 28.1% at 3-6 months. Surprisingly, with these coils, the recanalization rate did not correlate with the packing density (18% vs. 19% in aneurysms with packing densities >50% vs. <50%) (Cloft et al. 2007a), although the rationale behind the use of HydroCoils was that the increased packing density would reduce recurrences (Cloft et al. 2004).

Experimental coatings on coils, like extracellular matrix proteins, growth factors, and modified cells, have also been developed, but to date have only been

used in experimental animal models (Murayama et al. 1997, 1999, Kallmes et al. 1998b, Raymond et al. 1999, Abrahams et al. 2001) because of concern about excess thrombogenicity and eventual complications (discussed in section entitled: *Coiling of experimental aneurysms*).

2.2.2.5 Other endovascular methods

In addition to coils, stents, and balloons, other endovascular devices have also been used. Liquid embolic materials, which harden when they come into contact with an aqueous solution (like blood), can also be used for the endovascular occlusion of aneurysms, although these are more commonly used for occlusion of AVMs and AVFs. The first such agent (ethylene vinyl alcohol, EVAL) was presented in 1989 for the endovascular occlusion of malformations (Taki et.al. 1990). Today, the most widely used substance is Onyx (ethylene vinyl alcohol copolymer dissolved in dimethyl sulfoxide)(ev3, Plymouth, MN, USA), which was introduced in 1999 also for the treatment of aneurysms (Moret J, Annual Meeting of the American Society of Neuroradiology 2001). In the treatment of aneurysms, Onyx is constrained to the aneurysm with an inflatable balloon at the aneurysm neck. The outer surface of the Onyx cast starts to harden as the interior stays semi-liquid. With further filling, the added material breaks through the surface and makes the cast bigger. Onyx is injected at a very slow rate of 0.1 ml/min, after which the balloon is left inflated for 3 min. The balloon is deflated for 2 min, after which the cycle can be repeated for as many times as required to fill the aneurysm. Once occlusion is complete, a 10-min period is needed for the material to become completely solid. After this, the balloon is filled for the last time, in order to allow detachment of the microcatheter from the Onyx cast by traction.

Molyneux et al. (2004) conducted a prospective multicenter study to investigate the safety and efficacy of Onyx embolization of intracranial aneurysms. Complete or subtotal occlusion was initially seen in 99% of cases; after 3 months, this figure was 89%, and after 12 months 87%. For large (>10 mm) and giant (>25 mm) aneurysms, the figure was 67% at 12 months. The authors concluded that Onyx can provide more durable occlusion in large, giant, and wide-neck aneurysms, than endovascular coiling. For giant aneurysms, the recanalization rate has been 33% if initially completely occluded and 59% if initially incompletely occluded with coils (Murayama et al. 2003a). Drawbacks with Onyx treatment are the technical challenges and the multiple steps involved. Since Onyx is inert and nonadhesive, the results are likely to be highly dependent on initial occlusion rate. Procedure- and device-related permanent morbidity was 8.2% (8/92 patients), and mortality was 2.1% (2/92 patients). Morbidity was due to leakage of Onyx into the blood flow, extravasation of Onyx, and increased mass effect. Of patients, 9.7% (9/92) experienced delayed occlusion of the parent vessel, which was asymptomatic in

5.4% (5/92). Later studies have shown that also with Onyx the recanalization rate of large and giant aneurysms is high, being 36% in ICA aneurysms (Cekirge et al. 2006).

2.2.3 Clipping versus coiling

The first prospective, randomized (Vanninen et al. 1999) study comparing outcomes of early endovascular versus surgical treatment of ruptured aneurysms in 109 patients showed no significant difference in clinical outcome, measured by Glasgow outcome scale (GOS), at 3 or 12 months (Koivisto et al. 2000). Outcome was more dependent on initial Hunt and Hess grade, aneurysm size, and presence of vasospasm or hydrocephalus than on the treatment modality chosen. The treatment-related mortality was 2% in the endovascular group, compared with 4% in the surgical group. However, the angiographic occlusion rate was slightly lower in the endovascular group.

The results of the larger ISAT study (International Subarachnoid Aneurysm Trial), comprising 2143 patients with aneurysmal SAH, randomized between these treatment modalities, were published in 2002 and 2005. According to this multicenter trial, a significantly larger number of patients were dependent or dead at 1 year in the surgical group (30.6%) than in the endovascular group (23.7%) (Molyneux et al. 2002, 2005). However, complete occlusion of aneurysms was seen in 82% of patients in the surgical group, as opposed to only 66% in the endovascular group. Moreover, the risk of rebleeding was higher in the endovascular group than in the surgical group. The authors concluded that if the anatomy of the aneurysm indicates a high likelihood of success by endovascular techniques, the patients should be offered this option. There are, however, some concerns regarding this study, and so far it does not ultimately prove the superiority of endovascular treatment. In ISAT, the majority of patients (7416 / 9559) were excluded from the study; the study population therefore consisted of patients in better condition and with more anterior circulation aneurysms than on average. The majority of the excluded patients were eventually treated surgically. A major part of the participating centers and enrolled patients were from the UK, and thus, national circumstances confounded the results. A large number of centers performing microsurgical clipping with a low annual case flow were included, raising the question about the quality of their performance. Experience and high case flow have been demonstrated to lead to better outcome (Solomon et al. 1996, Cowan et al. 2003). The lower number of individual centers performing endovascular coiling all received a higher number of patients and were quickly gaining more experience. The ISAT study has been criticized as more or less being a comparison of expertise between these treatment modalities in the British healthcare system.

2.3 Experimental aneurysm models

2.3.1. Aneurysm models for the study of cerebral artery aneurysms

It has earlier been believed that the pathobiology of human SCAAs could be elucidated through work in experimental aneurysm models. However, although animal models may mimic some aspects of true aneurysms, such as morphology, hemodynamics, or wall cellular content, they never exhibit all of these characteristics at once. They also do not possess the same activated pathways at the cellular level as human SCAAs. Only in recent years has the complexity of the etiology and evolution of human SCAA really started to be appreciated. SCAAs evolve, degrade, and rupture when the processes weakening the aneurysm wall exceed those strengthening it. Today, the most important objective of experimental animal models has been the testing of endovascular devices for aneurysm occlusion. Coiling should cause thrombosis and fibrosis of the aneurysm and endothelialization of the aneurysm orifice. In order to be able to extrapolate the results to humans, the animal model must resemble human SCAAs as closely as possible.

There have been many attempts to create experimental aneurysm models in animals. The first model was established in 1954 when German and Black tried to elucidate the etiology of human SCAAs by studying the hemodynamics of the aneurysms. They used a venous pouch from the external jugular vein as a graft and constructed five experimental aneurysms in the common carotid arteries of dogs. The aneurysms remained patent for up to 5 months and were suitable for measurement of intra-aneurysmal and intra-arterial pressure and preliminary assessment of the motion of flow inside the aneurysm by cinefluorographic methods. However, they did not perform histological analysis. The venous pouch model has later been modified in many ways and adapted to different species of animals (Table 1). Forrest et al. (1989) introduced a technique in which the left and right common carotid arteries were anastomosed with each other, creating an artificial bifurcation for aneurysm construction. They also tried to relocate the aneurysm segment into the subarachoid space at the cranial vertex, but, unfortunately, these aneurysms did not remain patent (O'Reilly et al. 1981). Experimental intracranial aneurysms were created with a 55% success rate by transplanting venous grafts to the basilar artery (lingual-basilar branch) of dogs by Nishikawa et al. (1977). Macdonald et al. (1998) created a multiple aneurysm model using venous grafts in the carotid arteries of dogs. By anastomosing the cranial parts of the right and left common carotid arteries with each other and anastomosing the caudal end of the right common carotid artery to the caudal side of the newly formed arterial loop, they were able to form a Y-shaped vessel, which then was used as a platform to create both terminal and sidewall aneurysms in the same animal.

Arterial experimental aneurysms have also been created in the carotid arteries of rabbits without the need for an anastomosis, by ligating either the common carotid or the external carotid artery and infusing it with elastase (digestive enzyme) in order to destroy the internal elastic lamina and weaken the wall (Cawley et al. 1996, Altes et al. 2000, Hoh et al. 2004). A combination of intraluminal elastase and collagenase digestion has also been used (Yang et al. 2007), as has topical administration of elastase on the adventitial surface of the vessel (Miskolczi et al. 1998). Although these aneurysms remain patent for a longer time than the venous pouch aneurysms and due to their thin-walled nature are even susceptible to rupture, they have the least pathobiological resemblance to real SCAAs.

In humans, most aneurysms arise at arterial bifurcations, but some are pure sidewall aneurysms (e.g. Pcom and ICA aneurysms). Vascular pressure and sheer stress are different in bifurcation aneurysms than in sidewall aneurysms. The animal model should mimic the hemodynamic conditions of human SCAAs, and they have been produced in both ways.

Large animals, like dogs, sheep, and pigs, are much more expensive than rabbits, rats, or mice. The vasculature of the smallest animals (mice) is, however, not suited for the use of standard endovascular devices. Hence, mice can and should be used only in histopathological studies (Frösen, Marjamaa 2006a)

2.3.2 Other aneurysm models

The necessity of experimental aneurysm models for testing of improved surgical methods, like grafting and wrapping, has also arisen in the field of aortic aneurysm surgery. Experimental aneurysms have been produced by injecting nitrogen mustard into the adventitia of the thoracic aorta in dogs (McCune et al. 1953). This necrotizing agent was extremely potent and caused aneurysm formation and rupture within 4-14 days. Later fuciform abdominal aneurysms in rats have been produced more elegantly by elastase perfusion (Anidjar et al. 1990).

2.3.3 Coiling of experimental aneurysms

Coiling has been performed in animal models to evaluate histological changes with platinum coils and to test novel devices.

The first study, focusing on long-term histological changes in coiled experimental aneurysms, was performed in a canine jugular vein pouch model (Mawad et al. 1995). In this study, 10 aneurysms were coiled with various amounts of coils, and total occlusion was achieved in 9 of 10 cases. During the 6-month follow-up recanalization had occurred in 3 cases. However, in all cases, a neointima covering the coils was seen, but there was only a mild inflammatory reaction and small amount of desired thrombus organization.

Reul et al. (1997) compared GDC coils with tungsten coils in a rabbit model. Surprisingly, they found very high rates of incomplete occlusion in both groups (12/17), at 3 and 6 months. The lumen of GDC-coiled aneurysms was open in 6 of 8 cases and thrombus was present between the loops of the coils. In addition, a neointima was found in only one GDC-coiled aneurysm. This is consistent with Tamatani et al. (1997), who showed in an *in vitro* work that there was no endothelial proliferation on the surface of platinum coils.

Byrne et al. (1997) used the swine model to compare GDC and tungsten coils with untreated controls. They achieved a total initial occlusion in 10 of 18 coiled aneurysms. By the end of the 2- to 7-week follow-up, the remaining eight coiled aneurysms and also the five controls were completely occluded. They performed histological analysis at 2, 4, and 7 weeks. The inflammatory response in coiled aneurysms was greater during the first time-point than during later time-points. During later time-points the initial unorganized thrombus was replaced by fibrous tissue in-growth from the margins.

Testing of novel devices started in the mid-1990s, when the surface of GDC coils was coated with extracellular matrix proteins like collagen (Ahuja et al. 1993, Dawson et al. 1996, Szikora et al. 1997). The hypothesis was that these modifications would increase the thrombogenicity of the coil, accelerate fibrosis in the aneurysm and stimulate endothelialization of the aneurysm neck. The coatings were, however, weak and could be easily scraped off during delivery. To overcome this problem Murayama et al. (1997) used a physiochemical surface modification by ion implantation, which made the proteins adhere more tightly to the coil surface. They compared fibronectin-, fibrinogen-, albumin-, laminin-, vitronectin- and collagen-coated coils and found that all these coatings improved cellular adhesion and proliferation, with fibrinogen being the most thrombogenic. GDC coils have also been coated with growth factors and fibroblasts (Abrahams et al. 2001, Kallmes et al. 1998a). Furthermore, sponges impregnated with growth factors have been used to pack experimental swine aneurysms (Venne et al. 1999). Sponges with fibrinogen, vascular smooth muscle cells, and peripheral blood mononuclear cells were also used in jugular vein aneurysms in dogs (Raymond et al. 1999). All of these studies showed improved results in thrombus organization, neck endothelialization, and tissue integration into the aneurysm. However, none of these devices have been approved for clinical practice because of concern about excessive thrombosis and thromboembolic complications. Protein and especially cellular coatings are stripped when the device is passed through a microcatheter, both reducing the effects of treatment and increasing the risk of complications.

The next step has been the use of bioabsorbable polymeric materials such as PGA (polyglycolic acid) and PLA (polylactic acid) (Murayama et al. 2001). These materials are widely used in the field of tissue engineering and serve as scaffolds on which cells can grow and reconstitute tissues (Langer et al. 1993). The rationale is

that the polymer should permit cellular adhesion and growth and be reabsorbed after it has served its purpose to avoid chronic inflammation. Depending on the composition of the polymer, the absorption rate and the strength of the inflammatory reaction can be varied (Murayama et al. 2002). As a result, the Matrix coil coated with 90% PGA and 10% PLA was developed. The Matrix coil is absorbed slowly and elicits a moderate tissue reaction (inflammation).

These experimental devices were tested in jugular vein graft aneurysms in swine and elastase-induced carotid artery aneurysms in rabbits before clinical use. In the swine jugular vein model, the aneurysms were followed up by DSA for 14 days to 6 months and analyzed histologically at the end. During follow-up the tissue layer covering the neck was found to be thicker in the PGLA group and the aneurysms showed a more extensive area of thrombus organization and larger amount of inflammatory cell infiltration on day 14. In the rabbit carotid artery model, similar, strong inflammatory reactions around the PGLA-coated coils were found at 6 and 10 weeks, and neck tissue deposition in all PGLA-coiled aneurysms was present at 2 weeks. All of these changes were considered to be beneficial.

2.3.4 Rupture of experimental aneurysms

Standardizing the risk of rupture in experimental animal models has been impossible. The use of digestive enzymes (elastase, collagenase) or necrotizing agents severely weakens the vessel wall, causing a risk of rupture otherwise very seldom seen in experimental aneurysms. However, the variance in the time of rupture is very large even within the same study. Yang and collaborators (2007) observed the rupture of the first aneurysm within 24 h, while another ruptured 4 weeks after construction. It is not possible to mimic the natural fate and rupture rate of human cerebral aneurysms, and these models reflect real SCAA poorly. Moreover, this kind of heavy digestion is not seen in human SCAAs.

Table 1. Experimental aneurysm models.

Author	Animal	Aneurysm location	Technique	Endovascular coiling possible
German, Black N Eng J Med 1954	Dog	Common carotid artery Sidewall	External jugular vein pouch surgically anastomosed, V-incision	Angiography performed
Nishikawa M Surg Neurol 1976	Rat	Common carotid artery Bifurcation	Vein patch graft surgically sutured to artery	No
Nishikawa M Surg Neurol 1977	Dog	Basilar artery Sidewall and bifurcation	Vein graft surgically sutured to artery	Possible
Kerber CV Invest Radiol 1977	Dog	Common carotid artery Sidewall	External jugular vein pouch surgically anastomosed, I-incision	Angiography performed
Stehbens WE Surg Gyn Obst 1979	Sheep	Common carotid artery Sidewall	Modification of German et. al. in sheep	No
Stehbens WE Stroke 1981	Rabbit	Aortic bifurcation	External jugular vein pouch surgically anastomosed	No
Young PH Microsurgery 1987	Rat	Carotid artery Sidewall	Vein pouch sutured in variety of ways	No
Forrest, O'Reilly AJNR 1989	Rabbit	Common carotid artery Bifurcation	External jugular vein pouch surgically anastomosed in artificial bifurcation	Angiography performed. Intravascular laser attempted
Anidjar Circulation 1990	Rat	Abdominal Aorta Fuciform	Elastase perfusion	No
Graves AJNR 1993	Dog	Common carotid artery Terminal	External jugular vein pouch surgically anastomosed to artificial arterial arch made from right and left carotid	Embolization with GDC performed
Guglielmi Neuroradiology 1994	Swine	Common carotid artery Sidewall	Modification of German et. al. Arteriotomy made through fundus of vein graft	Endovascular approach possible
Massoud AJNR 1994	Swine	Bifurcation and terminal	External jugular vein pouch sutured in five different ways to carotid artery or ascending cervical artery	Not attempted
Tenjin Stroke 1995	Monkey	Carotid artery Sidewall	Femoral vein pouch surgically sutured to artery	Embolization with GDC performed
Cawley AJNR 1996	Rabbit	External carotid artery Bifurcation	Elastase perfusion of carotid stump trough femoral catheterization	
Spetzger J Neurosurg 1996	Rabbit	Common carotid artery Bifurcation	External jugular vein pouch surgically anastomosed in artificial bifurcation	Embolization with GDC and MDC performed.
Macdonald Stroke 1998	Dog	Common carotid artery Terminal and sidewall	Modification of Graves et. al. Includes sidewall aneurysms	Embolization with GDC and CAP performed
Miskolczi Neurosurgery 1998	Rabbit	Common carotid artery Superior thyroid artery origin Bifurcation	External application of elastase to artery wall	No

Altes AJR 2000	Rabbit	Common carotid artery Terminal	Modification of Cawley et. al. Retrograde catheterization of common carotid. Temporary proximal control with balloon	Yes
Hoh Acta Neurochirurgica 2004	Rabbit	Common carotid artery Terminal	Modification of Altes et. al. Temporary proximal ligation with microclip	Angiography performed
Frösen Marjamaa Neurosurgery 2006	Rat, Mouse	Abdominal Aorta Sidewall	Arterial graft surgically anastomosed	Embolization with GDC performed
Yang Jzus B 2007	Rabbit	Common carotid artery Terminal	Modification of Graves et. al. Arterial graft from carotid artery incubated in elastase	

GDC Guglielmi Detachable Coil

MDC Mechanically Detachable Coil

CAP Cellulose Acetate Polymer

2.4 Vascular imaging

In clinical practice, SAH or an intracerebral hematoma can be reliably diagnosed with computed tomography (CT) (van der Wee et al. 1995), but to visualize the vascular lesion itself (aneurysm, AVM, AVF), angiographic methods are needed. The gold standard for vascular imaging is digital subtraction angiography (DSA), but it is being gradually replaced by noninvasive alternatives such as magnetic resonance angiography (MRA) and computed tomography angiography (CTA).

2.4.1 Computed tomography angiography (CTA)

Since CTA is fast and readily available, it is often the first examination performed when a vascular lesion is suspected. The sensitivity to detect aneurysms >3 mm is very good (96%), but sensitivity decreases considerably when aneurysm size is ≤3 mm (61%) (White et al. 2000). With newer multislice helical CT scanners, the image resolution has improved (Kato et al. 2002), and even aneurysms as small as 2 mm can be detected with 99% sensitivity and 99% specificity (Kangasniemi et al. 2004). However, CTA cannot be used for follow-up of aneurysms treated with platinum coils because of the amount of artifact created by the coils. The follow-up of coiled aneurysms can only be performed with DSA or MRA, and these methods will be discussed and reviewed further in the following sections. In clinical use, CTA´s capability of showing small perforators or flow dynamics (e.g. in PCom) is limited.

2.4.2 Digital subtraction angiography (DSA)

DSA of cerebral vessels is usually performed through a femoral puncture. The catheter is advanced via the aorta to the carotid or vertebral arteries. Multiplane or rotational x-ray images are acquired after injection of contrast media. The pre-contrast image, including soft tissue and bony structures, is “subtracted” from the subsequent images, giving the final images, also in 3D, in which only blood vessels are apparent. Frequently repeated images add a dynamic component to the examination; this is important when assessing flow inside an aneurysm, arterial filling in cases with suspected embolism, or early venous filling associated with AVMs. If a vascular lesion is detected during the DSA imaging session, immediate endovascular treatment can be provided. Because DSA is invasive, it is associated with non-negligible morbidity and mortality, mainly due to thromboembolism, vessel spasm, or vessel dissection. Permanent neurological complications are reported to vary from 0.1% to 0.5%, and transient neurological complications are four times as common (0.4-2.6%) (Earnest et al. 1984, Dion et al. 1987, Grzyska, et al. 1990, Heiserman et al. 1994; Willinsky et al. 2003). Notably, one smaller study with high-risk patients

(carotid stenosis, previous transient ischemic attacks) reported transient neurological complications in 12.2% and permanent complications in 5.2% of patients (Faught et al. 1979). Other complications are also encountered (Leffers et al. 2000), such as hematomas at the puncture site, renal failure due to use of iodine-based contrast agents, or allergic reactions to the contrast agent. Other drawbacks are that it is time-consuming, which is not desirable for an unstable patient and might even necessitate general anesthesia. The radiation dose to the patient is highly dependent on the complexity of the procedure (angiography vs. endovascular treatment), but the average effective dose for a four-vessel angiogram (3.6 mSv) (Marshall et al. 1995) falls within the range of a multislice CTA exam (2.2 and 4.3 mSv for 4- and 64-slice CTAs respectively) (Klingebiel et al. 2008). Both CTA and DSA require the use of iodine-based contrast agents. DSA can be performed with smaller amounts of contrast agent and might be used even for patents with mild renal failure.

2.4.3 Magnetic resonance imaging (MRI)

The MRI technology was created by Paul Lauterbur and Peter Mansfield in the 1970s and the first study on a human subject was performed in 1977. The creators were awarded the Nobel Prize for Medicine in 2003. MRI enables detailed images of the body to be acquired without harmful radiation. The contrast between different soft tissues is also superior to CT, making MRI suitable for depicting anatomy. MRI is therefore often used for imaging of the nervous system and musculoskeletal system. MRI is also well-suited for detecting pathologies like tumors. MRI is generally safe, but the strong magnetic field interacts with metallic objects. It is contraindicated for the patient to have metal implants or implanted electrical devices e.g. cardiac pacemakers. The relatively long imaging time requires compliance from the patient, as in the case of DSA.

2.4.3.1 Principles of MRI

When a subject is placed into the magnet, it exerts a magnetic field of its own, which is parallel to the external magnetic field (longitudinal). This field is a result of the alignment of protons, in other words hydrogen nuclei (^{1}H), which are found in water-rich tissues. When a radio frequency pulse (RF pulse) is sent into the subject, it excites the protons and causes a decrease in the longitudinal magnetization and appearance of a transversal magnetization. The transversal magnetization is a result of the synchronization of the precession of the protons, which are put into ”phase” by the RF pulse. The newly developed transversal magnetization precesses and causes a magnetic resonance (MR) signal, that can be detected. When the RF pulse is switched off, the system goes back to its original state, the longitudinal

magnetization increases (= T1 relaxation) and the transversal magnetization decreases (= T2 relaxation). In a spin-echo pulse sequence, the normal 90° RF pulse is followed by a 180° refocusing pulse at TE/2. When this refocusing pulse is applied, the sign of the phase is reversed. Therefore, the precessing protons begin to rephase again and phase coherence is re-established at TE. Different tissues have a different ratio of free to bound hydrogen nuclei, and therefore, different T1 and T2 relaxation times. For water, both T1 and T2 are long, whereas for fat, they are short.

The contrast in MRI is affected by intrinsic (tissue-dependent) and extrinsic (user-selectable) factors. The intrinsic factors include the relaxation times (T1, T2, T2*), proton density and flow characteristics. Important extrinsic factors are repetition time (TR), echo time (TE), pulse angle (PA), sequence type, number of averages and coil type. TR is the time between two RF pulses in a pulse sequence. TE is the time from the RF pulse to the maximum intensity of spin-echo. TE less than 30 ms is considered short and TE longer than 80 ms is considered long. With short TR and short TE the image is T1-weighted, whereas with long TR and long TE the image is T2-weighted. The image is proton density-weighted when TR is long and TE is short. With short TE, the difference in T2 relaxation time does not influence contrast much. With long TE, the total signal intensity becomes smaller, the signal-to-noise ratio (SNR) becomes weaker, and the image becomes grainy. The spatial information in the image is due to the slice-, phase-, and frequency encoding gradients .

In MRI, contrast can be enhanced by the use of gadolinium contrast agent. gadolinium acts by shortening the T1 and T2 relaxation in the tissue that it penetrates.

2.4.3.2 Magnetic resonance angiography

Magnetic resonance angiograms can be acquired either without the use of a contrast agent (flow-dependent techniques and fresh blood imaging) or with the use of intravenously injected gadolinium (contrast-enhanced MRA). In flow-dependent techniques (time-of-flight [TOF] and phase contrast angiography) advantage is taken of the fact that blood flows through the vessels during the acquisition. Both flow-dependent techniques are based on gradient-recalled echo sequences. These techniques were originally created at the end of the 1980s (Laub et al. 1988, Dumoulin et al. 1989a, b). In the more recently developed fresh blood imaging (FBI) technique (Miyazaki et al. 2000), simultaneous ECG monitoring is used to acquire diastolic bright-blood images, systolic black-blood images and a subtraction image showing only the arteries.

TOF-MRA images are T1-weighted and blood should appear as hypo-intense, but because of the flow through the imaging volume, blood does not have time to become excited to the full extent, therefore appearing as hyper-intense. As

long as the TE values are kept relatively low, the signal intensity from the stationary background tissue will be very low, but the signal from fresh inflowing blood will be high and appear bright on the image. In a 3D imaging slab, the flow-related enhancement is highest near the inflow surface, but the signal gradually decreases (in more distal vessels) as the magnetized blood becomes saturated. The potential pitfalls in TOF-MRA, are related to the fact that wherever blood flow is slow, the spins (protons) in blood will become saturated along with the background tissue, and there will be no contrast. This is a problem when trying to visualize venous structures and sometimes also results in a signal-void within large aneurysms and is the reason why optimization of imaging protocols needs to be done. Fat suppression and magnetization transfer can be used for additional suppression of fat- and protein-containing background tissues.

Phase contrast angiography is more time-consuming than TOF-MRA. Phase contrast exploits the transverse magnetization dephasing of the moving spins which are subjected to a magnetic field gradient. In conventional sequences, the phase is only related to the spatial information. By the use of an additional bipolar RF pulse, the moving blood acquires a flow-induced phase. A second flow-compensated acquisition without the bipolar pulse is needed to complete the sequence. The final image, a subtraction of these two, has a very good suppression of the background and shows the vascular structures well. Phase contrast angiography enables the measurement of flow velocity and the detection of flow direction. However, image quality is dependent on the velocity-encoding coefficient (VENC [cm/s]), which the user needs to predetermine to a value near the real value. This might be difficult in situations with nonphysiological flow, e.g. in an aneurysm (Willinsky et al. 2003).

Contrast-enhanced MRA (CE-MRA) (Prince et al. 1993) gives a more accurate anatomical image of the vessels and possible aneurysms than flow-dependent techniques. The contrast agent is injected intravenously, and the image is acquired after a certain time. The determination of the time interval is the limitation of this technique.

Fresh blood imaging (FBI) is done with a 3D ultrafast spin-echo sequence with a half Fourier plane and requires prospective cardiac triggering, but is performed without any contrast agent. In FBI, the background is suppressed with an inversion pulse. The imaging volume needs to be parallel to the vessel.

The use of different MRA methods is justified since the information gathered may be complementary, and some methods are also better suited for venous imaging (Willinsky et al. 2003).

The latest development in the imaging of vascular pathologies is the use of USPIOs (Ultrasmall Superparamagnetic Particles of Iron Oxide) as a contrast agent in order to detect inflammatory cell infiltration in the arterial wall (Trivedi et al. 2006). USPIOs are taken up by macrophages present in, for example, atherosclerotic

plaques, and the iron component in these particles causes a susceptibility artifact that can be detected with MRI.

2.4.3.3 Clinical use of MRA in the imaging of SCAAs

A meta-analysis by White et al. (2000) showed almost a decade ago that MRA is equally sensitive to CTA in visualizing aneurysms > 3 mm (94% vs. 96%). However, aneurysms < 3 mm were visualized only in 38% of cases with MRA, compared with 61% with CTA. More recent studies have shown that the sensitivity is better when using MR scanners with higher field strength (3 Tesla) and closer to CTA (aneurysms < 3 mm MRA 67% vs. CTA 58%) (Hiratsuka et al. 2008).

The suitability of MRA (especially TOF-MRA) for the pre- and post-procedural evaluation of coiled aneurysms has been evaluated (Deutschmann et al. 2007). Using a 1.5 T scanner, Deutschmann et al. (2007) observed residual necks with a 94% sensitivity in cases where the aneurysm was > 3 mm, but only in 63.6% of cases where aneurysms were < 3 mm. They used both TOF-MRA and CE-MRA and found no difference between these techniques. Earlier studies did not correlate aneurysm size with the diagnostic accuracy of recanalization, but the overall sensitivity (72-97%) and specificity (91-100%) were within the same range (Kähärä et al. 1999, Anzalone et al. 2000, Boulin et al. 2001). In conclusion, TOF-MRA is especially suitable for follow-up of coiled aneurysms in cases with good initial correlation to DSA (Anzalone et al. 2000). Later, with the introduction of 3T scanners, reports have demonstrated that TOF-MRA is as suitable for follow-up as DSA (Ferré et al. 2008). CTA is not suited for this purpose because it is susceptible to artifacts created by the coils. However, the artifact from aneurysm clips is less obvious in CTA than in MRA.

3. Aims of the study

1. To optimize MRA imaging of the cerebral arteries and aorta of mice and to scan collagen 1a1-deficient mice for spontaneous aneurysms.

2. To develop an experimental aneurysm model in rats, characterize its histological features during a long-term follow-up, and evaluate its suitability for the testing of endovascular devices.

3. To optimize a MR imaging protocol for the follow-up of coiled rat aneurysms, including a high-resolution TOF MRA sequence for volumetric measurement of neck remnants.

4. To compare bare platinum GDC coils with PGLA-coated coils in the experimental rat aneurysm model.

4. Materials and methods

4.1 Study design

Study I

Mice with collagen I deficiency (Col-IntΔ) are prone to develop vascular defects. Collagen type I and III represent 80-90% of the total arterial wall collagen and are responsible for its tensile strength. Due to bleeding into the thoracic cavity, 54% of Col-IntΔ mice die before the age of 18 months. We optimized the protocol for imaging the entire aorta and the cerebral arteries of mice using spin-echo, pulse-echo and TOF-MRA sequences. Our aim was to determine whether Col-IntΔ mice develop detectable aneurysms in their aorta or other vessels, including the cerebral arteries, before they die. Moreover, we wanted to evaluate, whether this genetic mouse model helps to elucidate the hemodynamic conditions and pathobiological mechanisms involved in the formation of aneurysms and whether it can be used for the development of therapeutic methods.

Study II

Our goal was to develop an experimental aneurysm model in rats, that would be suitable for endovascular coiling. We characterized the histology of the aneurysm model and evaluated its long-term patency (Study II and unpublished data). Moreover, by adapting the aneurysm model to transgenic mice, we evaluated the contribution of bone marrow-derived progenitor cells in the formation of the neointima and the effect of atherosclerosis (discussed further in the thesis of J Frösen (2006c)).

Study III

Our goal was to develop a reliable MR imaging protocol for the follow-up of coiled experimental aneurysms in rats. We quantified the volume of the aneurysm neck remnants with 3D TOF-MRA. To enable the volumetric analysis, we had to reach a voxel size of < 150 µm. We performed optimization of the MR-imaging protocol along with the novel 3D TOF-MRA sequence in a simulation-based manner.

Study IV

The experimental rat aneurysm model was used to compare the efficacy of platinum and polyglycolic-polylactic acid-coated (PGLA) coils in aneurysms with initially deliberate incomplete occlusion. During a 4-week follow-up animals were noninvasively imaged six times with the optimized MRI protocol. We performed volumetric analysis of the neck remnants during the follow-up and analyzed the aneurysms histologically at the end.

4.2 Experimental animals and surgical procedures

4.2.1 Mice

In study I, collagen deficient (Col-IntΔ) mice were homozygous for a 1283 bp deletion in the 1462-bp-long first intron, of the *Col1a1* gene encoding the procollagen α1 chain of collagen type I. A silent mutation, which created a new X*ho*I site, was introduced in the *Col1a1* gene to assist in the detection of the mutant allele in genomic DNA. The mice were genotyped by polymerase chain reaction amplification and restriction digestion of DNA. A group of 5 homozygous Δ/Δ mice and 5 age- and weight-matched control +/+ mice were examined at the age of 16 months.

4.2.2 Rats

To create experimental aneurysms suitable for endovascular coiling, we used male Wistar rats (Harlan, Horst, Netherlands), weighing 300-450 g at the time of the aneurysm construction and coiling procedures (Studies II-IV). The procedures were approved by the Committee for Animal Welfare at the University of Helsinki, Finland.

4.2.3 Aneurysm construction and endovascular coiling

Aneurysms were constructed into the abdominal aorta of rats by transplanting an arterial graft from the descending thoracic aorta of sacrificed donor animals (Figure 3). First, the infrarenal part of the abdominal aorta of the recipient was exposed and room for vascular clamps was made. The donor animal was given an overdose of anesthetics, after which a bilateral thoracoabdominal incision was made. The descending thoracic aorta was exposed, the left subclavian artery identified, and a loose ligature was placed 5 mm distal to it. In this model, the length and aspect-ratio of the aneurysm can be varied (w x l = 2-3 x 3-6 mm) depending on the site of the ligature. The graft was removed and transplanted to the side of the abdominal aorta of the recipient. The graft walls were carefully aligned with the orifice of the arteriotomy. The anastomosis was made by using continuous 10-0 nylon sutures. After opening the vascular clamps, pulsation in the aneurysm and flow in the aorta were verified. A digital video camera (Sony Exwave® HAD SSC-DC58AP, Japan) attached to the stereomicroscope was used to document the final result at magnifications of 6-40x. Eighty-one aneurysms were constructed when setting up the model; their histology and patency, during follow-up, were confirmed. Six aneurysms were constructed in order to set up the coiling model (Study II + unpublished data). In study III 10 rats were used and in Study IV 40 rats. The

procedure in mice was identical (n=55), but the graft was smaller (1-1.5 x 2.5-3 mm), and it was sutured with interrupted 11-0 nylon sutures (Study II).

In Study IV the aneurysm grafts were coiled prior to their removal from the donor animal. A cannula with the catheter, including the coil, was inserted into the upper abdominal aorta in a retrograde manner. The aorta was flushed free from blood with heparinized saline, after which coiling was performed under visual inspection to ensure that the coils always align in the same way. The coils were detached by electolysis. Each aneurysm was coiled with either one PGLA-coated coil (Matrix® coil, SR-2mm x 2cm; Boston Scientific Corporation, CA, USA) or one platinum coil (GDC® coil, SR-2mm x 2cm; Boston Scientific Corporation, CA, USA). When the ligature around the fundus was tightened, it also grasped the end of the coil, ensuring that the coils did not protrude into the parent artery. We deliberately left a 1.5-mm-long neck remnant in each aneurysm because we wanted to compare the effect of the coils in a situation with an incomplete primary result. An effective coil should stimulate gradual occlusion even in a situation like this. Moreover, with an initial neck remnant, we were able to detect cases in which improper suturing of the anastomosis resulted in thrombosis at the site of the suture line. Whereas a gradual occlusion stimulated by the coils should begin at the interface between the coil mass and the blood.

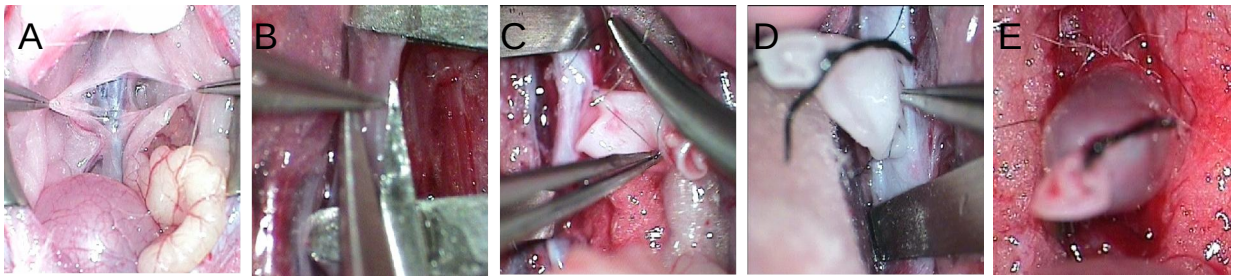

Figure 3:
Construction of experimental aneurysm into the abdominal aorta of a rat. Exposure of the aorta (A), arteriotomy (B), suturing of the graft (C), finished anastomosis (D) and pulsating aneurysm after removal of the vascular clamps (E).

4.2.4 Anesthesia

Anesthesia was used for both the surgical procedures and for the MR-imaging. During the anesthesia the animals were breathing spontaneously.

Mice were anesthetized with Hypnorm® (1.2 ml/kg; a mixture of fentanyl citrate 0.315 mg/ml and fluanisone 10 mg/ml, s.c.; Janssen Pharmaceutica Ltd., Beerse, Belgium) and Dormicum® (15 mg/kg; midazolamhydrochloride 5 mg/ml, i.p.; Roche, Basel, Switzerland).

Rats were anesthetized by using Domitor® (0.5 mg/kg; medetomidine 1 mg/ml, s.c.; Orion Pharma, Espoo, Finland) and Ketalar® (75 mg/kg; ketamine 50 mg/ml, i.p.; Pfizer, New York, NY,USA). Animals were allowed to wake up on their own in a warmed incubator and were given Temgesic® (5 mg/100g for mice and 0.3 mg/kg for rats; buprenorfin 0.3 mg/ml, s.c.; Schering-Plough, Kenilworth, NJ, USA) for postoperative pain.

4.3 Animal MRI

MRI was performed with a 4.7 T MR scanner (PharmaScan, Bruker®, Ettlingen, Germany) for experimental animals. The anesthetized animals were positioned headfirst and prone in the scanner within the linear Bruker receive-only birdcage radio frequency coil (RF coil). RF coils with three different inner diameters were used: 56 mm (for imaging of rat aortas), 38 mm (for mouse aorta), and 23 mm (for mouse cerebral vasculature).

4.3.1 Imaging of mice

In Study I, we performed optimization of the imaging protocol for the mouse aorta and cerebral arteries by systematically varying the imaging parameters (TR, TE, PA). The final protocol was the following:

For the aortic arch, we first obtained images in an axial plane using GEFC (Gradient echo imaging sequence, comprising 1st order flow compensation) sequence with the following parameters: repetition time (TR) 1000 ms; echo time (TE) 4.0 ms; bandwidth (BW) 101.01 kHz; pulse angle (PA) 90°; frequency x phase matrix 256 x 192; field of view (FOV) 3.0 cm and section thickness 1.0 mm (in-plane resolution 117 x 156 µm). Using these axial images for planning, double oblique images in a parallel plane to the aortic arch were obtained using the following pulse sequences: GEFC, RARE (Rapid acquisition with relaxation enhancement), and IR-RARE (RARE with inversion recovery). The imaging parameters for the GEFC images were TR 25.0 ms; TE 6.9 ms; BW 505.051 kHz; PA 30°; frequency x phase matrix 512 x 512; FOV 3.5 cm and section thickness 1.0 mm (in-plane resolution 68 x 68 µm). The imaging parameters for the RARE images were TR 5247 ms; effective TE (TE_{EF}) 20 ms; BW 101.01 kHz; echo train length (ETL) 16; frequency x phase matrix 256 x 256; FOV 3.0 cm and section thickness 1.5 mm (in-plane resolution 117 x 117 µm). The imaging parameters for the IR-RARE images were TR 5000 ms; TE_{EF} 4.2 ms; BW 101.01 kHz; ETL 8; frequency x phase matrix 192 x 192; FOV 3.0 cm and section thickness 1.5 mm (in-plane resolution 156 x 156 µm). An IR delay of 312 ms was used to suppress the surrounding tissues.

For the descending thoracic aorta, GEFC images were obtained in an axial plane with the following parameters: TR 25.0 ms; TE 4.2 ms; BW 101.01 kHz; PA 30°; frequency x phase matrix 256 x 256; FOV 3.5 cm and section thickness 1.0 mm (in-plane resolution 137 x 137 µm). Subsequently, GEFC images were taken in a nearly sagittal plane, perpendicular to the aortic arch, by using the following parameters: TR 25.0 ms; TE 4.2 ms; BW 101.01 kHz; PA 15°; frequency x phase matrix 192 x 192; FOV 3.0 cm and section thickness 1.0 mm (in-plane resolution 156 x 156 µm).

For the upper abdominal aorta behind the liver, GEFC images were taken in a nearly sagittal plane by using the following parameters: TR 25.0 ms; TE 4.2 ms; BW 101.01 kHz; PA 60°; frequency x phase matrix 192 x 192; FOV 3.0 cm and section thickness 1.0 mm (in-plane resolution 156 x 156 µm).

For the abdominal aorta, axial GEFC images ranging from the diaphragm to the iliac bifurcation were taken with the same parameters as for the aortic arch. IR-RARE images in the coronal plane were also taken with the same parameters as for the aortic arch.

The diameter of the aorta was measured from the MR images of all the obtained sequences at specific anatomic locations, e.g. aortic root.

For three-dimensional cerebral artery angiograms, time-of-flight (TOF) pulse sequence with magnetization transfer (MT) was used with the following parameters: TR 41.0 ms; TE 4.0 ms; BW 101.01 kHz; frequency x phase matrix 192 x 192 x 96; FOV 1.4 x 1.4 x 0.9 mm (spatial resolution 73 x 73 x 94 µm). MT parameters were: amplitude 5.9 µT; offset irradiation 2500 Hz and pulse length 25 ms. The angiograms were reconstructed with maximum intensity projections (MIPs). Both reconstructed images and raw data were used for evaluation.

4.3.2 Imaging of rats

In Study III we, determined the optimal protocol for the imaging of coiled (and noncoiled) rat aneurysms, which was later used in Study IV. Optimization of the TOF-MRA was done in a simulation-based manner by first making a theoretical simulation, and then finding the optimal values for imaging by varying the imaging parameters (TE, TR, PA) within the rational range obtained from the simulation.

The theoretical simulation was based on the T1, T2, and T2* relaxation times measured for the regions of interest (aneurysm, aorta) and for the surrounding tissues (fat, muscle). The simulation revealed the theoretically optimal TR and TE parameters for achieving maximal aneurysm-to-background contrast. The theoretically optimal pulse angle (PA) was calculated by using the Earnst angle equation. Signal intensity was measured from the acquired images in order to

calculate true contrast and the contrast-to-noise ratio (CNR). The theoretical contrast and measured true contrast were compared.

Because of the influence of noise, the image with the highest contrast is not necessarily optimal for the evaluation of anatomical structures (like aneurysm neck remnant). We therefore introduced another parameter, the CNR, to objectively assess the appearance and representativeness of the images. CNR can only be measured from actual images, since noise cannot be simulated. We also rated all images subjectively by two observers on how well the entire aneurysm neck remnant could be visualized.

To be able to measure the volume of the neck remnant with TOF-MRA, we determined that the voxel size should be less than 150 µm. This would result in an average in-plane resolution of 13 x 13 pixels in a neck remnant with an initial length and width of 2 x 2 mm. To achieve this goal, we used a phase x frequency matrix of 256 x 256 and FOV 3.0 x 3.0 cm, giving us a resolution of 117 x 117 µm. During the optimization we used a slice-encoding matrix of 16, which was zero filled to 256. This was done to reduce acquisition time to 8.11 min. Acquisition time was kept constant by increasing or reducing the number of averages (NEX) whenever TR was changed. Later, the acquisition time was changed to 54.36 min and the voxel was made isotropic (117 µm) by changing the matrix to 256 x 256 x 128 and the FOV to 3.0 x 3.0 x 1.5 cm. The shortest possible TE allowed by the imaging software was 6.6 ms for the chosen 256 x 256 matrix. The effects of fat suppression and magnetization transfer (MT), which suppress tissues that contain protein (e.g. muscle tissue), were also evaluated.

Measurement of relaxation times for simulation:

For determination of T_2-relaxation time a multi-spin multi-echo (MSME) sequence, based on CPMG (Carr-Purcell Meiboom-Gill) spin echoes was used. TR 1500 ms; TE 10-160 ms and 16 echoes; number of averages (NEX) 2; phase x frequency matrix 256 x 192; FOV 60 x 60 mm; single slice with slice thickness 2.0 mm; acquisition time 7 min 12 s.

For determination of T_1-relaxation time, a fast spin-echo saturation-recovery sequence was used. TR 101, 282, 503, 787, 1185, 1856 and 5000 ms; TE_{EF} 24 ms; RARE factor 4; NEX 2; phase x frequency matrix 128 x 128; FOV 60 x 60 mm; single slice with slice thickness 2.0 mm; acquisition time 10 min 21 s.

For determination of T_2* relaxation time, a multiple gradient echo sequence (MGE) was used. TR 1500 ms; TE 4.5 – 81.7 ms and 12 echoes; NEX 1, phase x frequency matrix 256 x 192; FOV 60 x 60 mm; single slice with slice thickness 2.0 mm; acquisition time 4 min 48 s.

Theoretical simulation:

It is possible to model moving blood approximately as a tissue having shorter T_1, the T_1 shortening dependent on the velocity of blood flow. This effective T_1, denoted by $T_{1,eff}$, is shorter when blood flow velocity is higher, as more of the imaging volume is refreshed by "unsaturated" spins. With slow flow, $T_{1,eff}$ approaches T_1 of stagnant blood. TOF contrast was simulated using the equation for gradient echo signal as follows:

$$S_{GE} \propto \sin\alpha \cdot \frac{1-e^{-TR/T_1}}{1-\cos\alpha \cdot e^{-TR/T_1}} \cdot e^{-TE/T_2*},$$

where α is the flip angle. The flip angle yielding a maximum signal in a gradient echo sequence for a tissue with relaxation time T_1 is given by the Ernst angle equation:

$$\cos\theta_E = e^{-TR/T_1},$$

where θ_E is the Ernst angle.

In the simulations, signal was normalized with TR to simulate varying TR while keeping imaging time constant (this operation implies continuity of number of excitations). Setting $\alpha = \theta_{E,\text{blood}}$, we have for the normalized gradient echo TOF signal

$$S_{GE} \propto \frac{\sin\theta_{E,blood}}{TR} \cdot \frac{1-e^{-TR/T_1}}{1-\cos\theta_{E,blood} \cdot e^{-TR/T_1}} \cdot e^{-TE/T_2*},$$

where $\theta_{E,blood} = \theta_{E,blood}(TR) = \arccos\left(e^{-TR/T_{1,eff}}\right)$ or the Ernst angle for flowing blood as a function of TR. This equation was used to simulate signal and contrast. The contrast was studied using difference curves calculated by subtracting background signal from blood signal. The effect of noise was omitted in the simulations.

The contrast (C) between two (1 and 2) tissues was calculated as:

$C_1=(S_1-S_2) / S_1$,

where S is measured signal intensity from region of interest (ROI), measured with Paravision 3.0 software (Bruker®, Ettlingen, Germany). The contrasts between the aorta, aneurysm neck remnant, fat tissue, and muscle tissue were calculated separately.

CNR was calculated as:

$CNR = (S_1 - S_A) / \Delta S_A$,

where ΔS_A is the standard deviation from the signal of the aorta. Standard deviation of an area outside the animal could not be measured since it was not included in the field of view (FOV). The standard deviation from a structurally and chemically homogeneous tissue, like the aorta, has earlier been used as an estimate for the noise (Prince et al. 1994).

The final imaging protocol for the rat aneurysm was the following:

Scout images were acquired in three directions, after which axial RARE images were obtained using the following parameters: Time to repetition (TR) 6103.2 ms; TE_{EF} 38.6 ms; ETL 16; BW 100.0 kHz; phase x frequency matrix 256 x 256; FOV 5.0 cm (in-plane resolution 195 x 195 µm) and section thickness 2.0 mm. The aneurysm was identified from these images and the sagittal sections were fitted so that they spanned the entire width of the aneurysm and the abdominal aorta. Using these sagittal images for planning, near-axial images, in the direction of the aneurysm, were obtained. Both sagittal and axial images were acquired using GEFC and RARE sequences. For RARE images, we used the following parameters: TR 6103.2 ms; TE_{EF} 38.6 ms; ETL 16; BW 100.0 kHz; phase x frequency matrix 256 x 256; FOV 3.5 cm (in-plane resolution 137 x 137 µm) and section thickness 2.0 mm. For GEFC images, we used the following parameters: TR 1000 ms; TE 4.0 ms; Pulse angle (PA) 90°; BW 100.0 kHz; phase x frequency matrix 256 x 256; FOV 3.5 cm (in-plane resolution 137 x 137 µm) and section thickness 2.0 mm.

The optimal TOF-MRA had the following parameters: TR 60 ms; TE 6.6 ms; PA 20°; BW 25.0 kHz; phase x frequency x slice matrix 256 x 256 x 128; FOV 3.0 x 3.0 x 1.5 cm (yielding a resolution of 117 x 117 x 117 µm). The optimization procedure for the 3D TOF-MRA is described in the results section.

4.3.3 Analysis of image data

The signal intensity from specific regions of interest was measured with Paravision 3.0 (Bruker, Germany).

Neck remnant volume was measured from the raw data of the 3D TOF-MRA using Image/J public domain software (developed at the U.S. National Institutes of Health and available on the Internet at http://rsb.info.nih.gov/ij/). First, the surrounding tissues were manually cropped. The image was then thresholded using the aortic diameter as a standard size reference, but taking to account its growth

during the follow-up. Groups were compared using independent samples t-test. Changes within a group were compared using Paired t-test.

The presence of dog ears was evaluated from both the 3D TOF-MRA and the GEFC images, which were sensitive to flowing blood. Groups were compared using the Fisher's exact test.

The RARE images were used to verify that the surrounding structures (i.e. the bowels) were not affecting the results.

4.4 Tissue preparation and histological analysis

In Study I, the tissues were perfusion-fixed with 3% phosphate-buffered paraformaldehyde (3% PFA) through cannulated left ventricles at a 140 mm Hg pressure. The aortas and hearts were removed entirely en block to the level of the iliac bifurcation. Brains with cerebral arteries were carefully removed via a craniotomy. Tissues were kept in 3% PFA for 6 h at room temperature and stored in PBS at +4°C until the time of paraffin-embedding. Axial and longitudinal cross-sections (5 µm) of entire aorta and axial cross-sections of brains with cerebral arteries were stained with Masson´s trichrome for detection of fibrillar collagens. For measurements of cerebral artery wall thickness, the internal carotid arteries were identified and serial cross-sections were taken from a location immediately proximal to the origin of the middle cerebral arteries. The area of the medial layer was measured from six separate cross-sections from each animal using a computer-assisted image analysis program (Image/J, U.S. National Institutes of Health). An average for each animal was calculated, and the values were compared between Col-IntΔ and control mice (t-test). The total number of spindle-shaped cells in the medial layer was counted from six separate cross-sections from each animal.

In Study II, the rats were perfusion-fixed through cannulated left ventricles with 3% paraformaldehyde followed by 6 h of incubation in 3% paraformaldehyde and paraffin-embedding. The samples were sectioned along the long axis of the aneurysm at 4-µm intervals and stained with hematoxylin and eosin. Immunohistochemistry was performed after deparaffinization and antigen retrieval in heated citrate buffer (pH 6.0) or heated Tris-ethylenediaminetetraacetic acid (pH 8.0–9.0) buffer. Monoclonal mouse antibodies were used to detect aSMA (clone 1A4, Sigma- Aldrich Co., St. Louis, MO, USA), anti-rat CD68 (clone ED1, Serotec, Oxford, UK), and CD3 (T-cell receptor, clone PC3/188A, Dako, Glostrup, Denmark). Terminal deoxynucleotidyl transferase biotin-dUTP nick end labeling reactions to detect apoptotic cells were performed with an InSituCell Death detection kit (Roche-Diagnostics, Roche, Basel, Switzerland).

In Studies III and IV, the tissues were perfusion-fixed with 10% formalin (phosphate-buffered to pH 7.0) through cannulated left ventricles. Tissue samples

were embedded in paraffin. Primary 1000-µm-thick sections were cut along the long axis of the aneurysm using an Isomet low-speed saw (Buehler, Lake Bluff, IL, USA) cutting through the platinum coils (Dai et al. 2005). After this, the coil loops were carefully removed with forceps. The final 5-µm-thick slices were then cut and stained with hematoxylin and eosin. Inflammatory cell infiltration and scar forming were evaluated. Measurements of neck tissue thickness were not performed since it was impossible to ensure that the histological sections were always taken from the same location.

4.5 Endoscopy

In Studies III and IV, the animals were sacrificed and the aneurysms were harvested immediately after the last imaging session (in Study IV on the 28th day). Before giving a lethal dose of the anesthetics, an inspection was made through laparotomy, to ensure that the aneurysm had not adhered to surrounding structures (i.e. the bowels), and to verify that the aneurysm was pulsating. The posterior wall of the aorta was gently opened with iris scissors, and the lumen of the aneurysm neck was inspected using a Storz (Karl Storz GmbH, Tuttlingen, Germany) endoscope, connected to a digital video camera (Sony Exwave® HAD SSC-DC58AP, Japan). The first aim of the endoscopic examination was to verify that the anastomosis had been made correctly. The second aim was to see whether the lumen of the neck remnant also contained dog ears protruding between the coils and the aneurysm wall. The third aim was to evaluate the transparency of the endothelial-like neointima over the coils. The live image was evaluated by two observers, but also recorded for later viewing. The results from endoscopy were compared with the MR images.

4.6 Statistics

Statistical analysis was performed by using NCSS 2000 (NCSS, Kaysville, UT, USA) statistics software. The level of significance was set at $p < 0.05$. Categorical variables were compared using Fisher's exact two-tailed test or Chi-square test. Continuous variables between groups were compared using the Mann-Whitney U-test or Student's t-test.

5. Results

5.1 Optimization of MRI for the aorta and cerebral arteries of mice

We imaged five Col-IntΔ mice and five age- and weight-matched control mice at the age of 16 months. We were able to obtain high-resolution MR images in three imaging planes (axial, sagittal, coronal) of the entire aorta, including the origin of the ascending aorta, without significant motion artifacts, even without pulse- and breath-triggering. Triggering would have multiplied the total acquisition time for the thoracic aorta, but with adequate fixation of the animals chest to the cradle with adhesive tape, we were able to eliminate thoracic motion during thoracic imaging. Similarly, for abdominal imaging, abdominal motion was eliminated by firm fixation of the lower body. The highest in-plane resolution of 68 x 68 µm was achieved with a GEFC sequence using a 1.0-mm slice thickness in a sagittal imaging plane of the thoracic aorta and an acquisition time of 8.32 min. For RARE and IR-RARE images, the maximum in-plane resolution varied from 117 x 117 to 156 x 156 µm with 1.5-mm slice thicknesses, and the acquisition times varied from 4.11 to 8.30 min. Intraluminal flow was primarily evaluated from the IR-RARE images, the GEFC images were the best to show the aortic root, and the RARE images were the best to show extravascular structures. All of the sequences in the plane of the aortic arch showed less motion artifacts than the GEFC sequences taken sagittally or axially to the descending aorta.

After optimizing 3D TOF-MRA, we achieved a resolution of 73 x 73 x 94 µm, using an acquisition time of 51 min. This was sufficient to visualize the entire circle of Willis and the distal branches of the cerebral arteries up to level of the anterior cerebral arteries (Figure 4). MRI of cerebral arteries was completed with four Col-IntΔ mice, while one mouse died during the acquisition.

To verify the imaging results, we immediately performed microsurgical dissection of the entire aorta, removed the brains through a craniotomy, and processed the tissues histologically.

5.2 Appearance of Col-IntΔ mice aortas and cerebral arteries in MRI and histology

Aortas of all Col-IntΔ mice appeared to be normal in MRI. There were no signs of aortic dilatation or aneurysm formation, and the mean diameter of the aortas measured from MR images at specific levels showed no difference between Col-IntΔ mice and controls (e.g. aortic root measured from GEFC sequence: Col-IntΔ 1.41 ± 0.023 mm vs. control 1.41 ± 0.071 mm; p=0.97). All MR images were also screened for narrowing of the lumen and for signs of previous rupture or aortic dissection,

which would have presumably appeared as a thickening of the aortic wall with laminar organization of hematomas of various ages or a parathoracic or retroperitoneal hematoma. None of these signs were seen in any of the Col-IntΔ or control mice.

Inspection of the aortas and surrounding tissues under a stereomicroscope was concordant with the MR images; no abnormalities suggesting aneurysms, dissections, or previous ruptures were seen, and the external aortic diameters in Col-IntΔ mice were similar to the diameters in control mice. Qualitative analysis from histologic samples showed no microaneurysms or dissections in the aortic wall.

With the resolution achieved, also the cerebral arteries appeared normal and there were no signs of aneurysms. However, histologic analysis revealed that the cerebral artery wall was 22% thinner in Col-IntΔ mice than in controls (p=0.01, t-test), but the numbers of spindle-shaped cells were similar in Col-IntΔ and control mice (p=0.97, t-test), suggesting that the thinning was related to decreased extracellular matrix protein (collagen) content rather than to cellular content (Figure 4).

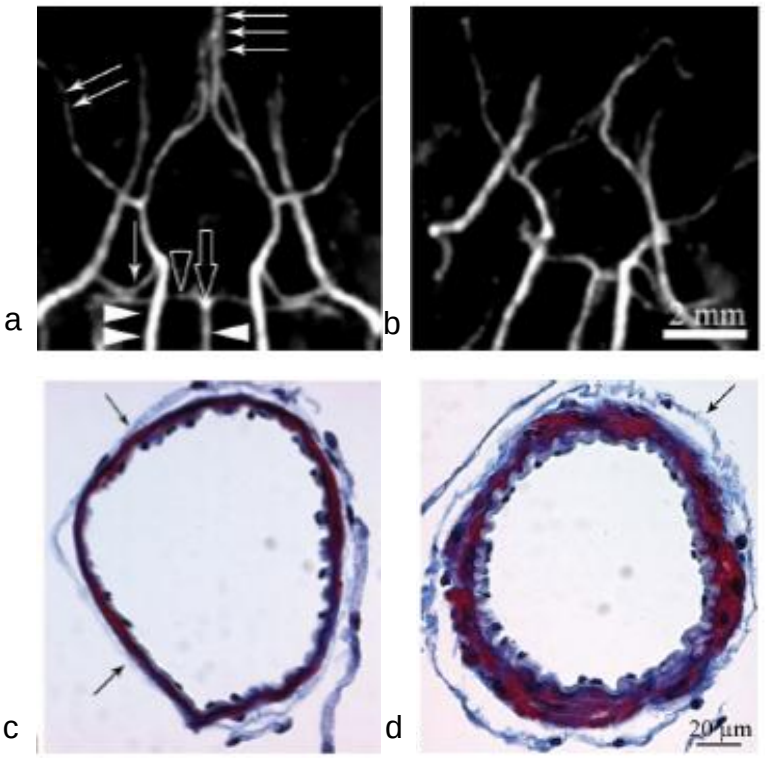

Figure 4:

TOF-MRA reconstruction of the cerebral arteries of Col-IntΔ mice (a,b). Photograph showing histological sections of cerebral arteries of Col-IntΔ (c) and control (d) mice. Cerebral arteries labelled in (a): basilar artery (arrowhead), basilar bifurcation (open arrow), superior cerebellar artery (open arrowhead), internal carotid artery (two arrowheads), posterior cerebral artery (arrow), distal branches of middle cerebral arteries (two arrows), pericallosal branches of anterior cerebral arteries (three arrows). In c and d the arrows point at the adventitial layer.

5.3 Experimental aneurysm model in rats

We established an experimental aneurysm model in rats by transplanting a segment of the descending thoracic aorta of a donor animal into the abdominal aorta of the recipient. The aneurysm model is easy to standardize, the patency of the aneurysms is excellent, and the mortality is low. We constructed a total of 112 experimental aneurysms in rats. Seven procedure-related deaths occurred, of which three happened in aneurysms being simultaneously coiled. The deaths were caused by profuse bleeding (n=3), aortic thrombosis (n=3), and an overdose of anesthetics (n=1). The overall mortality was 6.3% (4.7% for aneurysm construction alone, 11.5% for coiling procedure). All procedure-related deaths occurred within 24 h of the operation, and all in the first 30 operations. The high mortality associated with the coiling procedure (3/26 =11.5%) was due to three fatal cases during the six training operations. Native aneurysms (n=79) were followed up for a median of 6 weeks (range 3 days – 2 years). During this time, two animals died of unknown causes. Primary thrombosis of the aneurysm seen in the MR images on the first day occurred in two cases (2/79 = 2.5%) and early thrombosis seen in the MR images during the first 10 days occurred in four cases (4/79 = 5%). The overall patency of the aneurysms was therefore 92.5%. Three aneurysms enlarged during follow-up, and the rest remained the same size (measured from 2D MR images). In Study IV, all animals (n=20) survived the operation and coiling procedures, but four animals, exhibited primary thrombosis of the aneurysm (4/20 = 20%). As with naive aneurysms, the primary thrombosis was caused by an improperly placed suture or improper alignment of the graft and parent-artery walls, seen in endoscopy. In naive aneurysms, the primary thrombosis could also be caused by applying pressure to a leak from the anastomosis (n=2). The higher rate of primary thrombosis in coiled aneurysms is explained by the suturing being more technically demanding when coiling has been performed. The success rate of 80% can still be considered to be good. The mean procedure time for creating the aneurysm was 41 (range 24-61) min. Coiling prolonged the procedure by 20 (range 16-28) min. The length of the aneurysms in the long-term follow-up was easy to standardize (4.2 ± 0.3 mm). Moreover, the volume of the initial neck remnant in coiled aneurysms did not vary significantly (6.35 ± 1.58 mm^3).

The graft can be transplanted into two locations in the abdominal aorta, either superiorly or inferiorly to the lumbar vein. After the preliminary experiments, we found the superior location (directly distal to the renal arteries) preferable since this location is less susceptible to complications. Complications arise because the adventitia of the aorta and the inferior vena cava are more closely attached to each other, resulting in an easy tearing of the vena cava, causing hemorrhage. Moreover, in the preferred superior location, the aortic diameter is larger and there is usually

only one arterial branch arising from this site. This branch going to the back muscles can be ligated without any complications, and this should be done to avoid retrograde bleeding, which seriously interferes with proper anastomosis suturing. Repeated flushing with heparinized saline is recommended if there are any signs of bleeding from the arteriotomy of the unfinished anastomosis, e.g. because of slippage of the vascular clamps. If there is severe bleeding from the anastomosis after opening the vascular clamps, additional stitches can be applied either with or without temporary clamping of the vessel. If temporary clamping lasts for many minutes (>5 min), the patency of the anastomosis may be jeopardized due to accumulation of a thrombus; opening a part of the anastomosis and rinsing both the recipient artery and the graft with heparinized saline are advised to avoid primary thrombosis.

Coiling was successful on every occasion in Wistar rats weighing more than 350 g. In larger rats, the coiling procedure was easier because of the larger arterial diameter. In rats weighing less than 350 g, it was impossible to fit even the smallest GDC coils (diameter 2 mm) since they would not produce loops.

In Study IV, we created 20 standard-sized aneurysms, half of which were coiled with platinum coils and half with PGLA-coated coils and all of which possessed an approximately 2-mm-long neck remnant at surgery. There was no difference in the procedure time (coiling and suturing of anastomosis) between the two groups (mean: PGLA group 88 min, platinum group 86 min). The aneurysms did not differ in orientation. At the end of the follow-up, no aneurysm had adhered to the bowels. Sixteen animals exhibited a visible neck remnant on day 1, and these were included in the radiological evaluation and followed up. The remaining four animals (PGLA group n=1, platinum group n=3) were in good clinical condition, but exhibited complete initial thrombosis of the neck remnant. Although not included in the radiological evaluation, follow-up imaging of these thrombosed aneurysms was performed, but no recanalization was found. The endoscopic analysis at 4 weeks revealed that the thrombosis was caused by an improperly placed suture (n=2) or improper alignment of the graft and parent-artery walls (n=2). In conclusion, possible thrombosis of the graft caused by improper suturing of the anastomosis should be ruled out, by MRI at the first and seventh day after the procedure. If the aneurysm neck is patent at 1 week, it is reliable to begin follow-up of the interface of the coils and the aneurysm.

We have also conducted preliminary experiments using expandable nitinol stents. The stent causes an artifact inside the lumen of the vessel, but the aneurysm can be adequately evaluated. In the future, the model can be used to test flow-directing or porous stents developed for aneurysm treatment without additional coiling.

5.4 Histological changes in the rat aneurysm model

The histological changes in the murine experimental aneurysm wall were described in detail in Study II and have also been discussed in the thesis of Dr Juhana Frösen (2006c). The saccular aneurysms develop several histological changes that are characteristic of human SCAAs. These include: a) de-endothelialization, b) luminal thrombosis, c) organization of the luminal thrombosis and formation of neointima (myointimal hyperplasia), and d) inflammatory cell infiltration. However changes such as decellularization and degradation, which are found in ruptured human SCAAs do not occur in the murine model.

On day 3 a monolayer of endothelial-like cells (αSMA-negative) lined the luminal surface of the aneurysm fundus. At 3 weeks, a neointima had formed on the luminal side; this layer contained areas of organizing thrombus. At 3 months, the neointima had become thicker and capillaries were found in it in all samples (7/7). Inflammatory cells were seen at all time-points. At 3 days these consisted mostly of macrophages (CD68+) in the media and adventitia. From 3 weeks onwards macrophages were also found in the newly formed neointima, along with T-lymphocytes (CD3+). The neutrophils originally present in the adventitia had disappeared by 3 weeks. Apoptotic cells (TUNEL staining) were found in the media, and at 3 months also in the neointima.

Even though very different pathobiological mechanisms cause the histological changes in the wall of human SCAAs and the wall of the experimental rat aneurysm, there are many similarities in the end result, as described above. This leads us to believe that this model is suitable for studying thrombus formation and inflammatory cell infiltration after endovascular treatment. For histology of coiled aneurysms, see the section entitled: *Occlusion of the neck remnant after treatment with platinum-, or PGLA-coated coils.*

5.5 MRI of rat aneurysms

We were able to follow up the patency of the saccular aortic grafts with 4.7 T MRI. 2D MR images (GEFC and RARE) reliably showed the width, length, and shape of the aneurysm and neck remnant. From these images, it was also possible to detect thrombosis, verify parent artery integrity, and observe relation of the aneurysm to the surrounding structures and in this way exclude adhesion to intestines. The 3D TOF-MRA sequence was optimized for the measurement of neck remnant volume. In the coiled aneurysms, radiological signs of healing (disappearance of dog ears) could be seen with both 2D and 3D sequences.

One complete imaging session lasted 2 h per animal; during this time TOF-MRA was performed and GEFC and RARE images were taken in both axial and sagittal planes. 3D TOF-MRA was the most time-consuming, acquired in 32 min 40 s. The isotropic voxel size was 117 µm in the TOF-MRA. In the other sequences, the in-plane resolution was 137 x 137 µm, and the section thickness 2 mm.

During a total of 271 MRI sessions only one death occurred, yielding a mortality rate of 0.37%. Artifacts interfering with interpretation were seen in less than 1% of all images and the acquisition was repeated in these cases.

5.5.1 Optimization of TOF-MRI for coiled rat aneurysms and concordance with measurements

We successfully performed optimization of TOF-MRA in a simulation-based manner. By first measuring the relaxation times from the regions of interest (aneurysm and aorta) and from the surrounding tissues (intraperitoneal fat and spine musculature), a theoretical simulation was performed that gave maximal signal intensity and contrast between tissues as a function of TR and TE (Figure 5). We then performed imaging by systematically varying the TR and TE within the rational range of values depicted by the simulation. After imaging five animals, we measured signal intensity and calculated contrast and found that the TR and TE giving the highest values were concordant with the simulation (Figure 5).

The theoretically optimal pulse angle (PA) was calculated with the Earnst angle equation. During imaging the PA was varied from 10° to 50° at 10° intervals independently for different TR, TE, and mode of background suppression. The highest contrast was acquired with PA values near the theoretically optimal values. The good correlation between the simulation and the acquired images improves the validity of the following results.

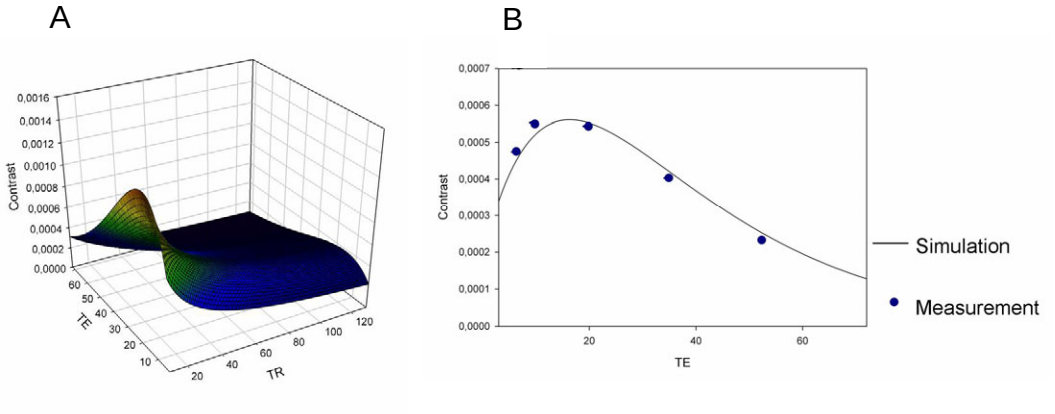

Figure 5:
Results of the simulation showing aneurysm-to-background contrast as a function of TR and TE (A). Figure B shows the agreement between simulation (line) and measurements (dots). In the simulation, aneurysm-to-background contrast is highest at TE 16.3 ms, for any given TR.

5.5.2 Achieving optimal imaging parameters

Effect of echo time (TE)

According to simulation, TE = 15.3 - 16.3 ms gave the highest contrast to background for both aorta and aneurysm at any given TR. We tested TE values ranging from 6.6 to 65 ms and found that contrast of aorta-to-background increases until 20 ms. Aneurysm-to-background contrast is highest at 10 ms. The correlation between simulation and imaging results is good. The center of the aneurysm (from where relaxation time is measured) is visible at all TE values, except 65 ms. However, with TE ≥10 ms, the turbulent and slow flow at the edge of the aneurysm is no longer visible (n=5/5), and the volume measurement is not reliable. The contrast-to-noise ratio from the entire aneurysm (center and edge) is highest at the shortest possible TE (6.6 ms). The optimal TE is therefore considered to be 6.6 ms.

Effect of repetition time (TR)

TR values ranging from 20 to 125 ms were tested, but the use of a TR value shorter than 30 ms required the use of a more robust matrix (128 x 256), which also reduced the resolution. The simulated and obtained aneurysm-to-background contrasts for different TRs differ in that simulation gives the highest contrast for the shortest possible TR, but measurements show that contrast does not increase further for TR values shorter than 30 ms. The CNR is higher for shorter TR. A TR of 30 ms was considered to be the best, but a problem occurred when making the voxel isotropic and the acquisition time longer since our scanner overheated. However, because images with TRs of 30 and 60 ms were both good for interpretation, we continued by using a TR of 60 ms as the longer TR did not cause overheating.

Effect of pulse angle (PA)

With the smallest PA (10°), the signal from the aneurysm is almost equal to the signal from the aorta and the contrast to the background is high. With higher PA, the background becomes suppressed, but also the signal from the aneurysm starts to decay, as the signal from fast-flowing blood in the aorta is intensified, suggesting the use of short PAs. CNR is highest for TR 60 ms at PA 20° and for TR 30 ms at PA 10°. These angels were considered optimal and correlated well to the theoretically optimal PA derived from the Earnst angle equation (19° for TR 60 ms and 14° for TR 30 ms). The changes in contrast and CNR are independent from the effects of TE, fat suppression, and magnetization transfer. Figure 6 shows the change of aneurysm signal for different PA and modes of background suppression.

Effect of background suppression

With the use of fat suppression and magnetization transfer, the signals from the aorta and aneurysm become more intense relative to fat and muscle tissue. However, when using background suppression, there is also a small signal loss from the aneurysm compared with the aorta, at tested PA, TR, and TE. We conclude that the images with suppression are all as valid for interpretation as the images without suppression, but the small loss of signal favors no background suppression. The maximum intensity projections (MIPs) are better with background suppression, but the raw data is used for the volume measurement.

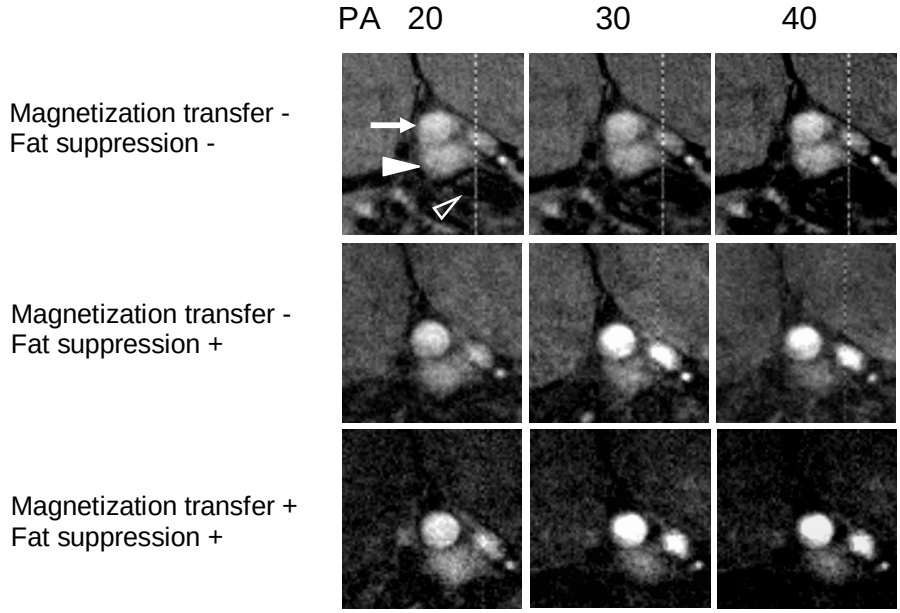

Figure 6:
The use of fat suppression or magnetization transfer results in reduced aneurysm to aorta contrast. This is also seen with increasing PA. Aorta (arrow), Neck (arrowhead), Coil (open arrowhead).

True high-resolution image

The in-plane resolution of 117 x 117 µm was achieved by choosing a phase x frequency matrix of 256 x 256 and a FOV of 3.0 x 3.0 cm. With a more robust matrix, we would not have been able to detect changes in the aneurysm neck sufficiently well. During the optimization we used a slice-encoding matrix of 16, which was zero filled to 256, in order to reduce acquisition time to 8.11 min. After the optimization, we repeated imaging with TR/TE/PA (60/6.6/20) and changed the acquisition time to 54.36 min and made the voxel isotropic (117 µm) by changing the matrix to 256 x 256 x 128 and FOV to 3.0 x 3.0 x 1.5 cm. This resulted in a true high-resolution (117 x 117 x 117 µm) image (Figure 7). The average volume obtained from imaging was 6.28 $\pm$ 1.52 mm^3 (n = 5, mean ± SD). Figure 8 shows how results from histological sections, endoscopy, and MRI correlate with each other.

TR 60 ms was used instead of 30 ms because short TR increased the risk for overheating of the MR scanner, which resulted in the need to abort acquisition. The interpretability of images with TR 60 ms was equal to that with TR 30 ms, despite a slightly lower CNR.

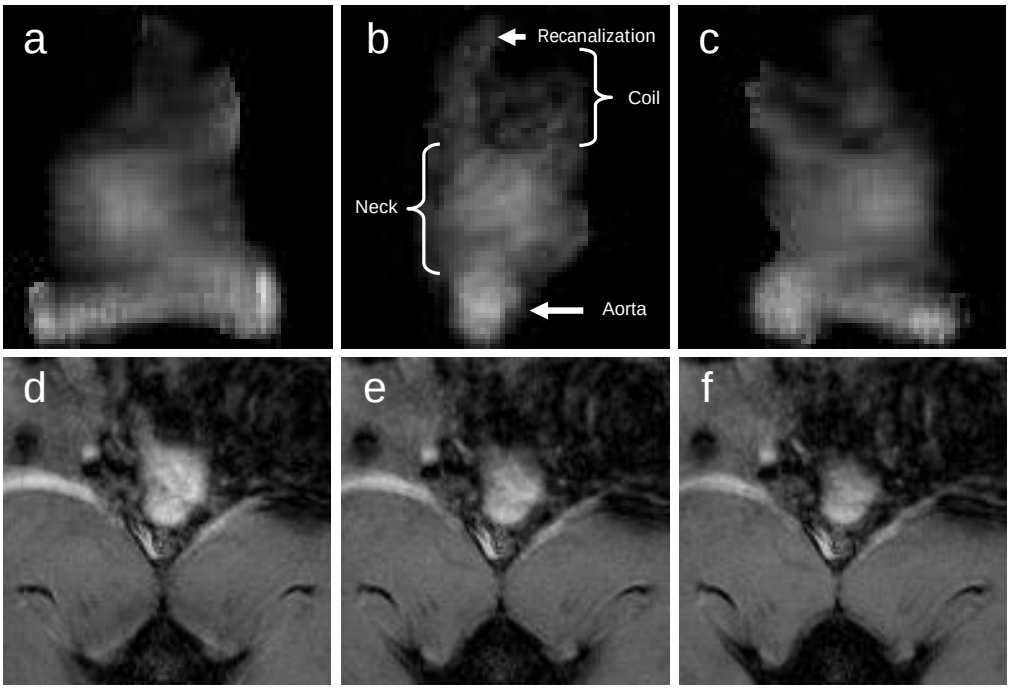

Figure 7:
3D-reformatted TOF MRA images showing in right lateral (a), superior (b), and left lateral (c) view. Raw data of 3D TOF used for volumetry (d-f).

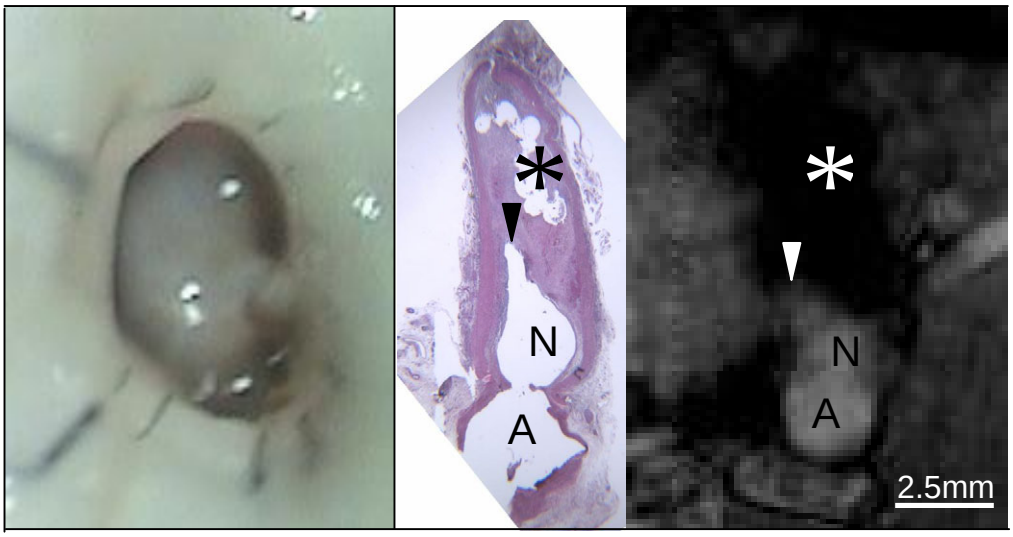

Figure 8:
Correlation between endoscopy, histology (HE-stain) and TOF-MRA immediately prior to harvesting. The morphology of the neck remnant (N) matches the shape seen in histology and endoscopy. A=Aorta, N=Neck remnant, * =Coils, Arrowhead=Open dog ear.

5.6 Occlusion of neck remnant after treatment with platinum or PGLA coated coils

The use of PGLA-coated coils resulted in an improved angiographic outcome, seen as disappearance of dog ears during follow-up (in 2D and 3D images) and a moderate progressive reduction of neck remnant size in volumetric analysis. In the endoscopic evaluation, the PGLA group exhibited a neointima which appeared thicker. Moreover, in histological analysis, thrombus organization and inflammatory cell infiltration were higher with PGLA.

5.6.1 Neck remnant analysis

At the beginning of follow-up, most aneurysms possessed visible dog ears in addition to the larger neck remnant (PGLA group 66.7% (n=6/9), and platinum group 71.4% (n=5/7)). Dog ears were defined as small blood-filled cavities, that protrude between the coil mass and the aneurysm wall in the distal part of the neck remnant. These can be seen with both conventional 2D sequences and 3D TOF-MRA.

Initially, no statistically significant differences in the presence of dog ears between the two groups were seen. However, by day 28, only 11.1% (n=1/9) of the aneurysms with PGLA-coated coils showed remaining dog ears, whereas all dog ears in platinum coiled aneurysms had persisted (n=5/7) (p=0.035) (Figure 9). No false-positive or -negative dog ears were observed when the 3D-TOF angiograms taken on day 28 were compared with the endoscopic images. Thus, the concordance between MRI and endoscopy was considered to be excellent.

5.6.2 MRI volumetry

There was no difference in the initial size of the aneurysm neck remnants between the two groups. Volumetric measurements from the TOF-MRA images of the 16 animals included for evaluation showed that the size (mean ± SD) was 6.84 ± 1.75 mm^3 for the PGLA group and 5.96 ± 1.40 mm^3 for the platinum group. During the first week an increase in the size of the neck remnant was seen in both groups, presumably due to hemodynamic stretching. After the first week, the neck remnant size in the PGLA group started to decrease, whereas in the platinum group it remained steady. By the end of the follow-up, the neck remnants of the PGLA-coiled aneurysms had reduced in size by 12.9 ± 17.4 % (p=0.044), while the neck remnants of the platinum-coiled aneurysms had increased by 6.63 ± 22.4 % (p=0.474). An increase in neck remnant size was observed in only 1/9 aneurysms in the PGLA group, whereas it was seen in 5/7 aneurysms in the platinum group (p=0.035).

5.6.3 Endoscopic analysis

A pale neointima covered the coils in 15/16 aneurysms (94%). Notably, one aneurysm with a platinum coil lacked the neointima completely. In 4/7 aneurysms (57%) in the platinum group, the neointima was translucent, whereas in the PGLA group 7/9 aneurysms (78%) exhibited such a thick neointima that it was impossible to see the coil loops through it. These changes were statistically nonsignificant (p=0.126).

5.6.4 Histological analysis

We found that 4/10 aneurysms in the PGLA group exhibited a dense fibrosis of the fundus and showed high amounts of inflammatory cell infiltration as well as growth of new capillaries. These changes were not seen at all in the platinum group; instead, in 2/10 aneurysms, only immature thrombosis was present. The remaining aneurysms from both groups exhibited intermediate changes consisting of varying amounts of fibrosis interspersed with areas of unorganized thrombosis (p=0.043) (Figure 10).

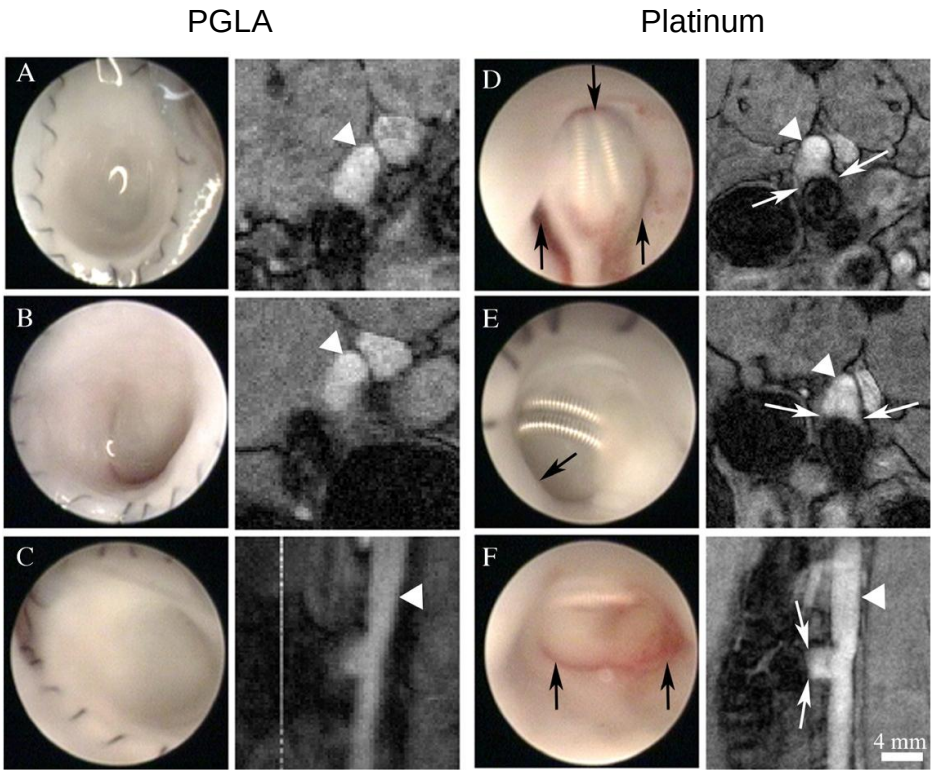

Figure 9:
Correlation between endoscopy and MRI on day 28. Endoscopic photographs and corresponding MR images (GEFC sequence) are shown adjacent to each other. A-C: PGLA-coiled aneurysms, notice smooth dome shape of aneurysm neck. D-F: Platinum coiled aneurysms, notice dog ears (arrows) in MRI and endoscopy. In the platinum coil group, the neointima is translucent, and coils are visible. Arrowhead indicates abdominal aorta.

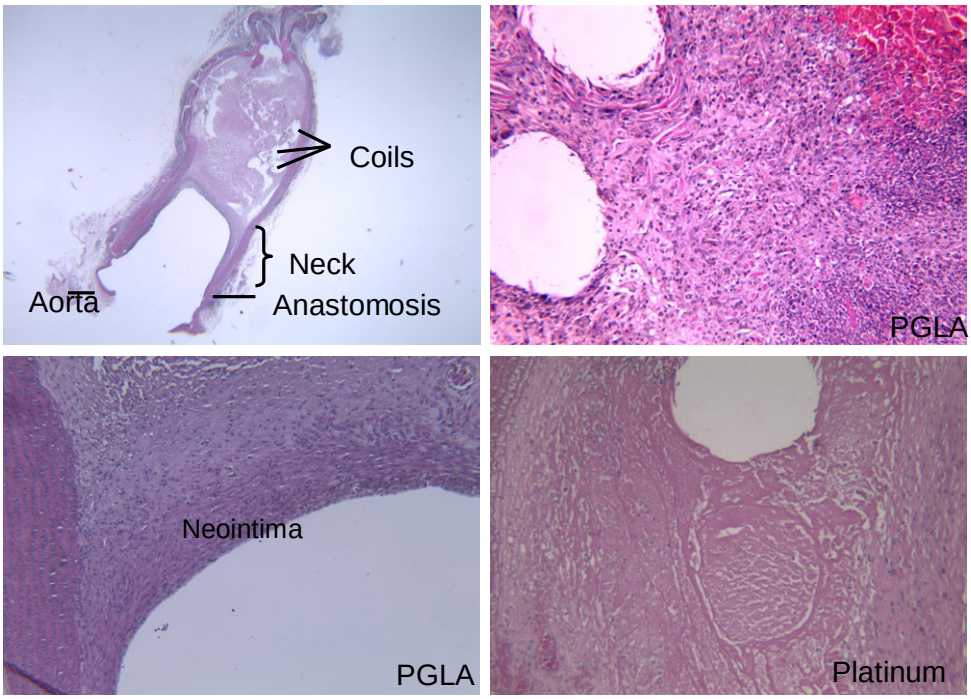

Figure 10:
Histological changes in coiled rat aneurysms. PGLA-coiled aneurysms exhibit higher inflammatory cell infiltration and maturation of thrombus and a neointima. Platinum coil is surrounded with an immature thrombus.

6. Discussion

Our main goals were I) to create a reliable high-resolution MRI protocol for the imaging of mice with genetic deficiencies predisposing to internal hemorrhage or spontaneous formation of aneurysms, II) to develop an experimental aneurysm model in rats, suitable for endovascular treatment, III) to optimize a reliable high-resolution MRI protocol suitable for repetitive follow-up of endovascularly treated aneurysms in rats including an optimized high-resolution TOF-MRA sequence suitable for quantitative volumetric analysis of neck remnants, and IV) to compare the efficacy of platinum coils with second-generation PGLA-coated coils in the rat model.

6.1 MRI of the mouse vasculature

For the purpose of studying the vasculature of mice, we created a high-resolution MRI protocol. The type I collagen-deficient mice (Col-IntΔ mice) that we imaged, had been shown to die of bleeding into the thoracic cavity (Rahkonen et al. 2004). Whether these mice develop a gradually enlarging aneurysm in the thoracic aorta or whether the aorta is acutely dissected was unknown. We were able to acquire images of this specific region of interest (thoracic aorta) with an in-plane resolution of 68 x 68 µm, using a GEFC sequence. An in-plane resolution of 100 x 100 µm has earlier been demonstrated to be sufficient to detect local aneurysm-like protrusions in a mouse model of Marfan's syndrome (Itskovich et al. 2003). Most studies concerning MRI of the mouse aorta have been done in order to detect atherosclerotic plaques. In these studies, the in-plane resolution has been similar to ours: 48 x 48 µm (Fayad et al. 1998), 49 x 98 µm (Weismann et al. 2003), 109 x 109 µm (Choudhury et al. 2002), and 140 x 187 µm (Hockings et al. 2002), although 7.0 or 9.4 T MR scanners have been used and the slice thickness has varied from 187 to 500 µm. Using a 4.7 T MR scanner, we had to use a thicker slice (1.0-1.5 mm) in order to get a sufficient amount of signal. However, this is not a large compromise since the slice is less than the diameter of the imaged vessel and there is no overlay of surrounding structures included in the image.

Our imaging protocol was fast since we were not constrained to use pulse- or breath-triggering. With proper fixation of the animal to the cradle and changing of the phase- and frequency-encoding directions, motion-based artifacts interfering with image interpretation were not seen. The use of heart- and breath-triggering is in general beneficial when imaging the body, but it is not necessary when imaging the abdominal area (Fayad et al. 1998). We tested heart-triggering with mice and were able to acquire cinematographic images of the intra-thoracic structures, including the heart, and measure the wall thickness of the heart chambers. However, the blood vessels were rather stabile, and image quality of the aorta was not significantly better with heart-triggering. Triggering always prolongs imaging time since the length of the

cardiac cycle may gradually increase as anesthesia becomes deeper. Imaging times are especially long if both heart- and breath-triggering are combined because heart and breath cycles needs to appear synchronously before acquisition takes place. Furthermore, with triggering, one is constrained to certain TE and TR values. The choice of anesthetic is important, as with isoflurane the animals breath more deeply and the motion from the diaphragm interferes with interpretation of abdominal structure (including aneurysm) if triggering is not used. Therefore, our observations support the use of heart-rate-lowering Hypnorm® or Ketalar®. When triggering is used (e.g. when imaging the heart), continuous isoflurane is better since its concentration can be adjusted during imaging. Triggering is not needed in imaging of the cerebral vasculature.

In cerebral artery imaging, we achieved a resolution of 73 x 73 x 94 µm using a TOF-MRA sequence with a 50.1-min acquisition time. There is only one earlier report concerning TOF-MRA of the cerebral arteries in mice; using a 4.7 T MR scanner, Beckmann et al. (2000) achieved an inferior resolution of 150 x 100 x 100 µm. Since the diameter of the M1 segment is approximately 300 µm, it should have been possible to detect aneurysms at least the size of the parent artery in the typical proximal locations (ICA, MCA, Acom) with the resolution achieved. However, the possibility remains that there are more distal or microaneurysms in the cerebral arteries of Col-IntΔ mice.

To verify the results of imaging the aorta and cerebral arteries had to be harvested immediately. No false-negative cases emerged, increasing the value of our imaging protocol.

6.2 Studies in mice with genetic deficiencies predisposing to vascular defects

6.2.1 Relevance of collagen in the formation of aneurysms

Type I collagen is found in all three layers of the vessel wall and is responsible for its tensile strength. It is the predominant protein in the outer layer, the adventitia, whereas type III collagen predominates in the media (Gay 1978, Miller 1987). Together these two collagens represent 80-90% of the total arterial wall collagens (Burke et al. 1977). A deficiency of type III collagen (Col3a1 mutation) leads to fatal consequences in patients suffering from the vascular form of Ehlers-Danlos syndrome, due to aortic rupture (Schwarze et al. 2001). Defective type I collagen can sometimes cause aortic dissection in patients suffering from variants of osteogenesis imperfecta (Ashraf et al. 1993, Mayer et al. 1996, Isotalo et al. 1999). In the formation of saccular cerebral artery aneurysms in humans, a variety of hereditary connective tissue disorders have been recognized, the most common of

which are autosomal dominant polycystic kidney disease (ADPKD) (Schievink et al. 1992), the vascular form of Ehlers-Danlos syndrome (Schievink et al. 2004), neurofibromatosis type I (Schievink et al. 1997, Pfohman et al 2001), fibromuscular dysplasia (Kalyanaraman et al. 1980), and Marfan's syndrome (Pfohman et al. 2001). Deficiencies of type I collagen may also play a role in the formation of saccular cerebral artery aneurysms. Mutations in *COL1A2,* encoding the α2(I) chain of type I collagen, have been shown to contribute to the formation of both familial and sporadic saccular cerebral artery aneurysms in the Japanese population (Yoneyama et al. 2004).

6.2.2 Significance of Col-IntΔ mouse strain for studies of aneurysm formation

The vessels of Col-IntΔ mice were found to be normal when we imaged them at the age of 16 months. An earlier study (Rahkonen et al. 2004) reported a survival rate of 46% at 18 months. The lack of aneurysm in MRI and microscopic inspection supports the theory of an acutely developed dissection. Although the animals were imaged only once it would have been exceedingly probable that the at least one of them would have developed an aneurysm by this age if aneurysm formation and rupture explain the thoracic hemorrhage seen in this subgroup of mice

The histology of the cerebral arteries of the Col-IntΔ mice was characterized for the first time. The analysis revealed that the cerebral artery wall was 22% thinner in Col-IntΔ mice than in controls. The number of spindle-shaped cells in the media layer being similar in both Col-IntΔ and control mice suggests that the thinning is related to decreased collagen content. This is in line with previous results showing that mRNA levels of proα1 collagen are decreased by 29% at the age of 2.5 months, decreasing further to 58% by the age of 12 months (Rahkonen et al. 2004). The total amount of collagen in the aorta, measured by the hydroxyproline assay, is decreased by 20% compared with controls.

MRI at 4.7 T is feasible for high-resolution imaging of the aorta and cerebral arteries of mice. Based on our findings, the Col-IntΔ mouse strain does not provide insight into the formation of saccular aneurysms. The mechanism causing thoracic hemorrhage appears to be an acute dissection of the aortic wall rather than a gradually developing aneurysm. This model might be beneficial in studies of drugs used to prevent aortic ruptures caused by a dissection.

6.3 Experimental aneurysm model in rats

A good experimental aneurysm model should exhibit characteristics similar to those in human aneurysms. The aneurysm should grow or remain patent and be of the same size as human SCAAs in order to be able to compare endovascular devices. The model should also be easy to standardize and reproduce and inexpensive.

A variety of different animal models have been developed to simulate human SCAAs (see review of literature). None of these models exhibit all of the pathobiological features of human SCAAs. The wide availability of different murine strains has favored the use of these animals for research over larger mammals. Different transgenic strains, especially in mice, are good tools for elucidating the pathological mechanisms involved in different diseases, including aneurysm pathophysiology. By inducing hypertension (renal artery ligation) and ligating one carotid artery in rats and mice it has been possible to produce intracranial aneurysms (anterior cerebral artery, olfactory artery) that closely resemble human SCAAs in that they have a thinning of the media, including apoptotic cells and a degenerated internal elastic lamina. There are, however, two major limitations in this model. First, standardizing the size of the aneurysms is not possible. In fact, even after 6 months of hypertension, 17% (6/35) of the animals show no visible aneurysms with light microscopy, and even the largest aneurysms (31%, 11/35) are only blebs, with a height of barely more than half of their orifice (Morimoto et al. 2002). The long incubation time and numerous animals needed make this model very expensive. To compare treated animals with controls, it is necessary to discover and verify the aneurysm size in vivo at the beginning of treatment and not just postmortem. Our high-resolution imaging techniques could be used for this purpose. The second limitation of the hypertension model is that treatment would need to be systemic, as the cerebral vessels in murines are not sufficiently large for catheterization and embolization with standard equipment. To overcome this size problem, we placed the experimental aneurysm in the abdominal aorta and were able to construct aneurysms of a standard size and equivalent to the small ruptured ones in humans.

Venous pouch models have been developed in swine, dogs, sheep, and rabbits. Criticism against the venous pouch models has mostly arisen due to the finding that these aneurysms contain more inflammatory cell infiltration and exhibit neointima formation (Cawley et al. 1996, Abruzzo et al. 1998) making the wall thicker than approximated for human SCAAs according to early autopsy studies (Walker et al. 1954, Stehbens 1963, Suzuki et al. 1978, Schlote et al. 1994). Nevertheless, it is now known that a significant number of both ruptured and especially unruptured aneurysms in humans do contain intimal thickening and inflammatory cell infiltration

(Frösen et al. 2004, Tulamo et al. 2006), supporting the use of venous pouch aneurysms or other surgically created aneurysms. The venous pouch aneurysms do, however, spontaneously thrombose (Guglielmi et al. 1994). In a study by Byrne et al. (1997), all aneurysms (5/5) were occluded by 2-7 weeks. This happened also in the venous pouch model in dogs (Kerber et al. 1977), where 6/30 aneurysms were occluded before the first examination, at 2-5 weeks. In addition, the venous pouch model requires an anastomosis, making the construction more difficult and time-consuming. The suture line has been speculated to contribute to the occlusion of the aneurysm (Cawley et al. 1996).

The advantage of the elastase-induced aneurysm model is that it lacks the suture line, which can affect the results in surgically created models. In histological analysis, the elastase-induced aneurysms have an attenuated media and internal elastic lamina, but the lack of inflammatory cells is a major difference compared with human SCAAs.

The problem with standardization of aneurysm size is common to most models. In the best swine jugular vein model to date (Byrne et al. 1997), aneurysms varied between 10 and 14 mm in length and between 5 and 6 mm in width. Still this is a 40% difference in size, twice as much as in our model. The elastase-induced aneurysms in rabbits have shown even larger size variation, with the length ranging between 2.6 and 12.5 mm (Ding et al. 2006). Similar substantial differences have been reported in other elastase-induced models, e.g. 4.3–10.8 mm by Hoh et al. (2004).

Our experimental aneurysm model in rats is reliable and suitable for trials comparing endovascular devices since the patency is good and the aneurysms are of standard size. The low mortality and complication rates and low costs of acquiring make the total costs of the model very low compared with other models.

The largest disadvantage with our aneurysm model is its rather small size. Although comparable with small ruptured SCAAs in humans, the model enables the use of only the smallest coils. It is not possible to simulate giant aneurysms, where the large coil-mass is more susceptible to significant compaction. However, in our model, coiling is performed using a predetermined number of coils, allowing a standard-sized neck remnant. Experimental and clinical studies have shown a clear correlation between packing density (occlusion rate) and recurrence. When the initial outcome of coiling is standardized, the result is not dependent on packing density, and therefore, only the actual characteristics of the coil are tested in our model.

6.4 Use of MRI for follow-up of experimental aneurysms in rats and mice

We proved that MRI is suitable for the follow-up of experimental aneurysms in rats and mice. The images are of good quality and interpretation is reliable. The use of perpendicular imaging planes enables the evaluation of the aneurysm or neck remnant from different directions. The most accurate view of an aneurysm and neck remnant is gained with the TOF-MRA sequence, which also enables quantification of the volume because of its high resolution (discussed in the next section). Because MR imaging is noninvasive and rather quick, all animals can be imaged repetitively and the evolution of the aneurysm (recanalization vs. gradual occlusion) can be followed. Inability to obtain images was very rare, and acquisition could be repeated, if for instance, motion-based artifacts were seen. In our series, only one death occurred over the course of 271 imaging sessions (0.37%). Images of the abdominal aorta are of high quality, even without the use of heart- and breath-triggering, particularly when ketamine instead of isoflurane is used as the main anesthetic.

One limitation of the MRI protocol is that the abdomen cannot be imaged if the rat weighs more than 600 g, since the rat will not fit into the RF coil of our system. Imaging of cerebral vessels does not have a similar size limitation. Growth of animals during follow-up has been a limitation also in other studies. For example, the use of DSA imaging of swine jugular vein graft aneurysms was totally hindered at 6 months because of poor radiographic quality due to growth of facial bones (Murayama et al. 2003b).

6.5 Optimized TOF-MRA sequence

Our optimized high-resolution TOF-MRA sequence allows accurate detection of morphological changes in neck remnant shape, such as harmful recanalization or beneficial induced occlusion. We performed optimization in a simulation-based manner. The good correlation between the theoretically calculated and the actual acquired contrast increases the validity of our findings.

In TOF-MRA, the image is created by saturating stagnant (background) tissue and collecting the signal from moving, unsaturated tissue (blood) that later arrives into the imaging volume (Dumoulin 1989). In this way, the image can be elegantly acquired even without the use of any contrast agent. The intensity of the intraluminal signal from the newly arrived fresh blood (flow-related enhancement) is dependent on the distance from the entry surface. Therefore, the aneurysm needs to

be positioned at a predetermined site in the imaging volume; if the distance to the entry surface increases, the flow-related enhancement and signal from the aneurysm decrease.

MRA is limited by factors affecting the saturation and relaxation of protons. 3D TOF-MRA is especially susceptible to spin-dephasing caused by turbulent flow, a problem relevant in such an environment as an aneurysm (Wilcock et al. 1995). Signal loss may also occur when the flow is slow, because of phase dispersion. We overcame these problems by using a short TE and a high resolution. With short echo times, the signal from the flowing blood is maximized. Longer TE would reduce the signal-to-noise ratio, yielding images with a grainy appearance. This is in concordance with earlier studies (Gonner et al. 1998, Krings et al. 2002, Yamada et al. 2004). TR 60 ms was used instead of 30 ms because short TR increased the risk for overheating of the MR scanner, resulting in a need to abort the acquisition. The interpretability of images with TR 60 ms was equal to that with TR 30 ms, although CNR was slightly lower.

A possible pitfall of TOF-MRA is that an acute or subacute thrombus containing methemoglobine can give rise to a hyperintense signal, thereby mimicing flow (Derdeyn et al. 1997, Moody et al. 1998, Yamada et al. 2004). We observed no false-positive flow signals in TOF-MRA; this result was confirmed by performing T2-weighted RARE imaging at every imaging session. At the end, the possibility of thrombosis was further ruled out by endoscopic inspection and histological analysis.

TOF-MRA was used for the first time to detect native cerebral aneurysms in humans by Sevick et al. (1990). Later, TOF-MRA has also been utilized for the imaging of coiled aneurysms. The suitability of MRA (especially TOF-MRA) for the pre- and post-procedural evaluation of coiled aneurysms has been studied earlier (Deutschmann et al. 2007). Using a 1.5 T, scanner Deutschmann and colleagues observed residual necks with a 94% sensitivity in cases where the aneurysm was > 3 mm, but only in 63.6% of cases with aneurysms < 3 mm. They did not find any difference between TOF-MRA and CE-MRA. Other studies have also found that the overall sensitivity (72-97%) and specificity (91-100%) are within the same range (Kähärä et al. 1999, Anzalone et al. 2000, Boulin et al. 2001).

Yamada et al. (2004) used TOF-MRA to evaluate residual flow in the neck region of 39 coiled aneurysms in humans. They found that TOF was as reliable as DSA in detecting residual flow. Gönner et al. (1998) used short and ultrashort TE when imaging coiled aneurysms in humans. They claim that MRA does not underestimate the size of the residual neck and even small dog ears can be seen. They predict that TOF-MRA could be more widely used in the follow-up of coiled aneurysms. Anzalone et.al (2000) also concluded that TOF-MRA is suitable for follow-up of coiled aneurysms, especially in cases with good initial correlation to DSA.

To our knowledge, MRA has been used in only one previous report for the imaging of experimental aneurysms (Krings et al. 2002). These authors imaged elastase-induced aneurysms in rabbits with a 1.5 T scanner, but only prior to coiling. Their resolution (703 x 703 x 500 µm) was inferior to ours and was not detailed enough for volumetric analysis. Moreover, they were compelled to use Gadolinium contrast agent in order to visualize all aneurysms. Their imaging parameters were within the same range as ours, although the pulse angle, which we found to correlate with the angle derived from the Earnst equation, was different.

In our study, image quality was very good even without the gratuitous step of contrast agent injection. Had the images not been satisfactory, intravenous Gadolinium injection and CE-MRA could have been used. In clinical practice, there seems to be an advantage in using CE-MRA to detect aneurysms and recanalization, although some contrary studies exist (Pierot et al. 2006, Deutschmann et al. 2007), showing that TOF-MRA and CE-MRA to be equally sensitive.

We also assessed the effect of i) fat suppression and ii) magnetization transfer (MT) which suppresses muscle tissue, on image quality (Figure 6). Blood consisting mostly of water should not be affected by either of these suppressions. Since the experimental aneurysm is closely surrounded by intraperitoneal fat tissue, while the muscle tissue is on the posterior side at a distance of several millimeters, needing fat suppression instead of MT seems more logical. In practice, we were able to produce enough contrast between the aneurysm and fat even without suppression. Fat suppression and MT made the automatic maximum intensity projection (MIP) reformats clearer. However, when analyzing data, the raw images are more important than MIP reformats. The relevance of background suppression is greater in a clinical setting since the aneurysm can be located in various places and it can project to a variety of directions. In our experimental model, the site of the aneurysm is clearly defined and it is easy to locate it even without background suppression. Since there was a slight signal loss from the aneurysm when using suppression, we decided not to use it.

The resolution achieved with the multislice TOF-MRA was 117 x 117 x 117 µm. With this resolution, it is possible to cover the aneurysm neck with an average of 21 slices from which the volume can be measured. We measured the volume by outlining the region of interest manually. In theory, this could be done automatically by having a program that recognizes the given intensities, but it would not eliminate the need for manually outlining the border between the aorta and the aneurysm neck.

6.6 Platinum versus PGLA-coated coils

In Study IV, we showed that aneurysms coiled with PGLA-coated coils exhibit progressive reduction in neck remnant size in MRI and increased fibrosis in histology, compared with platinum coils. However, the whole neck remnant was not abolished, but disappearance of dog ears was significantly more prominent in the PGLA group during the 4-week-long follow-up.

PGLA-coated coils were tested only in the jugular vein graft model in swine and the elastase-induced model in rabbits before introduction into clinical use (Murayama et al 2003b, Ding et al. 2005). Murayama et al. (2003b) constructed bilateral jugular vein graft aneurysms in 26 swine, 6 of which were followed up for 6 months. They used rather low packing densities (18.7-25.4%) and did not measure or monitor the aneurysm neck remnant. By using digital subtraction angiography (DSA), they were unable to obtain follow-up images on all planned imaging occasions. In histological analysis, they found that the aneurysms embolized with PGLA-coated coils showed a more extensive area of thrombus organization and higher amounts of leukocyte infiltration at 14 days, but complete fibrosis had occurred in both groups at 3 months. We used an intermediate time-point of 28 days and were also able to show that thrombus organization and inflammatory cell infiltration were more extensive in the PGLA group. However, we found that in neither group was the process complete at this point. In the swine model, using histological analysis and 2D DSA, the PGLA-coiled aneurysms were also demonstrated to possess significantly thicker neck tissue at 14 days and at 3 months such that the necks of all PGLA-coiled aneurysms were completely covered with a fibrous membrane (Murayama et al. 2003b). We considered the measurement of the neck tissue thickness from histological sections to be unreliable, but in endoscopic analysis the neointima covering the neck of aneurysms coiled with platinum coils was more often translucent or incomplete. We doubt that this transparency is explained by the difference in color of the devices, but rather represents true thickening. However, the difference was statistically nonsignificant.

Ding et al. (2005) compared PGLA-coated (Matrix®, Boston Scientific, Fremont, CA, USA) coils (n=15) with platinum coils and expandable hydrogel coils (HydroCoils®, Microvention, Aliso Viejo, CA, USA) in elastase-induced carotid aneurysms in rabbits (n=33). They found similar strong inflammatory reactions around the PGLA-coated coils at 6 and 10 weeks and observed neck tissue deposition in all PGLA-coiled aneurysms at 2 weeks. These findings are consistent with what we saw at 4 weeks. They then evaluated the angiographic outcome as complete/near-complete/incomplete occlusion by performing DSA at the time of sacrifice. Incomplete initial occlusion and aneurysm recurrence were more frequent in the PGLA group than in the other two groups. However, in their study, the number of PGLA-coated coils implanted was lower than that of other coil types. Moreover,

aneurysm neck occlusion was evaluated by a robust scale, and angiography was not frequently repeated.

In humans, PGLA-coated coils and platinum coils have not yet been compared in large, randomized, prospective, long-term studies. Human studies thus far have shown that initial angiographic results and overall treatment-related morbidity and mortality fall within the range of results reported in platinum coil studies (Pierot et al. 2006). Pierot et al. (2006, 2008) achieved complete initial occlusion in 44% of the cases coiled with PGLA-coated coils alone or combined with platinum coils. However, they had no control group and did not assess durability. The safety of using PGLA-coated coils has also been good in other studies (Katz et al. 2005, Linfante et al. 2005, Taschner et al. 2005). Niimi et al. (2006) conducted an average follow-up of 12 months of 47 aneurysms embolized with PGLA-coated coils and found a recanalization rate of 57.4%, which is worse than that reported for platinum coils. Other studies assessing durability and recanalization have reported moderate improvement in radiological outcome. In their 8-month follow-up of 87 patients, Murayama et al.(2006) noted that the aneurysms coiled with PGLA coils remained stable or exhibited progressive occlusion in up to 80.5% of cases. Moreover, no recanalization appeared in aneurysms that were initially completely occluded. Some aneurysms with a neck remnant showed progressive occlusion, similar to our results in rats. In addition, Katz et al. (2005) reported rather small recanalization rates – 14.3% in aneurysms (n=77) followed for an average of 12 months – when using predominantly PGLA-coated coils.

The variation in results may be due to varying primary occlusion rates, which were 17.6% in the Niimi study (Niimi et al. 2006), 26.3% in the Murayama study (Murayama et al. 2006) and 56.3% in the Katz study (Katz et al. 2005). The generally low occlusion rates with PGLA-coated coils are partially explained by the additional stiffness and friction that come with the coating. These technical shortcomings are currently under investigation. The results may also vary because the wall histology and cellularity of human aneurysms can differ from case to case (Frösen et al. 2004, 2006), and some aneurysms may therefore be less suitable for coiling.

Gonzales et al. (2005) estimated aneurysm neck tissue thickness from DSA images. In concordance with findings in the swine model and our rat model, the neck tissue had increased with PGLA-coated coils. Because of controversy regarding the clinical results, a larger clinical trial is needed to elucidate this issue.

In Study IV, the experimental rat model was for the first time used to compare two different coils. Our success rate for producing standard-sized aneurysms was high (80%), and the costs were low. Imaging was performed repeatedly with MRI. It would have improved the value of this study had DSA also been performed at one time-point.

Our results suggest that the PGLA-coated coils have a biological effect on the neck remnant. Previous experimental studies have not focused on evaluating and quantifying this phenomenon. We performed the aneurysm coiling so that residual filling – the dog ears – remained between the coil mass and the aneurysm wall, and we were able to adequately evaluate their status during follow-up. It is generally believed that the dog ears are potential sites for further growth and aneurysm recurrence (Raymond et al. 1997a,b). The PGLA-coated coils significantly stimulated the occlusion of these dog ears, whereas the total reduction in neck remnant size was rather moderate (12.9%). The process of neointima formation, which occluded the dog ears, accounts for most of the quantified reduction of the neck remnant. Coils were not, however, able to stimulate total occlusion of the neck remnant.

In our experimental arterial model, we were able to mimic the real-life situation by having a neck remnant with dog ears. By frequently performed, high-resolution MR imaging with newly optimized 3D TOF-MRA and volumetric measurements, we showed progressive occlusion of neck remnants and better angiographic outcome, seen as disappearance of dog ears during follow-up in aneurysms treated with PGLA-coated coils. We also performed endoscopic and histological analyses at the 28-day endpoint.

The true benefit of PGLA-coated coils in clinical practice may be to improve the occlusion of residual filling between coils and the aneurysm wall, possibly preventing aneurysm recurrence. However, because of the marginal influence of the coils on the neck remnant itself, achieving high packing densities and good primary angiographic outcome is still necessary with these coils. Knowledge is growing regarding aneurysm pathobiology (Peters et al. 1999, 2001, Frösen et al. 2004, 2006b, Tulamo et al. 2006, Laaksamo et al. 2008), and ongoing technical development of coils should emphasize the biological effects. In the future, biologically active, but otherwise simple coils may work in such a way that even incompletely coiled aneurysms would progressively and completely occlude. It should not be necessary for the interventionist to make a perfect architectural construction of the coil mass. Instead, putting only a small coil loop into the aneurysm should be sufficient to induce aneurysm occlusion.

6.7 Future visions for endovascular treatment

The greatest challenge in aneurysm microneurosurgery has always been the treatment of giant aneurysms, especially those in difficult locations like the basilar artery. The mass of a large aneurysm interferes with the surgical maneuvering and preparation of the aneurysm neck. Locations such as the basilar artery are very delicate also because of the many arterial perforators going to the brainstem, the cranial nerves passing at a close distance, and the deep and narrow surgical corridor to the lesion. All of these are even more relevant in acute surgery after SAH. Endovascular coiling has become a good alternative to surgery in the treatment of cerebral aneurysms in general, but it has not become the definite solution for the awkward lesion like giant aneurysms or aneurysms with a very wide neck.

Still today, almost 20 years after the introduction of endovascular coiling, incomplete angiographic occlusion of coiled aneurysms remains a problem. There have been attempts to overcome this problem by developing biologically active coatings on platinum coils, e.g. PGLA. However, for the time being, the long-term results appear to be highly dependent on the initial angiographic result (Sluzewski et al. 2004). To prevent recurrence, the volume of the aneurysm needs to occluded with as many coils as possible. This is an unsustainable condition when treating giant aneurysms that might contain thrombi and already by themselves might generate a mass effect and compress cerebral structures. When these giant aneurysms are treated with numerous coils, the coil mass causes additional compression, especially if re-treatment is needed. On the other hand effective scar formation would cause beneficial constriction of tissues. When the coating of PGLA-coated coils is absorbed and replaced by mature connective tissue, the total volume of the aneurysm has been thought to decrease. However, thus far, this has only been demonstrated in experimental aneurysms (Murayama et al 2003b).

The trend of developing biologically inert embolization materials, such as Onyx and HydroCoils, is irrational in the sense that the aneurysm is filled with a cast made of foreign material, which has no biological effect and is not replaced by fibrous tissue. This cast holds the aneurysm walls apart, exhibits pressure on the wall itself, and actually interferes with aneurysm healing. Although the treatment may be satisfactory in many cases and aneurysms might not recanalize, the rationale of the treatment is nevertheless somewhat illogical. The primary justification of the use of HydroCoils was that the improved packing density would reduce recurrences (Cloft et al. 2004). However, the first follow-up study with these coils did not confirm this (Cloft et al. 2007). Hypothetically, the expanding of the coil inside the aneurysm can be considered a dangerous event.

One should also focus on the significance of incomplete occlusion. Raymond et al. (2003) debated the risks worth taking to make the angiographic occlusion perfect since the true risk of rebleeding might be low, even with a small remnant. This is reinforced by the observation that despite the vast number of coiled aneurysms worldwide, we see less cases of rebleeding after coiling in clinical practice than we would expect. However, systematic, population-based, long-term follow-up studies are needed to confirm this.

The rapid and constant evolution of new endovascular devices (3D coils, soft coils, coated coils, stents, flow diverters, liquid agents) and combined use of techniques have lead to a point where reliable results concerning safety and efficacy are difficult or even impossible to find. The results from using new devices are often reported as single-center studies, with small study populations and often without control groups or with historic series as controls (Kang et al. 2005). Very few studies provide reliable long-term results of the use of one device and even fewer compare two devices in a randomized way. There has also been a drive to develop more efficient techniques, but as procedures become more demanding and complex (balloon-remodeling, stent placement), overall safety has not necessarily improved (Raymond et al. 2003, Nelson et al. 2006).

In the future, focus will be on the biological activity of the endovascular device. The treatment will rely less on skilful positioning of the coil into the aneurysm and more on the biological activity of an otherwise simple device. The placement of even a small device inside the aneurysm should promote gradual occlusion and healing with good long-term results, despite an imperfect initial angiographic result. In our experimental rat aneurysm model, we were able to deliberately perform coiling so that there is an initial neck remnant. An efficient endovascular device should promote gradual occlusion of this neck. The neck remnant also possessed additional blood-filled cavities projecting between the coils and the aneurysm wall, namely the “dog ears”. A poor endovascular device permits further growth of these dog ears. Growth of intimal hyperplasia (neointima) is the goal in the endovascular treatment of aneurysms (Raymond et al. 1999) and this would occlude the dog ears and the neck remnant.

We will use the rat model to test novel endovascular devices, including coated coils and porous stents. The detection of inflammation (macrophage infiltration) in a vessel wall by in vivo imaging can be done by injecting USPIOs (ultrasmall superparamagnetic particles of iron oxide). We are currently studying the characteristics of USPIOs and will use USPIOs to evaluate inflammation in experimental aneurysms in order to elucidate whether this contrast agent can help to identify rupture prone aneurysms.

7. Conclusions

MRI is a reliable method for the detection of experimental murine aneurysms. Using a 4.7 T MR scanner, we were able to scan the cerebral arteries of mice up to the distal branches with a resolution of 73 x 73 x 94 µm. The Col-IntΔ mouse strain is, however, not suitable for studies of aneurysm formation and pathobiology, but other stains can be examined.

The surgically created experimental aneurysm model in rats is easy to standardize and reproduce. Moreover, it is suitable for endovascular treatment. The low mortality rate makes the model affordable. The aneurysms remain patent for up to 2 years and sometimes even grow.

The optimized MRI protocol provides detailed and accurate follow-up images of the experimental aneurysms. With the high-resolution TOF-MRA sequence, it is possible to quantify changes in neck remnant volume during follow-up.

Aneurysms coiled with PGLA-coated coils show progressive reduction in neck remnant size in MRI and increased fibrosis in histology compared with platinum coils. During follow-up, disappearance of dog ears was significantly more prominent in the PGLA group, suggesting a true biological benefit of this device.

Acknowledgements

This study was carried out in the Neurosurgery Research Group in 2003-2008. I wish to thank my co-workers, colleagues and friends for their help and support during these years.

Mika Niemelä and Marko Kangasniemi for their work as thesis supervisors. Both of you worked hard in making my research possible by preparing excellent research plans and establishing the necessary contacts to collaborators in the University of Turku and abroad. You never gave up hope even when I sometimes needed to stretch the timetables. Moreover, I value how you shared your knowledge in how to write scientific papers.

Juha Hernesniemi as the honorary custos and head of the department. You are an excellent role model for young surgeons. You have gained reputation both as a clinician, researcher and chairman by hard work and shown how many faces a man needs to have in order to become highly respected in his own field.

Juha Jääskeläinen as the first leader of the research group for teaching how to constantly ask questions in order to find new solutions, and always strive for accuracy.

Jaakko Rinne and Leo Keski-Nisula, reviewers of the thesis, for their excellent comments.

Juhana Frösen, Riikka Tulamo, Usama Abo-Ramadan and Henrik Antell, my closest co-workers in the research group, for their contribution in the research. Especially Juhana for the hands-on teaching of many of the methods used.

My other co-workers in the research group and in the department of neurosurgery for your friendship, support, understanding and backup.

Jorma Greijer for technical support in the endovascular procedures and valuable help in establishing international contacts, and participation in the ever so important recreational activities of the research group.

Carol Ann Pelli for revising the English language of the thesis.

My friends for providing alternative activities and not forgetting me even in times when I have been too absorbed in my studies, work and carrier.

My family for their understanding, enthusiasm, support and love, and for making me who I am. Most of all I thank my companion and lovely wife Annukka, for pushing me forward, forcing me to realise my goals and sharing everyday life with me.

This research has been funded by grants from the Helsinki University Central Hospital, Finnish Neurosurgical Association, Finska Läkaresällskapet, Maire Taposen säätiö and Biomedicum Helsinki Foundation. Endovascular devices have been provided by Boston Scientific Corporation, Fremont, CA, USA.

References

Abrahams JM, Forman MS, Grady MS and Diamond SL (2001). Delivery of human vascular endothelial growth factor with platinum coils enhances wall thickening and coil impregnation in a rat aneurysm model. *AJNR Am J Neuroradiol.* 22(7): 1410-7.

Abruzzo T, Shengelaia GG, Dawson RC, 3rd, Owens DS, Cawley CM and Gravanis MB (1998). Histologic and morphologic comparison of experimental aneurysms with human intracranial aneurysms. *AJNR Am J Neuroradiol.* 19(7): 1309-14.

Ahuja AA, Hergenrother RW, Strother CM, Rappe AA, Cooper SL and Graves VB (1993). Platinum coil coatings to increase thrombogenicity: a preliminary study in rabbits. *AJNR Am J Neuroradiol.* 14(4): 794-8.

Altes TA, Cloft HJ, Short JG, DeGast A, Do HM, Helm GA and Kallmes DF (2000). 1999 ARRS Executive Council Award. Creation of saccular aneurysms in the rabbit: a model suitable for testing endovascular devices. American Roentgen Ray Society. *AJR Am J Roentgenol.* 174(2): 349-54.

Anidjar S, Salzmann JL, Gentric D, Lagneau P, Camilleri JP, Michel JB. (1990) Elastase-induced experimental aneurysms in rats. *Circulation*. 82(3):973-81

Anzalone N, Righi C, Simionato F, Scomazzoni F, Pagani G, Calori G, Santino P and Scotti G (2000). Three-dimensional time-of-flight MR angiography in the evaluation of intracranial aneurysms treated with Guglielmi detachable coils. *AJNR Am J Neuroradiol.* 21(4): 746-52.

Araki C, Handa H, Yoshida K et.al. (1966) Electrically induced thrombosis for the treatment of intracranial aneurysms and angiomas. Proceedings of the third international congress of neurological surgery, Copenhagen 1965, *Excerpta Medica* 110: 651-654

Ashraf SS, Shaukat N, Masood M, Lyons TJ and Keenan DJ (1993). Type I aortic dissection in a patient with osteogenesis imperfecta. *Eur J Cardiothorac Surg* 7(12): 665-6.

Auer LM, Brandt L, Ebeling U, Gilsbach J, Groeger U, Harders A, Ljunggren B, Oppel F, Reulen HJ, Saeveland H (1986). Nimodipine and early aneurysm operation in good condition SAH patients. *Acta Neurochir (Wien)* 82(1-2):7-13.

Beckmann N (2000). High resolution magnetic resonance angiography non-invasively reveals mouse strain differences in the cerebrovascular anatomy in vivo. *Magn Reson Med* 44(2): 252-8.

Belz MM, Hughes RL, Kaehny WD, Johnson AM, Fick-Brosnahan GM, Earnest MP and Gabow PA (2001). Familial clustering of ruptured intracranial aneurysms in autosomal dominant polycystic kidney disease. *Am J Kidney Dis* 38(4): 770-6.

Bederson JB, Connolly ES Jr, Batjer HH, Dacey RG, Dion JE, Diringer MN, Duldner JE Jr, Harbaugh RE, Patel AB, Rosenwasser RH; American Heart Association (2009). Guidelines for the management of aneurysmal subarachnoid hemorrhage: a statement for healthcare professionals from a special writing group of the Stroke Council, American Heart Association. *Stroke*. 40(3):994-1025. Epub 2009 Jan 22. Review.

Bendszus M and Solymosi L (2006). Cerecyte coils in the treatment of intracranial aneurysms: a preliminary clinical study. *AJNR Am J Neuroradiol.* 27(10): 2053-7.

Benoit BG and Wortzman G (1973). Traumatic cerebral aneurysms. Clinical features and natural history. *J Neurol Neurosurg Psychiatry.* 36(1): 127-38.

Bonita R (1986). Cigarette smoking, hypertension and the risk of subarachnoid hemorrhage: a population-based case-control study. *Stroke.* 17(5): 831-5.

Boulin A and Pierot L (2001). Follow-up of intracranial aneurysms treated with detachable coils: comparison of gadolinium-enhanced 3D time-of-flight MR angiography and digital subtraction angiography. *Radiology.* 219(1): 108-13.

Brilstra EH, Rinkel GJ, van der Graaf Y, van Rooij WJ, Algra A. (1999) Treatment of intracranial aneurysms by embolization with coils: a systematic review. *Stroke*. 30(2):470-6. Review

Burke JM, Balian G, Ross R and Bornstein P (1977). Synthesis of types I and III procollagen and collagen by monkey aortic smooth muscle cells in vitro. *Biochemistry* 16(14): 3243-9.

Butler WE, Barker FG, 2nd and Crowell RM (1996). Patients with polycystic kidney disease would benefit from routine magnetic resonance angiographic screening for intracerebral aneurysms: a decision analysis. *Neurosurgery.* 38(3): 506-15; discussion 515-6.

Byrne JV & GuglielmiG (1998) Endovascular treatment of intracranial aneurysms. Springer-Verlag, Berlin, Heidelberg.

Byrne JV, Hope JK, Hubbard N and Morris JH (1997). The nature of thrombosis induced by platinum and tungsten coils in saccular aneurysms. *AJNR Am J Neuroradiol.* 18(1): 29-33.

Cawley CM, Dawson RC, Shengelaia G, Bonner G, Barrow DL and Colohan AR (1996). Arterial saccular aneurysm model in the rabbit. *AJNR Am J Neuroradiol.* 17(9): 1761-6.

Cekirge HS, Saatci I, Ozturk MH, Cil B, Arat A, et al. (2006). Late angiographic and clinical follow-up results of 100 consecutive aneurysms treated with Onyx reconstruction: largest single-center experience. *Neuroradiology.* 48(2): 113-26. Epub 2006 Jan 4.

Choi IS and David C (2003). Giant intracranial aneurysms: development, clinical presentation and treatment. *Eur J Radiol.* 46(3): 178-94.

Choudhury RP, Aguinaldo JG, Rong JX, Kulak JL, Kulak AR, et al. (2002). Atherosclerotic lesions in genetically modified mice quantified in vivo by non-invasive high-resolution magnetic resonance microscopy. *Atherosclerosis* 162(2): 315-21.

Clare CE and Barrow DL (1992). Infectious intracranial aneurysms. *Neurosurg Clin N Am.* 3(3): 551-66.

Cloft HJ, Joseph GJ, Tong FC, Goldstein JH, Dion JE. (2000) Use of three-dimensional Guglielmi detachable coils in the treatment of wide-necked cerebral aneurysms. *AJNR Am J Neuroradiol*. 21(7):1312-4

Cloft HJ and Kallmes DF (2004). Aneurysm packing with HydroCoil Embolic System versus platinum coils: initial clinical experience. *AJNR Am J Neuroradiol.* 25(1): 60-2.

Cloft HJ (2006). HydroCoil for Endovascular Aneurysm Occlusion (HEAL) study: periprocedural results. *AJNR Am J Neuroradiol.* 27(2): 289-92.

Cloft HJ (2007). HydroCoil for Endovascular Aneurysm Occlusion (HEAL) study: 3-6 month angiographic follow-up results. *AJNR Am J Neuroradiol.* 28(1): 152-4.

Cognard C, Weill A, Castaings L, Rey A and Moret J (1998). Intracranial berry aneurysms: angiographic and clinical results after endovascular treatment. *Radiology.* 206(2): 499-510.

Cowan JA, Jr., Dimick JB, Wainess RM, Upchurch GR, Jr. and Thompson BG (2003). Outcomes after cerebral aneurysm clip occlusion in the United States: the need for evidence-based hospital referral. *J Neurosurg.* 99(6): 947-52.

Dai D, Ding YH, Danielson MA, Kadirvel R, Lewis DA, Cloft HJ and Kallmes DF (2005a). Modified histologic technique for processing metallic coil-bearing tissue. *AJNR Am J Neuroradiol.* 26(8): 1932-6.

Dawson RC, 3rd, Shengelaia GG, Krisht AF and Bonner GD (1996). Histologic effects of collagen-filled interlocking detachable coils in the ablation of experimental aneurysms in swine. *AJNR Am J Neuroradiol.* 17(5): 853-8.

Debrun G, Fox A, Drake C, Peerless S, Girvin J and Ferguson G (1981). Giant unclippable aneurysms: treatment with detachable balloons. *AJNR Am J Neuroradiol.* 2(2): 167-73.

Debrun GM, Aletich VA, Kehrli P, Misra M, Ausman JI, Charbel F and Shownkeen H (1998). Aneurysm geometry: an important criterion in selecting patients for Guglielmi detachable coiling. f*Neurol Med Chir (Tokyo).* 38 Suppl: 1-20.

Derdeyn CP, Graves VB, Turski PA, Masaryk AM and Strother CM (1997). MR angiography of saccular aneurysms after treatment with Guglielmi detachable coils: preliminary experience. *AJNR Am J Neuroradiol.* 18(2): 279-86.

Derdeyn CP, Cross DT, 3rd, Moran CJ, Brown GW, Pilgram TK, et al. (2002). Postprocedure ischemic events after treatment of intracranial aneurysms with Guglielmi detachable coils. *J Neurosurg.* 96(5): 837-43.

de Rooij NK, Linn FH, van der Plas JA, Algra A, Rinkel GJ (2007). Incidence of subarachnoid haemorrhage: a systematic review with emphasis on region, age, gender and time trends. *J Neurol Neurosurg Psychiatry*. 78(12):1365-72. Epub 2007 Apr 30. Review

Deutschmann HA, Augustin M, Simbrunner J, Unger B, Schoellnast H, Fritz GA and Klein GE (2007). Diagnostic accuracy of 3D time-of-flight MR angiography compared with digital subtraction angiography for follow-up of coiled intracranial aneurysms: influence of aneurysm size. *AJNR Am J Neuroradiol.* 28(4): 628-34.

Ding YH, Dai D, Lewis DA, Cloft HJ and Kallmes DF (2005). Angiographic and histologic analysis of experimental aneurysms embolized with platinum coils, Matrix, and HydroCoil. *AJNR Am J Neuroradiol* 26(7): 1757-63.

Ding YH, Dai D, Lewis DA, Danielson MA, Kadirvel R, Mandrekar JN, Cloft HJ and Kallmes DF (2006). Can neck size in elastase-induced aneurysms be controlled? A retrospective study. *AJNR Am J Neuroradiol.* 27(8): 1681-4.

Dion JE, Gates PC, Fox AJ, Barnett HJ and Blom RJ (1987). Clinical events following neuroangiography: a prospective study. *Stroke.* 18(6): 997-1004.

Donaghy RM (1979). The history of microsurgery in neurosurgery. *Clin Neurosurg.* 26: 619-25.

Dorai Z, Hynan LS, Kopitnik TA and Samson D (2003). Factors related to hydrocephalus after aneurysmal subarachnoid hemorrhage. *Neurosurgery.* 52(4): 763-9; discussion 769-71.

Dowd CF, Halbach VV, Higashida RT, Barnwell SL and Hieshima GB (1990). Endovascular coil embolization of unusual posterior inferior cerebellar artery aneurysms. *Neurosurgery.* 27(6): 954-61.
Dumoulin CL, Cline HE, Souza SP, Wagle WA and Walker MF (1989a). Three-dimensional time-of-flight magnetic resonance angiography using spin saturation. *Magn Reson Med.* 11(1): 35-46.
Dumoulin CL, Souza SP, Walker MF and Wagle W (1989b). Three-dimensional phase contrast angiography. *Magn Reson Med.* 9(1): 139-49.
Earnest Ft, Forbes G, Sandok BA, Piepgras DG, Faust RJ, Ilstrup DM and Arndt LJ (1984). Complications of cerebral angiography: prospective assessment of risk. *AJR Am J Roentgenol.* 142(2): 247-53.
Faught E, Trader SD and Hanna GR (1979). Cerebral complications of angiography for transient ischemia and stroke: prediction of risk. *Neurology.* 29(1): 4-15.
Fayad ZA, Fallon JT, Shinnar M, Wehrli S, Dansky HM, et al. (1998). Noninvasive In vivo high-resolution magnetic resonance imaging of atherosclerotic lesions in genetically engineered mice. *Circulation* 98(15): 1541-7.
Ferre JC, Carsin-Nicol B, Morandi X, Carsin M, de Kersaint-Gilly A, Gauvrit JY and Desal HA (2008). Time-of-flight MR angiography at 3T versus digital subtraction angiography in the imaging follow-up of 51 intracranial aneurysms treated with coils. *Eur J Radiol* 21: 21.
Finlay HM, Whittaker P and Canham PB (1998). Collagen organization in the branching region of human brain arteries. *Stroke.* 29(8): 1595-601.
Fogelholm R (1981) Subarachnoid hemorrhage in middle-Finland: incidence, early prognosis and indications for neurosurgical treatment. Stroke 12: 296-301.
Fogelholm R (1992). Subarachnoid hemorrhage in Finland. *Stroke.* 23(3): 437.
Forrest MD and O'Reilly GV (1989). Production of experimental aneurysms at a surgically created arterial bifurcation. *AJNR Am J Neuroradiol.* 10(2): 400-2.
Frazee JG, Cahan LD and Winter J (1980). Bacterial intracranial aneurysms. *J Neurosurg.* 53(5): 633-41.
Frosen J, Piippo A, Paetau A, Kangasniemi M, Niemela M, Hernesniemi J and Jaaskelainen J (2004). Remodeling of saccular cerebral artery aneurysm wall is associated with rupture: histological analysis of 24 unruptured and 42 ruptured cases. *Stroke.* 35(10): 2287-93. Epub 2004 Aug 19.
Frosen J, Marjamaa J, Myllarniemi M, Abo-Ramadan U, Tulamo R, Niemela M, Hernesniemi J and Jaaskelainen J (2006a). Contribution of mural and bone marrow-derived neointimal cells to thrombus organization and wall remodeling in a microsurgical murine saccular aneurysm model. *Neurosurgery.* 58(5): 936-44; discussion 936-44.
Frosen J, Piippo A, Paetau A, Kangasniemi M, Niemela M, Hernesniemi J and Jaaskelainen J (2006b). Growth factor receptor expression and remodeling of saccular cerebral artery aneurysm walls: implications for biological therapy preventing rupture. *Neurosurgery.* 58(3): 534-41; discussion 534-41.
Frosen J (2006c) The pathobiology of saccular cerebral artery aneurysms rupture and repair - a clinicipathological and experimental approach, Helsinki, Yliopistopaino
Gay S and Miller E (1978). Collagen in the Physiology and Pathology of Connective Tissue. New York, Gustav Fischer Verlag.
Gelabert-González M, Fernández-Villa JM, Iglesias-Pais M, González-García J, García-Allut A (2004). [Acute spontaneous subdural haematoma of arterial origin] *Neurocirugia (Astur).* 15(2):165-70. Review. Spanish.
Geyik S, Yavuz K, Ergun O, Koc O, Cekirge S and Saatci I (2008). Endovascular treatment of intracranial aneurysms with bioactive Cerecyte coils: effects on treatment stability. *Neuroradiology.* 50(9): 787-93. Epub 2008 May 16.
Gonner F, Heid O, Remonda L, Nicoli G, Baumgartner RW, Godoy N and Schroth G (1998). MR angiography with ultrashort echo time in cerebral aneurysms treated with Guglielmi detachable coils. *AJNR Am J Neuroradiol.* 19(7): 1324-8.
Gonzalez NR, Patel AB, Murayama Y and Vinuela F (2005). Angiographic evidence of aneurysm neck healing following endovascular treatment with bioactive coils. *AJNR Am J Neuroradiol* 26(4): 912-4.
Goto K, Halbach VV, Hardin CW, Higashida RT, Hieshima GB. (1988) Permanent inflation of detachable balloons with a low-viscosity, hydrophilic polymerizing system.*Radiology*. 169(3):787-90
Graves VB, Ahuja A, Strother CM and Rappe AH (1993a). Canine model of terminal arterial aneurysm. *AJNR Am J Neuroradiol.* 14(4): 801-3.

Graves VB, Strother CM and Rappe AH (1993b). Treatment of experimental canine carotid aneurysms with platinum coils. *AJNR Am J Neuroradiol.* 14(4): 787-93.
Grzyska U, Freitag J and Zeumer H (1990). Selective cerebral intraarterial DSA. Complication rate and control of risk factors. *Neuroradiology.* 32(4): 296-9.
Guglielmi G, Vinuela F, Dion J and Duckwiler G (1991a). Electrothrombosis of saccular aneurysms via endovascular approach. Part 2: Preliminary clinical experience. *J Neurosurg.* 75(1): 8-14.
Guglielmi G, Vinuela F, Sepetka I and Macellari V (1991b). Electrothrombosis of saccular aneurysms via endovascular approach. Part 1: Electrochemical basis, technique, and experimental results. *J Neurosurg.* 75(1): 1-7.
Guglielmi G, Vinuela F, Duckwiler G, Dion J, Lylyk P, et al. (1992). Endovascular treatment of posterior circulation aneurysms by electrothrombosis using electrically detachable coils. *J Neurosurg.* 77(4): 515-24.
Guglielmi G, Ji C, Massoud TF, Kurata A, Lownie SP, Vinuela F and Robert J (1994). Experimental saccular aneurysms. II. A new model in swine. *Neuroradiology.* 36(7): 547-50.
Hawkins J, Quisling RG, Mickle JP and Hawkins IF (1986). Retrievable Gianturco-coil introducer. *Radiology.* 158(1): 262-4.
Heifetz MD (1963) A new intracranial aneurysm clip. *J Neurosurg.* 30(6):753.
Heiserman JE, Dean BL, Hodak JA, Flom RA, Bird CR, Drayer BP and Fram EK (1994). Neurologic complications of cerebral angiography. *AJNR Am J Neuroradiol.* 15(8): 1401-7; discussion 1408-11.
Hernesniemi J, Vapalahti M, Niskanen M, Tapaninaho A, Kari A, Luukkonen M, Puranen M, Saari T, Rajpar M (1993). One-year outcome in early aneurysm surgery: a 14 years experience. *Acta Neurochir (Wien).* 122(1-2):1-10.
Hernesniemi J, Niemela M, Karatas A, Kivipelto L, Ishii K, et al. (2005). Some collected principles of microneurosurgery: simple and fast, while preserving normal anatomy: a review. *Surg Neurol.* 64(3): 195-200.
Hieshima GB, Higashida RT, Wapenski J, Halbach VV, Cahan L and Bentson JR (1986). Balloon embolization of a large distal basilar artery aneurysm. Case report. *J Neurosurg.* 65(3): 413-6.
Higashida RT, Halbach VV, Barnwell SL, Dowd C, Dormandy B, Bell J and Hieshima GB (1990). Treatment of intracranial aneurysms with preservation of the parent vessel: results of percutaneous balloon embolization in 84 patients. *AJNR Am J Neuroradiol.* 11(4): 633-40.
Higashida RT, Smith W, Gress D, Urwin R, Dowd CF, Balousek PA and Halbach VV (1997). Intravascular stent and endovascular coil placement for a ruptured fusiform aneurysm of the basilar artery. Case report and review of the literature. *J Neurosurg.* 87(6): 944-9.
Hillbom M and Kaste M (1981). Does alcohol intoxication precipitate aneurysmal subarachnoid haemorrhage? *J Neurol Neurosurg Psychiatry.* 44(6): 523-6.
Hiratsuka Y, Miki H, Kiriyama I, Kikuchi K, Takahashi S, Matsubara I, Sadamoto K and Mochizuki T (2008). Diagnosis of Unruptured Intracranial Aneurysms: 3T MR Angiography versus 64-channel Multi-detector Row CT Angiography. *Magn Reson Med Sci.* 7(4): 169-78.
Hockings PD, Roberts T, Galloway GJ, Reid DG, Harris DA, Vidgeon-Hart M, Groot PH, Suckling KE and Benson GM (2002). Repeated three-dimensional magnetic resonance imaging of atherosclerosis development in innominate arteries of low-density lipoprotein receptor-knockout mice. *Circulation* 106(13): 1716-21.
Hoh BL, Rabinov JD, Pryor JC and Ogilvy CS (2004). A modified technique for using elastase to create saccular aneurysms in animals that histologically and hemodynamically resemble aneurysms in human. *Acta Neurochir (Wien).* 146(7): 705-11. Epub 2004 May 17.
Hop JW, Rinkel GJ, Algra A and van Gijn J (1997). Case-fatality rates and functional outcome after subarachnoid hemorrhage: a systematic review. *Stroke.* 28(3): 660-4.
Hosobuchi Y (1979). Direct surgical treatment of giant intracranial aneurysms. *J Neurosurg.* 51(6): 743-56.
Ingall TJ, Whisnant JP, Wiebers DO and O'Fallon WM (1989). Has there been a decline in subarachnoid hemorrhage mortality? *Stroke.* 20(6): 718-24.
Ishibashi T, Murayama Y, Urashima M, Saguchi T, Ebara M, Arakawa H, Irie K, Takao H, Abe T (2009). Unruptured intracranial aneurysms: incidence of rupture and risk factors. *Stroke*. 40(1):313-6. Epub 2008 Oct 9.
Isotalo PA, Guindi MM, Bedard P, Brais MP and Veinot JP (1999). Aortic dissection: a rare complication of osteogenesis imperfecta. *Can J Cardiol* 15(10): 1139-42.
Itskovich VV, Lieb M, Aguinaldo JG, Samber DD, Ramirez F and Fayad ZA (2003). Magnetic resonance microscopy quantifies the disease progression in Marfan syndrome mice. *J Magn Reson Imaging* 17(4): 435-9.

Juvela S, Porras M and Poussa K (2000). Natural history of unruptured intracranial aneurysms: probability of and risk factors for aneurysm rupture. *J Neurosurg.* 93(3): 379-87.
Juvela S, Poussa K and Porras M (2001). Factors affecting formation and growth of intracranial aneurysms: a long-term follow-up study. *Stroke.* 32(2): 485-91.
Kahara VJ, Seppanen SK, Ryymin PS, Mattila P, Kuurne T and Laasonen EM (1999). MR angiography with three-dimensional time-of-flight and targeted maximum-intensity-projection reconstructions in the follow-up of intracranial aneurysms embolized with Guglielmi detachable coils. *AJNR Am J Neuroradiol.* 20(8): 1470-5.
Kallmes DF, Borland MK, Cloft HJ, Altes TA, Dion JE, Jensen ME, Hankins GR and Helm GA (1998a). In vitro proliferation and adhesion of basic fibroblast growth factor-producing fibroblasts on platinum coils. *Radiology.* 206(1): 237-43.
Kallmes DF, Williams AD, Cloft HJ, Lopes MB, Hankins GR and Helm GA (1998b). Platinum coil-mediated implantation of growth factor-secreting endovascular tissue grafts: an in vivo study. *Radiology.* 207(2): 519-23.
Kallmes DF, Helm GA, Hudson SB, Altes TA, Do HM, Mandell JW and Cloft HJ (1999). Histologic evaluation of platinum coil embolization in an aneurysm model in rabbits. *Radiology* 213(1): 217-22.
Kallmes DF, Lin HB, Fujiwara NH, Short JG, Hagspiel KD, Li ST, Matsumoto AH (2007). Dr. Gary J. Becker young investigator award: comparison of small-diameter type 1 collagen stent-grafts and PTFE stent-grafts in a canine model--work in progress. *J Vasc Interv Radiol*.12(10):1127-33.
Kalyanaraman UP and Elwood PW (1980). Fibromuscular dysplasia of intracranial arteries causing multiple intracranial aneurysms. *Hum Pathol* 11(5): 481-4.
Kang HS, Han MH, Kwon BJ, Kwon OK, Kim SH, Choi SH and Chang KH (2005). Short-term outcome of intracranial aneurysms treated with polyglycolic acid/lactide copolymer-coated coils compared to historical controls treated with bare platinum coils: a single-center experience. *AJNR Am J Neuroradiol.* 26(8): 1921-8.
Kangasniemi M, Makela T, Koskinen S, Porras M, Poussa K and Hernesniemi J (2004). Detection of intracranial aneurysms with two-dimensional and three-dimensional multislice helical computed tomographic angiography. *Neurosurgery.* 54(2): 336-40; discussion 340-1.
Kassell NF, Sasaki T, Colohan AR, Nazar G (1985). Cerebral vasospasm following aneurysmal subarachnoid hemorrhage. *Stroke*. 16(4):562-72. Review.
Kassell NF, Torner JC, Haley EC, Jr., Jane JA, Adams HP and Kongable GL (1990a). The International Cooperative Study on the Timing of Aneurysm Surgery. Part 1: Overall management results. *J Neurosurg.* 73(1): 18-36.
Kassell NF, Torner JC, Jane JA, Haley EC, Jr. and Adams HP (1990b). The International Cooperative Study on the Timing of Aneurysm Surgery. Part 2: Surgical results. *J Neurosurg.* 73(1): 37-47.
Kato Y, Nair S, Sano H, Sanjaykumar MS, Katada K, Hayakawa M and Kanno T (2002). Multi-slice 3D-CTA - an improvement over single slice helical CTA for cerebral aneurysms. *Acta Neurochir (Wien).* 144(7): 715-22.
Katz JM, Tsiouris AJ, Biondi A, Salvaggio KA, Ougorets I, Stieg PE, Riina HA and Gobin YP (2005). Advances in endovascular aneurysm treatment: are we making a difference? *Neuroradiology* 47(9): 695-701. Epub 2005 Jul 19.
Kerber CW and Buschman RW (1977). Experimental carotid aneurysms: I. Simple surgical production and radiographic evaluation. *Invest Radiol.* 12(2): 154-7.
Kivisaari RP, Porras M, Ohman J, Siironen J, Ishii K and Hernesniemi J (2004). Routine cerebral angiography after surgery for saccular aneurysms: is it worth it? *Neurosurgery.* 55(5): 1015-24.
Klingebiel R, Kentenich M, Bauknecht HC, Masuhr F, Siebert E, Busch M and Bohner G (2008). Comparative evaluation of 64-slice CT angiography and digital subtraction angiography in assessing the cervicocranial vasculature. *Vasc Health Risk Manag.* 4(4): 901-7.
Koffijberg H, Buskens E, Algra A, Wermer MJ, Rinkel GJ (2008). Growth rates of intracranial aneurysms: exploring constancy. *J Neurosurg*. 109(2):176-85.
Koivisto T, Vanninen R, Hurskainen H, Saari T, Hernesniemi J and Vapalahti M (2000). Outcomes of early endovascular versus surgical treatment of ruptured cerebral aneurysms. A prospective randomized study. *Stroke.* 31(10): 2369-77.
Krayenbuhl HA, Yasargil MG, Flamm ES and Tew JM, Jr. (1972). Microsurgical treatment of intracranial saccular aneurysms. *J Neurosurg.* 37(6): 678-86.
Krings T, Hans FJ, Moller-Hartmann W, Thiex R, Brunn A, et al. (2002). Time-of-flight-, phase contrast and contrast enhanced magnetic resonance angiography for pre-interventional determination of aneurysm size, configuration, and neck morphology in an aneurysm model in rabbits. *Neurosci Lett.* 326(1): 46-50.

Kriss TC, Kriss VM. (1998) History of the operating microscope: from magnifying glass to microneurosurgery. *Neurosurgery.* 42(4):899-907; discussion 907-8

Kuether TA, Nesbit GM and Barnwell SL (1998). Clinical and angiographic outcomes, with treatment data, for patients with cerebral aneurysms treated with Guglielmi detachable coils: a single-center experience. *Neurosurgery.* 43(5): 1016-25.

Kumar M and Kitchen ND (1998). Infective and traumatic aneurysms. *Neurosurg Clin N Am.* 9(3): 577-86.

Laaksamo E, Tulamo R, Baumann M, Dashti R, Hernesniemi J, Juvela S, Niemelä M, Laakso A. (2008) Involvement of mitogen-activated protein kinase signaling in growth and rupture of human intracranial aneurysms. *Stroke*. 39(3):886-92. Epub 2008 Jan 31

Langer R and Vacanti JP (1993). Tissue engineering. *Science.* 260(5110): 920-6.

Lanzino G, Wakhloo AK, Fessler RD, Hartney ML, Guterman LR and Hopkins LN (1999). Efficacy and current limitations of intravascular stents for intracranial internal carotid, vertebral, and basilar artery aneurysms. *J Neurosurg.* 91(4): 538-46.

Laub GA and Kaiser WA (1988). MR angiography with gradient motion refocusing. *J Comput Assist Tomogr.* 12(3): 377-82.

Leffers AM and Wagner A (2000). Neurologic complications of cerebral angiography. A retrospective study of complication rate and patient risk factors. *Acta Radiol.* 41(3): 204-10.

Lin T, Fox AJ and Drake CG (1989). Regrowth of aneurysm sacs from residual neck following aneurysm clipping. *J Neurosurg.* 70(4): 556-60.

Linfante I, Akkawi NM, Perlow A, Andreone V and Wakhloo AK (2005). Polyglycolide/polylactide-coated platinum coils for patients with ruptured and unruptured cerebral aneurysms: a single-center experience. *Stroke* 36(9): 1948-53. Epub 2005 Jul 28.

Loeb GE, McHardy J, Kelliher EM et.al. (1982) Neural prosthesis in Williams DF: Biocompatibility in clinical practice. *CRC Press* 1982; 123-150

Macdonald RL, Mojtahedi S, Johns L and Kowalczuk A (1998). Randomized comparison of Guglielmi detachable coils and cellulose acetate polymer for treatment of aneurysms in dogs. *Stroke.* 29(2): 478-85; discussion 485-6.

Mahindu A, Koivisto T, Ronkainen A, Rinne J, Assaad N, Morgan MK (2008). Similarities and differences in aneurysmal subarachnoid haemorrhage between eastern Finland and northern Sydney. *J Clin Neurosci*. 15(6):617-21. Epub 2008 Apr 18.

Malek AM, Higashida RT, Phatouros CC, Dowd CF and Halbach VV (1999). Treatment of an intracranial aneurysm using a new three-dimensional-shape Guglielmi detachable coil: technical case report. *Neurosurgery.* 44(5): 1142-4; discussion 1144-5.

Marks MP, Steinberg GK and Lane B (1995). Combined use of endovascular coils and surgical clipping for intracranial aneurysms. *AJNR Am J Neuroradiol.* 16(1): 15-8.

Marshall NW, Noble J and Faulkner K (1995). Patient and staff dosimetry in neuroradiological procedures. *Br J Radiol.* 68(809): 495-501.

Massoud TF, Guglielmi G, Ji C, Vinuela F and Duckwiler GR (1994a). Experimental saccular aneurysms. I. Review of surgically-constructed models and their laboratory applications. *Neuroradiology.* 36(7): 537-46.

Massoud TF, Ji C, Guglielmi G, Vinuela F and Robert J (1994b). Experimental models of bifurcation and terminal aneurysms: construction techniques in swine. *AJNR Am J Neuroradiol.* 15(5): 938-44.

Mawad ME, Mawad JK, Cartwright J, Jr. and Gokaslan Z (1995). Long-term histopathologic changes in canine aneurysms embolized with Guglielmi detachable coils. *AJNR Am J Neuroradiol.* 16(1): 7-13.

Mayer SA, Rubin BS, Starman BJ and Byers PH (1996). Spontaneous multivessel cervical artery dissection in a patient with a substitution of alanine for glycine (G13A) in the alpha 1 (I) chain of type I collagen. *Neurology* 47(2): 552-6.

Mayfield FH and Kees G, Jr. (1971). A brief history of the development of the Mayfield clip. Technical note. *J Neurosurg.* 35(1): 97-100.

McCormick WF and Acosta-Rua GJ (1970). The size of intracranial saccular aneurysms. An autopsy study. *J Neurosurg.* 33(4): 422-7.

McCune WS, Samadi A and Blades B (1953). Experimental aneurysms. *Ann Surg.* 138(2): 216-8.

Mericle RA, Lanzino G, Wakhloo AK, Guterman LR and Hopkins LN (1998). Stenting and secondary coiling of intracranial internal carotid artery aneurysm: technical case report. *Neurosurgery.* 43(5): 1229-34.

Miller EJ and Gay S (1987). The collagens: an overview and update. *Methods Enzymol* 144: 3-41.

Miskolczi L, Guterman LR, Flaherty JD and Hopkins LN (1998). Saccular aneurysm induction by elastase digestion of the arterial wall: a new animal model. *Neurosurgery.* 43(3): 595-600; discussion 600-1.
Miyazaki M, Sugiura S, Tateishi F, Wada H, Kassai Y and Abe H (2000). Non-contrast-enhanced MR angiography using 3D ECG-synchronized half-Fourier fast spin echo. *J Magn Reson Imaging.* 12(5): 776-83.
Molyneux A, Kerr R, Stratton I, Sandercock P, Clarke M, Shrimpton J and Holman R (2002). International Subarachnoid Aneurysm Trial (ISAT) of neurosurgical clipping versus endovascular coiling in 2143 patients with ruptured intracranial aneurysms: a randomised trial. *Lancet.* 360(9342): 1267-74.
Molyneux AJ, Cekirge S, Saatci I and Gal G (2004). Cerebral Aneurysm Multicenter European Onyx (CAMEO) trial: results of a prospective observational study in 20 European centers. *AJNR Am J Neuroradiol.* 25(1): 39-51.
Molyneux AJ, Kerr RS, Yu LM, Clarke M, Sneade M, Yarnold JA and Sandercock P (2005). International subarachnoid aneurysm trial (ISAT) of neurosurgical clipping versus endovascular coiling in 2143 patients with ruptured intracranial aneurysms: a randomised comparison of effects on survival, dependency, seizures, rebleeding, subgroups, and aneurysm occlusion. *Lancet.* 366(9488): 809-17.
Moody AR, Pollock JG, O'Connor AR and Bagnall M (1998). Lower-limb deep venous thrombosis: direct MR imaging of the thrombus. *Radiology.* 209(2): 349-55.
Moret J, Cognard C, Weill A, Castaings L and Rey A (1997). [Reconstruction technic in the treatment of wide-neck intracranial aneurysms. Long-term angiographic and clinical results. Apropos of 56 cases]. *J Neuroradiol.* 24(1): 30-44.
Morimoto M, Miyamoto S, Mizoguchi A, Kume N, Kita T and Hashimoto N (2002). Mouse model of cerebral aneurysm: experimental induction by renal hypertension and local hemodynamic changes. *Stroke.* 33(7): 1911-5.
Mullan S, Raimondi AJ, Dobben G, Vailati G and Hekmatpanah J (1965). Electrically induced thrombosis in intracranial aneurysms. *J Neurosurg.* 22(6): 539-47.
Mullan S (1969). Stereotactic thrombosis of intracranial aneurysms. *Confin Neurol.* 31(1): 94.
Murayama Y, Vinuela F, Suzuki Y, Do HM, Massoud TF, et al. (1997). Ion implantation and protein coating of detachable coils for endovascular treatment of cerebral aneurysms: concepts and preliminary results in swine models. *Neurosurgery.* 40(6): 1233-43; discussion 1243-4.
Murayama Y, Suzuki Y, Vinuela F, Kaibara M, Kurotobi K, Iwaki M and Abe T (1999). Development of a biologically active Guglielmi detachable coil for the treatment of cerebral aneurysms. Part I: in vitro study. *AJNR Am J Neuroradiol.* 20(10): 1986-91.
Murayama Y, Vinuela F, Tateshima S, Song JK, Gonzalez NR and Wallace MP (2001). Bioabsorbable polymeric material coils for embolization of intracranial aneurysms: a preliminary experimental study. *J Neurosurg.* 94(3): 454-63.
Murayama Y, Vinuela F, Tateshima S, Gonzalez NR, Song JK, Mahdavieh H and Iruela-Arispe L (2002). Cellular responses of bioabsorbable polymeric material and Guglielmi detachable coil in experimental aneurysms. *Stroke.* 33(4): 1120-8.
Murayama Y, Nien YL, Duckwiler G, Gobin YP, Jahan R, Frazee J, Martin N and Vinuela F (2003a). Guglielmi detachable coil embolization of cerebral aneurysms: 11 years' experience. *J Neurosurg.* 98(5): 959-66.
Murayama Y, Tateshima S, Gonzalez NR and Vinuela F (2003b). Matrix and bioabsorbable polymeric coils accelerate healing of intracranial aneurysms: long-term experimental study. *Stroke* 34(8): 2031-7. Epub 2003 Jul 17.
Murayama Y, Vinuela F, Ishii A, Nien YL, Yuki I, Duckwiler G and Jahan R (2006). Initial clinical experience with matrix detachable coils for the treatment of intracranial aneurysms. *J Neurosurg.* 105(2): 192-9.
Nadel L, Braun IF, Kraft KA, Fatouros PP and Laine FJ (1991). Intracranial vascular abnormalities: value of MR phase imaging to distinguish thrombus from flowing blood. *AJR Am J Roentgenol.* 156(2): 373-80.
Nelson PK, Sahlein D, Shapiro M, Becske T, Fitzsimmons BF, Huang P, Jafar JJ and Levy DI (2006). Recent steps toward a reconstructive endovascular solution for the orphaned, complex-neck aneurysm. *Neurosurgery.* 59(5 Suppl 3): S77-92; discussion S3-13.
Niimi Y, Song J, Madrid M and Berenstein A (2006). Endosaccular treatment of intracranial aneurysms using matrix coils: early experience and midterm follow-up. *Stroke.* 37(4): 1028-32. Epub 2006 Mar 2.
Nishikawa M, Yonekawa Y and Matsuda I (1976). Experimental aneurysms. *Surg Neurol.* 5(1): 15-8.

Niskanen M, Koivisto T, Ronkainen A, Rinne J and Ruokonen E (2004). Resource use after subarachnoid hemorrhage: comparison between endovascular and surgical treatment. *Neurosurgery.* 54(5): 1081-6; discussion 1086-88.

Norlen G, Olivecrona H (1953) The treatment of aneurysms of the circle of Willis. *J Neurosurg*. 10(4):404-15.

Nyström SH (1966) Some aspects of the treatment of intracranial aneurysms. *Int Surg*. 45(1):19-23

Ohkuma H, Fujita S and Suzuki S (2002). Incidence of aneurysmal subarachnoid hemorrhage in Shimokita, Japan, from 1989 to 1998. *Stroke.* 33(1): 195-9.

Ohman J, Heiskanen O (1988). Effect of nimodipine on the outcome of patients after aneurysmal subarachnoid hemorrhage and surgery. *J Neurosurg*. 69(5):683-6.

Ohman J, Heiskanen O. (1989) Timing of operation for ruptured supratentorial aneurysms: a prospective randomized study. *J Neurosurg.* 170(1):55-60.

O'Reilly GV, Utsunomiya R, Rumbaugh CL and Colucci VM (1981). Experimental arterial aneurysms:modification of the production technique. *J Microsurg.* 2(3): 219-23.

Pakarinen S (1967) Incidence, aetiology, and prognosis of primary subarachnoid haemorrhage. Astudy based on 589 cases diagnosed in a defined urban population during a defined period. Acta Neurol Scand 29: 1-28.

Park HK, Horowitz M, Jungreis C, Genevro J, Koebbe C, Levy E and Kassam A (2005). Periprocedural morbidity and mortality associated with endovascular treatment of intracranial aneurysms. *AJNR Am J Neuroradiol.* 26(3): 506-14.

Peters DG, Kassam A, St Jean PL, Yonas H and Ferrell RE (1999). Functional polymorphism in the matrix metalloproteinase-9 promoter as a potential risk factor for intracranial aneurysm. *Stroke.* 30(12): 2612-6.

Peters DG, Kassam AB, Feingold E, Heidrich-O'Hare E, Yonas H, Ferrell RE and Brufsky A (2001). Molecular anatomy of an intracranial aneurysm: coordinated expression of genes involved in wound healing and tissue remodeling. *Stroke.* 32(4): 1036-42.

Pfohman M and Criddle LM (2001). Epidemiology of intracranial aneurysm and subarachnoid hemorrhage. *J Neurosci Nurs* 33(1): 39-41.

Phillips LH, 2nd, Whisnant JP, O'Fallon WM and Sundt TM, Jr. (1980). The unchanging pattern of subarachnoid hemorrhage in a community. *Neurology.* 30(10): 1034-40.

Pickard JD, Murray GD, Illingworth R, Shaw MD, Teasdale GM, Foy PM, Humphrey PR, Lang DA, Nelson R, Richards P, et al (1990). Oral nimodipine and cerebral ischaemia following subarachnoid haemorrhage. *Br J Clin Pract*. 44(2):66-7. No abstract available.

Pierot L, Bonafe A, Bracard S and Leclerc X (2006). Endovascular treatment of intracranial aneurysms with matrix detachable coils: immediate posttreatment results from a prospective multicenter registry. *AJNR Am J Neuroradiol.* 27(8): 1693-9.

Pierot L, Spelle L and Vitry F (2008). Immediate clinical outcome of patients harboring unruptured intracranial aneurysms treated by endovascular approach: results of the ATENA study. *Stroke.* 39(9): 2497-504. Epub 2008 Jul 10.

Prince MR, Yucel EK, Kaufman JA, Harrison DC and Geller SC (1993). Dynamic gadolinium-enhanced three-dimensional abdominal MR arteriography. *J Magn Reson Imaging.* 3(6): 877-81.

Prince MR (1994). Gadolinium-enhanced MR aortography. *Radiology.* 191(1): 155-64.

Raaymakers TW, Rinkel GJ, Limburg M and Algra A (1998). Mortality and morbidity of surgery for unruptured intracranial aneurysms: a meta-analysis. *Stroke.* 29(8): 1531-8.

Rahkonen O, Su M, Hakovirta H, Koskivirta I, Hormuzdi SG, Vuorio E, Bornstein P and Penttinen R (2004). Mice with a deletion in the first intron of the Col1a1 gene develop age-dependent aortic dissection and rupture. *Circ Res* 94(1): 83-90. Epub 2003 Nov 20.

Raymond J and Roy D (1997). Safety and efficacy of endovascular treatment of acutely ruptured aneurysms. *Neurosurgery.* 41(6): 1235-45; discussion 1245-6.

Raymond J, Roy D, Bojanowski M, Moumdjian R and L'Esperance G (1997). Endovascular treatment of acutely ruptured and unruptured aneurysms of the basilar bifurcation. *J Neurosurg.* 86(2): 211-9.

Raymond J, Desfaits AC and Roy D (1999). Fibrinogen and vascular smooth muscle cell grafts promote healing of experimental aneurysms treated by embolization. *Stroke.* 30(8): 1657-64.

Raymond J, Guilbert F, Weill A, Georganos SA, Juravsky L, Lambert A, Lamoureux J, Chagnon M and Roy D (2003). Long-term angiographic recurrences after selective endovascular treatment of aneurysms with detachable coils. *Stroke.* 34(6): 1398-403. Epub 2003 May 29.

Reul J, Weis J, Spetzger U, Konert T, Fricke C and Thron A (1997). Long-term angiographic and histopathologic findings in experimental aneurysms of the carotid bifurcation embolized with platinum and tungsten coils. *AJNR Am J Neuroradiol.* 18(1): 35-42.

Rinkel GJ, Djibuti M, Algra A and van Gijn J (1998). Prevalence and risk of rupture of intracranial aneurysms: a systematic review. *Stroke.* 29(1): 251-6.
Rinkel GJ, Feigin VL, Algra A, Vermeulen M, van Gijn J (2002). Calcium antagonists for aneurysmal subarachnoid haemorrhage. *Cochrane Database Syst Rev*. 2002;(4):CD000277. Review. Update in: *Cochrane Database Syst Rev*. 2005;(1):CD000277.
Rinne JK, Hernesniemi JA (1993). De novo aneurysms: special multiple intracranial aneurysms. *Neurosurgery.* 33(6):981-5. Review.
Rinne J, Hernesniemi J, Puranen M, Saari T. (1994) Multiple intracranial aneurysms in a defined population: prospective angiographic and clinical study. Neurosurgery. 1994 Nov;35(5):803-8
Rinne J, Hernesniemi J, Niskanen M & Vapalahti M (1996) Analysis of 561 patients with 690 middle cerebral artery aneurysms: anatomic and clinical features as correlated to management outcome. Neurosurgery 38: 2-11.
Romodanov AP and Shcheglov VI (1979). Endovascular method of excluding from the circulation saccular cerebral arterial aneurysms, leaving intact vessels patient. *Acta Neurochir Suppl (Wien).* 28(1): 312-5.
Ronkainen A and Hernesniemi J (1992). Subarachnoid haemorrhage of unknown aetiology. *Acta Neurochir (Wien).* 119(1-4): 29-34.
Ronkainen A, Miettinen H, Karkola K, Papinaho S, Vanninen R, Puranen M and Hernesniemi J (1998). Risk of harboring an unruptured intracranial aneurysm. *Stroke.* 29(2): 359-62.
Roy D, Milot G and Raymond J (2001). Endovascular treatment of unruptured aneurysms. *Stroke.* 32(9): 1998-2004.
Sarti C, Tuomilehto J, Salomaa V, Sivenius J, Kaarsalo E, Narva EV, Salmi K and Torppa J (1991). Epidemiology of subarachnoid hemorrhage in Finland from 1983 to 1985. *Stroke.* 22(7): 848-53.
Schievink WI, Torres VE, Piepgras DG and Wiebers DO (1992). Saccular intracranial aneurysms in autosomal dominant polycystic kidney disease. *J Am Soc Nephrol* 3(1): 88-95.
Schievink WI (1997). Genetics of intracranial aneurysms. *Neurosurgery* 40(4): 651-62; discussion 662-3.
Schievink WI (2004). Cerebrovascular Involvement in Ehlers-Danlos Syndrome. *Curr Treat Options Cardiovasc Med* 6(3): 231-236.
Schlote W, Gaus C. (1994) Histologic aspects from ruptured and nonruptured aneurysms.*Neurol Res*. 6(1):59-62.
Schwarze U, Schievink WI, Petty E, Jaff MR, Babovic-Vuksanovic D, Cherry KJ, Pepin M and Byers PH (2001). Haploinsufficiency for one COL3A1 allele of type III procollagen results in a phenotype similar to the vascular form of Ehlers-Danlos syndrome, Ehlers-Danlos syndrome type IV. *Am J Hum Genet* 69(5): 989-1001. Epub 2001 Sep 27.
Sekhon LH, Morgan MK, Sorby W and Grinnell V (1998). Combined endovascular stent implantation and endosaccular coil placement for the treatment of a wide-necked vertebral artery aneurysm: technical case report. *Neurosurgery.* 43(2): 380-3; discussion 384.
Serbinenko FA (1971). [Catheterization and occlusion of major cerebral vessels and prospects for the development of vascular neurosurgery]. *Vopr Neirokhir.* 35(5): 17-27.
Serbinenko FA (1974). Balloon catheterization and occlusion of major cerebral vessels. *J Neurosurg.* 41(2): 125-45.
Sevick RJ, Tsuruda JS and Schmalbrock P (1990). Three-dimensional time-of-flight MR angiography in the evaluation of cerebral aneurysms. *J Comput Assist Tomogr.* 14(6): 874-81.
Sluzewski M, van Rooij WJ, Slob MJ, Bescos JO, Slump CH and Wijnalda D (2004). Relation between aneurysm volume, packing, and compaction in 145 cerebral aneurysms treated with coils. *Radiology.* 231(3): 653-8. Epub 2004 Apr 29.
Solomon RA, Mayer SA and Tarmey JJ (1996). Relationship between the volume of craniotomies for cerebral aneurysm performed at New York state hospitals and in-hospital mortality. *Stroke.* 27(1): 13-7.
Song JK, Elliott JP, Eskridge JM (1997). Neuroradiologic diagnosis and treatment of vasospasm. *Neuroimaging Clin N Am.* 7(4):819-35. Review.
Spaziante R, De Chiara A, Iaccarino V, Stella L, Benvenuti D and Giamundo A (1986). Intracavernous giant fusiform aneurysm of the carotid artery treated with Gianturco coils. *Neurochirurgia (Stuttg).* 29(1): 34-41.
Spetzger U, Reul J, Weis J, Bertalanffy H, Thron A and Gilsbach JM (1996). Microsurgically produced bifurcation aneurysms in a rabbit model for endovascular coil embolization. *J Neurosurg.* 85(3): 488-95.
Stehbens WE (1963) Histopathology of cerebral aneurysms. A*ch Neurol.* 8:272-85.

Stehbens WE (1973). Experimental production of aneurysms by microvascular surgery in rabbits. *Vasc Surg.* 7(3): 165-75.
Stehbens WE (1979). Chronic changes in the walls of experimentally produced aneurysms in sheep. *Surg Gynecol Obstet.* 149(1): 43-8.
Stehbens WE (1981). Chronic vascular changes in the walls of experimental berry aneurysms of the aortic bifurcation in rabbits. *Stroke.* 12(5): 643-7.
Suzuki J, Ohara H. (1978) Clinicopathological study of cerebral aneurysms. Origin, rupture, repair, and growth.*J. Neurosurg*. 48(4):505-14.
Szikora I, Wakhloo AK, Guterman LR, Chavis TD, Dawson RC, 3rd, Hergenrother RW, Twyford RH and Hopkins LN (1997). Initial experience with collagen-filled Guglielmi detachable coils for endovascular treatment of experimental aneurysms. *AJNR Am J Neuroradiol.* 18(4): 667-72.
Taha MM, Nakahara I, Higashi T, Iwamuro Y, Iwaasa M, Watanabe Y, Tsunetoshi K and Munemitsu T (2006). Endovascular embolization vs surgical clipping in treatment of cerebral aneurysms: morbidity and mortality with short-term outcome. *Surg Neurol.* 66(3): 277-84; discussion 284.
Takahashi T, Nakamura K, Andoh K, Tajima M. (1988) Bilateral nontraumatic intracavernous internal carotid aneurysms presenting with massive epistaxis. *Neurol Med Chir* (Tokyo). 28(9):904-9.
Taki W, Handa H, Yamagata S, Ishikawa M, Iwata H and Ikada Y (1980). Radiopaque solidifying liquids for releasable balloon technique: a technical note. *Surg Neurol.* 13(2): 140-2.
Taki W, Yonekawa Y, Iwata H, Uno A, Yamashita K and Amemiya H (1990). A new liquid material for embolization of arteriovenous malformations. *AJNR Am J Neuroradiol.* 11(1): 163-8.
Tamatani S, Ozawa T, Minakawa T, Takeuchi S, Koike T and Tanaka R (1997). Histological interaction of cultured endothelial cells and endovascular embolic materials coated with extracellular matrix. *J Neurosurg.* 86(1): 109-12.
Tapaninaho A, Hernesniemi J, Vapalahti M, Niskanen M, Kari A, Luukkonen M, Puranen M (1993). Shunt-dependent hydrocephalus after subarachnoid haemorrhage and aneurysm surgery: timing of surgery is not a risk factor. *Acta Neurochir (Wien)* 123(3-4):118-24.
Taschner CA, Leclerc X, Rachdi H, Barros AM and Pruvo JP (2005). Matrix detachable coils for the endovascular treatment of intracranial aneurysms: analysis of early angiographic and clinical outcomes. *Stroke* 36(10): 2176-80. Epub 2005 Sep 8.
Tenjin H, Fushiki S, Nakahara Y, Masaki H, Matsuo T, Johnson CM and Ueda S (1995). Effect of Guglielmi detachable coils on experimental carotid artery aneurysms in primates. *Stroke.* 26(11): 2075-80.
ter Berg HW, Bijlsma JB, Veiga Pires JA, Ludwig JW, van der Heiden C, Tulleken CA and Willemse J (1986). Familial association of intracranial aneurysms and multiple congenital anomalies. *Arch Neurol.* 43(1): 30-3.
Teunissen LL, Rinkel GJ, Algra A and van Gijn J (1996). Risk factors for subarachnoid hemorrhage: a systematic review. *Stroke.* 27(3): 544-9.
Toma N, Imanaka-Yoshida K, Takeuchi T, Matsushima S, Iwata H, Yoshida T and Taki W (2005). Tenascin-C-coated platinum coils for acceleration of organization of cavities and reduction of lumen size in a rat aneurysm model. *J Neurosurg* 103(4): 681-6.
Trivedi RA, Mallawarachi C, U-King-Im JM, Graves MJ, Horsley J, Goddard MJ, Brown A, Wang L, Kirkpatrick PJ, Brown J, Gillard JH (2006) Identifying inflamed carotid plaques using in vivo USPIO-enhanced MR imaging to label plaque macrophages. *Arterioscler Thromb Vasc Biol.* 26(7):1601-6. Tsutsumi K, Ueki K, Usui M, Kwak S and Kirino T (1998). Risk of recurrent subarachnoid hemorrhage after complete obliteration of cerebral aneurysms. *Stroke.* 29(12): 2511-3.
Tsutsumi K, Ueki K, Usui M, Kwak S and Kirino T (1999). Risk of subarachnoid hemorrhage after surgical treatment of unruptured cerebral aneurysms. *Stroke.* 30(6): 1181-4.
Tsutsumi K, Ueki K, Morita A, Usui M and Kirino T (2001). Risk of aneurysm recurrence in patients with clipped cerebral aneurysms: results of long-term follow-up angiography. *Stroke.* 32(5): 1191-4.
Tulamo R, Frosen J, Junnikkala S, Paetau A, Pitkaniemi J, et al. (2006). Complement activation associates with saccular cerebral artery aneurysm wall degeneration and rupture. *Neurosurgery.* 59(5): 1069-76; discussion 1076-7.
Unruptured intracranial aneurysms--risk of rupture and risks of surgical intervention. International Study of Unruptured Intracranial Aneurysms Investigators. (1998). *N Engl J Med.* 339(24): 1725-33.
Vale FL, Bradley EL and Fisher WS, 3rd (1997). The relationship of subarachnoid hemorrhage and the need for postoperative shunting. *J Neurosurg.* 86(3): 462-6.

Walker AE, Allegre GW. (1954) The pathology and pathogenesis of cerebral aneurysms. *J Neuropathol Exp Neurol*. 13(1):248-59.
van den Berg R, Rinkel GJ and Vandertop WP (2003). Treatment of ruptured intracranial aneurysms: implications of the ISAT on clipping versus coiling. *Eur J Radiol.* 46(3): 172-7.
van der Wee N, Rinkel GJ, Hasan D and van Gijn J (1995). Detection of subarachnoid haemorrhage on early CT: is lumbar puncture still needed after a negative scan? *J Neurol Neurosurg Psychiatry.* 58(3): 357-9.
van Gijn J and van Dongen KJ (1980). Computed tomography in the diagnosis of subarachnoid haemorrhage and ruptured aneurysm. *Clin Neurol Neurosurg.* 82(1): 11-24.
van Gijn J and Rinkel GJ (2001). Subarachnoid haemorrhage: diagnosis, causes and management. *Brain.* 124(Pt 2): 249-78.
van Gijn J, Kerr RS, Rinkel GJ (2007). Subarachnoid haemorrhage. *Lancet*. 369(9558):306-18. Review.
van Munster CE, von und zu Fraunberg M, Rinkel GJ, Rinne J, Koivisto T, Ronkainen A (2008). Differences in aneurysm and patient characteristics between cohorts of Finnish and Dutch patients with subarachnoid hemorrhage: time trends between 1986 and 2005. *Stroke*. 39(12):3166-71. Epub 2008 Oct 30.
Wanke I, Doerfler A, Schoch B, Stolke D and Forsting M (2003). Treatment of wide-necked intracranial aneurysms with a self-expanding stent system: initial clinical experience. *AJNR Am J Neuroradiol.* 24(6): 1192-9.
Vanninen R, Koivisto T, Saari T, Hernesniemi J and Vapalahti M (1999). Ruptured intracranial aneurysms: acute endovascular treatment with electrolytically detachable coils--a prospective randomized study. *Radiology.* 211(2): 325-36.
Vanninen R, Manninen H and Ronkainen A (2003). Broad-based intracranial aneurysms: thrombosis induced by stent placement. *AJNR Am J Neuroradiol.* 24(2): 263-6.
Venne D, Raymond J, Allas S, Roy D, Leclerc G, Boushira M and Brazeau P (1999). Healing of experimental aneurysms. II: Platelet extracts can increase the thickness of the neointima at the neck of treated aneurysms. *J Neuroradiol.* 26(2): 92-100.
Weir B & MacDonald L (1996) Intracranial aneurysms and subarachnoid hemorrhage: an overview. In: Wilkins RH & Rengachary SS (eds) Neurosurgery. St Louis, McGraw-Hill, 2191-2213.
White PM, Wardlaw JM and Easton V (2000). Can noninvasive imaging accurately depict intracranial aneurysms? A systematic review. *Radiology.* 217(2): 361-70.
Wiebers DO, Whisnant JP, Huston J, 3rd, Meissner I, Brown RD, Jr., et al. (2003). Unruptured intracranial aneurysms: natural history, clinical outcome, and risks of surgical and endovascular treatment. *Lancet.* 362(9378): 103-10.
Wiesmann F, Szimtenings M, Frydrychowicz A, Illinger R, Hunecke A, Rommel E, Neubauer S and Haase A (2003). High-resolution MRI with cardiac and respiratory gating allows for accurate in vivo atherosclerotic plaque visualization in the murine aortic arch. *Magn Reson Med* 50(1): 69-74.
Wilcock DJ, Jaspan T and Worthington BS (1995). Problems and pitfalls of 3-D TOF magnetic resonance angiography of the intracranial circulation. *Clin Radiol.* 50(8): 526-32.
Wilkinson IM (1972). The vertebral artery. Extracranial and intracranial structure. *Arch Neurol.* 27(5): 392-6.
Willing MC, Pruchno CJ, Atkinson M and Byers PH (1992). Osteogenesis imperfecta type I is commonly due to a COL1A1 null allele of type I collagen. *Am J Hum Genet* 51(3): 508-15.
Willinsky RA, Taylor SM, TerBrugge K, Farb RI, Tomlinson G and Montanera W (2003). Neurologic complications of cerebral angiography: prospective analysis of 2,899 procedures and review of the literature. *Radiology.* 227(2): 522-8. Epub 2003 Mar 13.
Vinuela F, Duckwiler G and Mawad M (1997). Guglielmi detachable coil embolization of acute intracranial aneurysm: perioperative anatomical and clinical outcome in 403 patients. *J Neurosurg.* 86(3): 475-82.
Woo D, Khoury J, Haverbusch MM, Sekar P, Flaherty ML, Kleindorfer DO, Kissela BM, Moomaw CJ, Deka R, Broderick JP (2009). Smoking and family history and risk of aneurysmal subarachnoid hemorrhage. *Neurology*. 72(1):69-72.
Yamada N, Hayashi K, Murao K, Higashi M and Iihara K (2004). Time-of-flight MR angiography targeted to coiled intracranial aneurysms is more sensitive to residual flow than is digital subtraction angiography. *AJNR Am J Neuroradiol.* 25(7): 1154-7.
Yang XJ, Li L and Wu ZX (2007). A novel arterial pouch model of saccular aneurysm by concomitant elastase and collagenase digestion. *J Zhejiang Univ Sci B.* 8(10): 697-703.
Yasargil MG and Fox JL (1975). The microsurgical approach to intracranial aneurysms. *Surg Neurol.* 3(1): 7-14.

Yasargil MG (1984) Microsurgical anatomy of the basal cisterns and vessels of the brain, diagnostic studies, general operative techniques and pathological considerations of the intracranial aneurysms. Volume 1. Georg Thieme Verlag, New York.

Yeh HS, Tomsick TA and Tew JM, Jr. (1985). Intraventricular hemorrhage due to aneurysms of the distal posterior inferior cerebellar artery. Report of three cases. *J Neurosurg.* 62(5): 772-5.

Yoneyama T, Kasuya H, Onda H, Akagawa H, Hashiguchi K, Nakajima T, Hori T and Inoue I (2004). Collagen type I alpha2 (COL1A2) is the susceptible gene for intracranial aneurysms. *Stroke* 35(2): 443-8. Epub 2004 Jan 22.

Young PH, Fischer VW, Guity A and Young PA (1987). Mural repair following obliteration of aneurysms: production of experimental aneurysms. *Microsurgery.* 8(3): 128-37.